Algebraic & Geometric Topology 17 (2017) 3461–3518

Quasistabilization and basepoint moving maps in link Floer homology

IAN ZEMKE

We analyze the effect of adding, removing, and moving basepoints on link Floer homology. We prove that adding or removing basepoints via a procedure called quasistabilization is a natural operation on a certain version of link Floer homology, which we call CFL^∞_{UV}. We consider the effect on the full link Floer complex of moving basepoints, and develop a simple calculus for moving basepoints on the link Floer complexes. We apply it to compute the effect of several diffeomorphisms corresponding to moving basepoints. Using these techniques we prove a conjecture of Sarkar about the map on the full link Floer complex induced by a finger move along a link component.

57M25, 57M27, 57R58

1 Introduction

Introduced by Ozsváth and Szabó, Heegaard Floer homology associates algebraic invariants to closed three-manifolds. To a three-manifold Y with embedded nullhomologous knot K, there is a refinement of Heegaard Floer homology called knot Floer homology, introduced by Ozsváth and Szabó [8] and independently by Rasmussen [11]. A similar invariant was defined by Ozsváth and Szabó for links [10].

To a nullhomologous knot $K \subseteq Y$ with two basepoints z and w and a relative Spin^c structure $\mathfrak{t} \in \mathrm{Spin}^c(Y, K)$, Ozsváth and Szabó [8] define a $\mathbb{Z} \oplus \mathbb{Z}$–filtered chain complex $\mathrm{CFK}^\infty(Y, K, w, z, \mathfrak{t})$. The $\mathbb{Z} \oplus \mathbb{Z}$–filtered chain homotopy type of $\mathrm{CFK}^\infty(Y, K, w, z, \mathfrak{t})$ is an invariant of the data $(Y, K, w, z, \mathfrak{t})$.

One of the nuances of Heegaard Floer homology is the dependence on basepoints. In the case of closed three-manifolds, if $\boldsymbol{w} \subseteq Y$ is a collection of basepoints, $w \in \boldsymbol{w}$ and γ is a curve in $\pi_1(Y, w)$, then one can consider the diffeomorphism ϕ_γ resulting from a finger move along γ. According to Juhász and Thurston [4], the based mapping class group $\mathrm{MCG}(Y, w)$ acts on $\mathrm{CF}^\circ(Y, \boldsymbol{w}, \mathfrak{s})$ and hence there is an induced map $(\phi_\gamma)_*$ on the closed three-manifold invariant $\mathrm{CF}^\circ(Y, \boldsymbol{w}, \mathfrak{s})$, which is a $\mathbb{Z}_2[U]$–equivariant chain

Published: 4 October 2017 DOI: 10.2140/agt.2017.17.3461

homotopy type. In [14], the author computes the equivariant chain homotopy type of $(\phi_\gamma)_*$ to be

$$(\phi_\gamma)_* \simeq \mathrm{id} + [\gamma] \circ \Phi_w,$$

where $[\gamma]$ is the $\Lambda^*(H_1(Y;\mathbb{Z})/\operatorname{Tors})$ action and Φ_w is an analogue of a map appearing also on link Floer homology, which we describe below.

In this paper, we consider the analogous question about basepoint dependence for link Floer homology. In link Floer homology, the basepoints are constrained to be on the link component, so the analogous operation is to consider the map on link Floer homology induced by a finger move ς around a link component, in the positive direction according to the link's orientation. Using grid diagrams, Sarkar [13] computes the map associated to the diffeomorphism ς on a certain version of link Floer homology (the associated graded complex) for links in S^3. For links in arbitrary three-manifolds, and for the induced map on the full link Floer complex, he conjectures the formula. We prove his formula in full generality (Theorem B), but before we state that theorem we will provide a brief description of the complexes and maps which appear.

We will work with a slightly different version of CFL^∞ than the one which most often appears in the literature. For a multibased link $\mathbb{L} = (L, \boldsymbol{w}, \boldsymbol{z})$ inside of Y and a Spin^c structure $\mathfrak{s} \in \mathrm{Spin}^c(Y)$, we construct a chain complex

$$\mathrm{CFL}^\infty_{UV}(Y, \mathbb{L}, \mathfrak{s}),$$

which is a module over the polynomial ring $\mathbb{Z}_2[U_{\boldsymbol{w}}, V_{\boldsymbol{z}}]$, generated by variables U_w with $w \in \boldsymbol{w}$ and V_z with $z \in \boldsymbol{z}$. The module $\mathrm{CFL}^\infty_{UV}(Y, \mathbb{L}, \mathfrak{s})$ has generators of the form

$$\boldsymbol{x} \cdot U_{\boldsymbol{w}}^I V_{\boldsymbol{z}}^J = \boldsymbol{x} \cdot U_{w_1}^{i_1} \cdots U_{w_n}^{i_n} V_{z_1}^{j_1} \cdots V_{z_n}^{j_n}$$

for multi-indices $I = (i_1, \dots, i_n)$ and $J = (j_1, \dots, j_n)$, though we identify two variables V_z and $V_{z'}$ if z and z' are on the same link component. Thus, $\mathrm{CFL}^\infty_{UV}(Y, \mathbb{L}, \mathfrak{s})$ has a filtration by $\mathbb{Z}^{|\boldsymbol{w}|} \oplus \mathbb{Z}^{|L|}$ given by filtering over powers of the variables, where $|L|$ denotes the set of components of L.

As with the free stabilization maps from [14], to define functorial maps corresponding to adding or removing basepoints in link Floer homology, we must work with colored complexes. A coloring $(\sigma, \mathfrak{P})$ of a link with basepoints, $(L, \boldsymbol{w}, \boldsymbol{z})$, is a set $\mathfrak{P}$ indexing a collection of formal variables, together with a map $\sigma\colon \boldsymbol{w} \cup \boldsymbol{z} \to \mathfrak{P}$ which maps all $\boldsymbol{z}$–basepoints on a component of L to the same color. Given a coloring $(\sigma, \mathfrak{P})$ of a link $\mathbb{L} = (L, \boldsymbol{w}, \boldsymbol{z})$, we create a $\mathbb{Z}_2[U_{\mathfrak{P}}]$–chain complex

$$\mathrm{CFL}^\infty_{UV}(Y, \mathbb{L}, \sigma, \mathfrak{P}, \mathfrak{s}).$$

The powers of the $U_{\mathfrak{P}}$ variables yield a filtration by $\mathbb{Z}^{\mathfrak{P}}$, which we call the $\mathfrak{P}$–filtration.

In the context of link Floer homology, analogously to adding or removing a free basepoint in a closed 3–manifold, one can add or remove a pair of adjacent basepoints, w and z, on a link component. Some authors refer to this operation as a "special stabilization". Manolescu and Ozsváth [6] consider certain questions about the operation, calling it "quasistabilization", which is the phrase we will use. A full description and proof of naturality of the operation has not been completed, so we do that in this paper:

Theorem A *Suppose z and w are new basepoints on a link $\mathbb{L}=(L,\boldsymbol{w},\boldsymbol{z})$, ordered so that w comes after z, which aren't separated by any basepoints in $\boldsymbol{w}$ or $\boldsymbol{z}$. If $\sigma\colon \boldsymbol{w}\cup\boldsymbol{z}\to\mathfrak{P}$ is a coloring which is extended by $\sigma'\colon \boldsymbol{w}\cup\boldsymbol{z}\cup\{w,z\}\to\mathfrak{P}$, then there are $\mathfrak{P}$–filtered $\mathbb{Z}_2[U_{\mathfrak{P}}]$–chain maps*

$$S_{w,z}^{+}\colon \mathrm{CFL}_{UV}^{\infty}(Y,L,\boldsymbol{w},\boldsymbol{z},\sigma,\mathfrak{P},\mathfrak{s})\to \mathrm{CFL}_{UV}^{\infty}(Y,L,\boldsymbol{w}\cup\{w\},\boldsymbol{z}\cup\{z\},\sigma',\mathfrak{P},\mathfrak{s})$$

and

$$S_{w,z}^{-}\colon \mathrm{CFL}_{UV}^{\infty}(Y,L,\boldsymbol{w}\cup\{w\},\boldsymbol{z}\cup\{z\},\sigma',\mathfrak{P},\mathfrak{s})\to \mathrm{CFL}_{UV}^{\infty}(Y,L,\boldsymbol{w},\boldsymbol{z},\sigma,\mathfrak{P},\mathfrak{s}),$$

which are well-defined invariants, up to $\mathfrak{P}$–filtered, $\mathbb{Z}_2[U_{\mathfrak{P}}]$–equivariant chain homotopy. If z comes after w, there are maps $S_{z,w}^{+}$ and $S_{z,w}^{-}$ defined analogously.

Following Sarkar [13], we consider endomorphisms Φ_w and Ψ_z of $\mathrm{CFL}_{UV}^{\infty}(Y,\mathbb{L},\mathfrak{s})$ ($\Phi_{i,j}$ and $\Psi_{i,j}$ in his notation). We can think of the maps Φ_w and Ψ_z as formal derivatives of the differential ∂ with respect to the variables U_w and V_z, respectively. The maps Φ_w and Ψ_z are invariants of $\mathrm{CFL}_{UV}^{\infty}(Y,\mathbb{L},\sigma,\mathfrak{P},\mathfrak{s})$ up to $\mathfrak{P}$–filtered chain homotopy.

The maps Ψ_z can be thought of as analogues of the relative homology maps A_λ defined in [14] for the closed three-manifold invariants, since they play the role in the basepoint moving maps for link Floer homology that the relative homology maps introduced in [14] played in the basepoint moving maps for the closed three-manifolds invariants. Indeed the objects $\mathrm{CFL}_{UV}^{\infty}(Y,\mathbb{L},\mathfrak{s})$ and the maps Ψ_z and $S_{w,z}^{\pm}$ fit into the framework of a "graph TQFT" for surfaces embedded in four-manifolds with some extra decoration, similar to the TQFT for $\widehat{\mathrm{HFL}}$ constructed using sutured Floer homology by Juhász [2] and considered further by Juhász and Marengon [3] for concordances. Such a TQFT construction for $\mathrm{CFL}_{UV}^{\infty}$ will appear in a future paper.

We finally state Sarkar's conjecture, cast into the framework of $\mathrm{CFL}_{UV}^{\infty}(Y,\mathbb{L},\sigma,\mathfrak{P},\mathfrak{s})$:

Theorem B *Suppose that $\mathbb{L}=(L,\boldsymbol{w},\boldsymbol{z})$ is a multibased link in an arbitrary 3–manifold Y and K is a component of L. Suppose that the basepoints on K are $z_1,w_1,\dots,z_n,w_n$. Letting ς denote the diffeomorphism resulting from a finger move* *around a link component* K, *the induced map* ς_* *on* $\mathrm{CFL}^\infty_{UV}(Y, \mathbb{L}, \sigma, \mathfrak{P}, \mathfrak{s})$ *has the* $\mathfrak{P}$*–filtered equivariant chain homotopy type*

$$\varsigma_* \simeq \mathrm{id} + \Phi_K \Psi_K,$$

where

$$\Phi_K = \sum_{j=1}^n \Phi_{w_j} \quad \textit{and} \quad \Psi_K = \sum_{j=1}^n \Psi_{z_j}.$$

Sarkar's conjecture for the effect on the filtered link Floer complex, which we will denote by $\mathrm{CFL}^\infty(Y, \mathbb{L}, \mathfrak{t})$ for $\mathfrak{t}$ a relative $\mathrm{Spin}^c(Y, L)$ structure, follows by setting $(\sigma, \mathfrak{P})$ to be the trivial coloring (ie $\mathfrak{P} = \boldsymbol{w} \cup |L|$ and $\sigma\colon (\boldsymbol{w} \cup \boldsymbol{z}) \to (\boldsymbol{w} \cup |L|)$ the natural map) since the complex $\mathrm{CFL}^\infty(Y, \mathbb{L}, \mathfrak{t})$ becomes a $\mathbb{Z}_2$–subcomplex of $\mathrm{CFL}^\infty_{UV}(Y, \mathbb{L}, \sigma, \mathfrak{P}, \mathfrak{s})$ which is preserved by ς_*, where $\mathfrak{s}$ is the underlying Spin^c structure associated to the relative Spin^c structure $\mathfrak{t}$.

There are several other formulations of this conjecture for different versions of link Floer homology. For example, the conjectured formula for ς_* on $\mathrm{CFK}^\infty(S^3, K)$ for $K \subseteq S^3$ is useful for computations in the involutive Heegaard Floer homology theory developed by Hendricks and Manolescu (see [1, Section 6]). In their notation, for a choice of diagrams, the complex $\mathrm{CFK}^\infty(S^3, K)$ for a knot $K \subseteq S^3$ is generated by elements of the form $[\boldsymbol{x}, i, j]$ where i and j satisfy $A(\boldsymbol{x}) = i - j$, and A denotes the Alexander grading. In their notation, the U map takes the form $U \cdot [\boldsymbol{x}, i, j] = [\boldsymbol{x}, i-1, j-1]$. Again, the complex $\mathrm{CFK}^\infty(S^3, K)$ is a $\mathbb{Z}_2$–subcomplex

$$\mathrm{CFK}^\infty(S^3, K) \subseteq \mathrm{CFL}^\infty_{UV}(S^3, K, w, z, \mathfrak{s}_0)$$

which is preserved by ς_*. Recasting Theorem B into this notation and recalling that we are using coefficients in $\mathbb{Z}_2$, we arrive at the following:

Corollary C *For a knot* $K \subseteq S^3$, *the involution* ς_* *on* $\mathrm{CFK}^\infty(S^3, K)$ *takes the form*

$$\varsigma_* \simeq 1 + U^{-1}\Big(\sum_{\substack{i,j\ge 0\\ i \text{ odd}}} \partial_{ij}\Big) \circ \Big(\sum_{\substack{i,j\ge 0\\ j \text{ odd}}} \partial_{ij}\Big),$$

if we write the differential $\partial = \sum_{i,j\ge 0} \partial_{ij}$. *Here* ∂_{ij} *decreases the first filtration by* i *and the second filtration by* j.

For other flavors, such as $\widehat{\mathrm{CFL}}$ or CFL^-, the formula conjectured by Sarkar also follows, since those cases correspond to setting various variables equal to zero in the formula for ς_*.

In addition, we consider the effect of another diffeomorphism obtained by twisting a link component. Suppose that K is a component of a link $\mathbb{L}$ and suppose that the basepoints of K are $z_1, w_1, \dots, z_n$ and w_n, appearing in that order. We can consider the diffeomorphism $\tau\colon (Y, \mathbb{L}) \to (Y, \mathbb{L})$ which twists $(1/n)^{\text{th}}$ of the way around K. The diffeomorphism τ maps z_i and w_i to z_{i+1} and w_{i+1}, respectively, with indices taken modulo n. If $(\sigma, \mathfrak{P})$ is a coloring of $\mathbb{L}$ which sends all of the $\boldsymbol{w}$–basepoints on K to the same color, then τ naturally induces an automorphism of

$$\mathrm{CFL}^\infty_{UV}(Y, \mathbb{L}, \sigma, \mathfrak{P}, \mathfrak{s}).$$

Using the techniques of this paper, we can compute the following:

Theorem D *Suppose that $\mathbb{L}$ is an embedded link in Y, and K is a component of $\mathbb{L}$ with basepoints $z_1, w_1, \dots, z_n$ and w_n, appearing in that order. Assume that $n > 1$. If τ denotes the diffeomorphism induced by twisting $(1/n)^{th}$ of the way around K, then for a coloring where all $\boldsymbol{w}$–basepoints on K have the same color, we have*

$$\tau_* \simeq (\Psi_{z_1}\Phi_{w_1}\Psi_{z_2}\Phi_{w_2}\cdots\Phi_{w_{n-1}}\Psi_{z_n}\Phi_{w_n}) + (\Phi_{w_1}\Psi_{z_2}\Phi_{w_2}\cdots\Phi_{w_{n-1}}\Psi_{z_n}).$$

Organization In Section 2 we define the complexes which will appear in this paper, as well as their algebraic structures as $\mathfrak{P}$–filtered chain complexes over certain modules. In Section 3 we define the maps Φ_w and Ψ_z which feature prominently in this paper. In Sections 5–7 we define quasistabilization maps $S^{\pm}_{w,z}$ and show that they are independent of the choice of diagrams and auxiliary data, proving Theorem A. In Sections 8 and 9 we prove useful relations amongst the maps Ψ_z, Φ_w and $S^{\pm}_{w,z}$. In Section 10 we compute several maps associated with moving basepoints, proving Theorems B and D.

Acknowledgments I would like to thank my advisor, Ciprian Manolescu, for helpful conversations, especially about quasistabilization. I would also like to thank Faramarz Vafaee and Robert Lipshitz for helpful conversations.

2 Background, the complexes CFL^∞_{UV}, and $\mathfrak{P}$–filtrations

In this section we provide some background and describe the complexes $\mathrm{CFL}^\infty_{UV}(Y, \mathbb{L}, \mathfrak{s})$ which will appear.

2.1 Spin^c structures and relative Spin^c structures

Ozsváth and Szabó [9] define a Spin^c structure on Y to be a homology class of nonvanishing vector fields on Y. For a Heegaard diagram $\mathcal{H} = (\Sigma, \boldsymbol{\alpha}, \boldsymbol{\beta}, \boldsymbol{w})$ they define a map

$$\mathfrak{s}_{\boldsymbol{w}}\colon \mathbb{T}_\alpha \cap \mathbb{T}_\beta \to \mathrm{Spin}^c(Y).$$

The vector field $\mathfrak{s}_{\boldsymbol{w}}(\boldsymbol{x})$ is obtained by taking an upward gradient-like vector field associated to a Morse function yielding $\mathcal{H}$, and modifying it in a neighborhood of the flowlines passing through the points in $\boldsymbol{w}$ and $\boldsymbol{x}$ to obtain a nonvanishing vector field. Ozsváth and Szabó [10] provide a notion of relative Spin^c structures for a link in a 3–manifold. These are homology classes of vector fields on $Y \setminus N(L)$ which are tangent to the torus $\partial N(L)$. They define a map

$$\mathfrak{s}_{\boldsymbol{w},\boldsymbol{z}} \colon \mathbb{T}_\alpha \cap \mathbb{T}_\beta \to \mathrm{Spin}^c(Y, L).$$

We note that in general there are two natural ways to obtain an absolute Spin^c structure from a relative Spin^c structure. We take the convention that the filling map covers the map $\mathfrak{s}_{\boldsymbol{w}}$ (compare [10, Section 3.7]). In more generality, one has $\mathfrak{s}_{\boldsymbol{w}}(\boldsymbol{x}) - \mathfrak{s}_{\boldsymbol{z}}(\boldsymbol{x}) = \mathrm{PD}[L]$, so if we restrict to links whose total homology class vanishes, then there is no distinction. Since we include the versions of link Floer homology which use relative Spin^c structures only for the sake of comparison, whenever we consider relative Spin^c structures, we will assume that Y is a integer homology sphere. We will primarily be interested in working with the version CFL^∞_{UV}, which uses absolute Spin^c structures.

2.2 The complex $\mathrm{CFL}^\infty_{UV}(Y, \mathbb{L}, \mathfrak{s})$

Here we describe the uncolored complex $\mathrm{CFL}^\infty_{UV}(Y, \mathbb{L}, \mathfrak{s})$. We first describe an intermediate object, $\mathrm{CFL}^\infty_{UV,0}(Y, \mathbb{L}, \mathfrak{s})$.

Let $\mathbb{Z}_2[U_{\boldsymbol{w}}, U_{\boldsymbol{w}}^{-1}, V_{\boldsymbol{z}}, V_{\boldsymbol{z}}^{-1}]$ denote the ring generated by variables U_w, V_z and their inverses U_w^{-1}, V_z^{-1} for $w \in \boldsymbol{w}$ and $z \in \boldsymbol{z}$. Given a diagram $\mathcal{H} = (\Sigma, \boldsymbol{\alpha}, \boldsymbol{\beta}, \boldsymbol{w}, \boldsymbol{z})$ for $(Y, L, \boldsymbol{w}, \boldsymbol{z})$, we define $\mathrm{CFL}^\infty_{UV,0}(\mathcal{H}, \mathfrak{s})$ to be the free $\mathbb{Z}_2[U_{\boldsymbol{w}}, U_{\boldsymbol{w}}^{-1}, V_{\boldsymbol{z}}, V_{\boldsymbol{z}}^{-1}]$–module generated by $\boldsymbol{x} \in \mathbb{T}_\alpha \cap \mathbb{T}_\beta$ with $\mathfrak{s}_{\boldsymbol{w}}(\boldsymbol{x}) = \mathfrak{s}$. We refer the reader to eg [10] for the definition of a Heegaard diagram for a link, though we emphasize that in light of the results of [4], we must assume that

$$\boldsymbol{w} \cup \boldsymbol{z} \subseteq \Sigma \subseteq Y$$

and that the embedding of Σ in Y is part of the data of a Heegaard splitting.

We now define a map

$$\partial \colon \mathrm{CFL}^\infty_{UV,0}(\mathcal{H}, \mathfrak{s}) \to \mathrm{CFL}^\infty_{UV,0}(\mathcal{H}, \mathfrak{s})$$

by

$$\partial(\boldsymbol{x}) = \sum_{\boldsymbol{y} \in \mathbb{T}_\alpha \cap \mathbb{T}_\beta} \sum_{\substack{\phi \in \pi_2(\boldsymbol{x}, \boldsymbol{y}) \\ \mu(\phi) = 1}} \# \widehat{\mathcal{M}}(\phi) U_{\boldsymbol{w}}^{n_{\boldsymbol{w}}(\phi)} V_{\boldsymbol{z}}^{n_{\boldsymbol{z}}(\phi)} \cdot \boldsymbol{y}.$$

The map ∂ does not square to zero, but we do have the following:

Lemma 2.1 *The map* $\partial\colon \mathrm{CFL}^\infty_{UV,0}(\mathcal{H},\mathfrak{s}) \to \mathrm{CFL}^\infty_{UV,0}(\mathcal{H},\mathfrak{s})$ *satisfies*

$$\partial^2 = \sum_{K\in|L|}(U_{w_{K,1}}V_{z_{K,1}} + V_{z_{K,1}}U_{w_{K,2}} + U_{w_{K,2}}V_{z_{K,2}} + \cdots + V_{z_{K,n_K}}U_{w_{K,1}}),$$

where $w_{K,1}, z_{K,1}, \dots, w_{K,n_K}, z_{K,n_K}$ *are the basepoints on the link component* K*, in the order that they appear on* K.

Proof This follows from the usual proof that the differential squares to zero, now just counting boundary degenerations carefully. If there are exactly two basepoints, there are no boundary degenerations by [10, Theorem 5.5], and the above formula is satisfied. If there are more than two, then each $\boldsymbol{\alpha}$– and $\boldsymbol{\beta}$–degeneration has a unique holomorphic representative by [10, Theorem 5.5] and each crosses over a $\boldsymbol{w}$–basepoint and a $\boldsymbol{z}$–basepoint. The formula follows. $\square$

To get a chain complex, we must color $\mathrm{CFL}^\infty_{UV,0}(Y,\mathbb{L},\mathfrak{s})$ by setting certain variables equal. Let $C_{\mathbb{L}}$ denote the ideal generated by elements of the form $V_{z_i} - V_{z_j}$, where z_i and z_j are in the same link component. We let $\mathcal{L} = \mathbb{Z}_2[U_{\boldsymbol{w}}, U_{\boldsymbol{w}}^{-1}, V_{\boldsymbol{z}}, V_{\boldsymbol{z}}^{-1}]/C_{\mathbb{L}}$.

We now define

$$\mathrm{CFL}^\infty_{UV}(\mathcal{H},\mathfrak{s}) = \mathrm{CFL}^\infty_{UV,0}(\mathcal{H},\mathfrak{s}) \otimes_{\mathbb{Z}_2[U_{\boldsymbol{w}},U_{\boldsymbol{w}}^{-1},V_{\boldsymbol{z}},V_{\boldsymbol{z}}^{-1}]} \mathcal{L}.$$

We have the following:

Lemma 2.2 *The map* ∂ *defined above is a differential on* $\mathrm{CFL}^\infty_{UV}(\mathcal{H},\mathfrak{s})$*, ie* $\partial^2 = 0$.

Proof This follows from the formula in Lemma 2.1 since the module $\mathcal{L}$ simply identifies all V_z variables for z which lie in the same link component. $\square$

Remark 2.3 There are other modules that we could tensor with to make the differential square to zero. The module $\mathcal{L}$ is actually a quite natural choice. As we will see in the proof of Proposition 5.3, terms of the form $V_z + V_{z'}$ appear in the differential after quasistabilization, and these terms must be zero for $S^{\pm}_{w,z}$ to be chain maps.

The $\mathbb{Z}_2[U_{\boldsymbol{w}}, V_{\boldsymbol{z}}]$–module $\mathrm{CFL}^\infty_{UV}(\mathcal{H},\mathfrak{s})$ has a natural $\mathbb{Z}^{|\boldsymbol{w}|} \oplus \mathbb{Z}^{|L|}$ filtration given by filtering over powers of the variables $U_{\boldsymbol{w}}$ and $V_{\boldsymbol{z}}$.

There are of course many different Heegaard diagrams $\mathcal{H}$ for a given multibased link $(L,\boldsymbol{w},\boldsymbol{z})$. As in the case of closed three-manifolds, using [4], given two diagrams $\mathcal{H}$ and $\mathcal{H}'$, there is a $\mathbb{Z}^{|\boldsymbol{w}|} \oplus \mathbb{Z}^{|L|}$–filtered map

$$\Phi_{\mathcal{H}\to\mathcal{H}'}\colon \mathrm{CFL}^\infty_{UV}(\mathcal{H},\mathfrak{s}) \to \mathrm{CFL}^\infty_{UV}(\mathcal{H}',\mathfrak{s})$$

which is a filtered chain homotopy equivalence, and is an invariant up to $\mathbb{Z}^{|\boldsymbol{w}|} \oplus \mathbb{Z}^{|L|}$–filtered chain homotopy. The maps $\Phi_{\mathcal{H} \to \mathcal{H}'}$ are functorial in the sense that if $\mathcal{H}, \mathcal{H}'$ and $\mathcal{H}''$ are three diagrams, then

$$\Phi_{\mathcal{H}' \to \mathcal{H}''} \circ \Phi_{\mathcal{H} \to \mathcal{H}'} \simeq \Phi_{\mathcal{H} \to \mathcal{H}''}.$$

The strongest invariant, which we will occasionally refer to as the *coherent filtered chain homotopy type*, is the collection of all of the complexes $\mathrm{CFL}^\infty_{UV}(\mathcal{H}, \mathfrak{s})$ for all admissible diagrams $\mathcal{H}$ for $(Y, L, \boldsymbol{w}, \boldsymbol{z})$, as well as the maps $\Phi_{\mathcal{H} \to \mathcal{H}'}$. We let

$$\mathrm{CFL}^\infty_{UV}(Y, \mathbb{L}, \mathfrak{s})$$

denote this invariant. Note that since we are working with embedded Heegaard surfaces, the set of Heegaard diagrams for a link is a set, and not a proper class.

Remark 2.4 As we remarked earlier, since $\mathrm{CFL}^\infty_{UV}(Y, \mathbb{L}, \mathfrak{s})$ is generated by intersection points with $\mathfrak{s}_{\boldsymbol{w}}(\boldsymbol{x}) = \mathfrak{s}$, there is some asymmetry between the $\boldsymbol{w}$ and $\boldsymbol{z}$ basepoints in the construction of CFL^∞_{UV}. We note that $\mathfrak{s}_{\boldsymbol{w}}(\boldsymbol{x}) - \mathfrak{s}_{\boldsymbol{z}}(\boldsymbol{x}) = \mathrm{PD}[L]$, so if L is null-homologous, this doesn't affect the chain complexes. As a toy example, one can consider $(S^1 \times S^2, S^1 \times \{\mathrm{pt}\})$ to see how the modules change over different choices of $\mathfrak{s}$.

2.3 Other versions of the link Floer complex

Supposing for simplicity that Y is an integer homology sphere, we briefly describe a complex $\mathrm{CFL}^\infty(Y, \mathbb{L}, \mathfrak{t})$, for a relative Spin^c structure $\mathfrak{t} \in \mathrm{Spin}^c(Y, L)$. It will not feature in any of the sections after this, but we describe it as a comparison with CFL^∞_{UV}. Let μ_i be a positive meridian of the i^{th} link component. The complex $\mathrm{CFL}^\infty(Y, \mathbb{L}, \mathfrak{t})$ is defined as the subcomplex of $\mathrm{CFL}^\infty_{UV}(\mathcal{H}, \mathfrak{s})$ generated over $\mathbb{Z}_2$ by elements of the form $\boldsymbol{x} \cdot U^{\boldsymbol{I}}_{\boldsymbol{w}} V^{\boldsymbol{J}}_{\boldsymbol{z}}$, where

$$J \cdot \mathrm{PD}[M] = (\mathfrak{t} - \mathfrak{s}_{\boldsymbol{w},\boldsymbol{z}}(\boldsymbol{x})) + I \cdot \mathrm{PD}[M], \tag{1}$$

where PD denotes Poincaré duality. Here, if $J = (j_1, \dots, j_\ell)$, then $J \cdot \mathrm{PD}[M]$ is defined to be $j_1 \cdot \mathrm{PD}[\mu_1] + \cdots + j_\ell \cdot \mathrm{PD}[\mu_\ell]$, and $I \cdot \mathrm{PD}[M]$ is defined similarly.

In the case that $\mathbb{L} = (K, w, z)$ is a knot with exactly two basepoints, we see that $\mathrm{CFL}^\infty(Y, K, w, z, \mathfrak{t})$ is generated by elements of the form $\boldsymbol{x} \cdot U^i_w V^j_z$ with

$$j \cdot \mathrm{PD}[\mu] = (\mathfrak{t} - \mathfrak{s}_{\boldsymbol{w},\boldsymbol{z}}(\boldsymbol{x})) + i \cdot \mathrm{PD}[\mu],$$

which is exactly the complex $\mathrm{CFK}^\infty(K, \mathfrak{t})$ found in [8]. More often one writes $[\boldsymbol{x}, i, j]$ for what we write $\boldsymbol{x} \cdot U^{-i}_w V^{-j}_z$. Most authors also write U for the action defined by $U \cdot [\boldsymbol{x}, i, j] = [\boldsymbol{x}, i-1, j-1]$, though in our notation this action corresponds to multiplication by $U_w V_z$. It's also common to consider an object $\mathrm{CFK}^\infty(Y, K)$, generated by monomials $U_w^i V_z^j \cdot \boldsymbol{x}$ satisfying $A(\boldsymbol{x}) = i - j$, where A is the symmetrized Alexander grading.

Given a relative Spin^c structure $\mathfrak{t} \in \mathrm{Spin}^c(Y, L)$, we write

$$\iota_{\mathfrak{t}} \colon \mathrm{CFL}^\infty(Y, L, \mathfrak{t}) \hookrightarrow \mathrm{CFL}^\infty_{UV}(Y, L, \mathfrak{s})$$

for inclusion.

As a direct sum of $\mathbb{Z}_2$–modules, we have

$$\mathrm{CFL}^\infty_{UV}(\mathcal{H}, \mathfrak{s}) = \bigoplus_{\mathfrak{t} \in \mathrm{Spin}^c(Y,L)} \mathrm{CFL}^\infty(\mathcal{H}, \mathfrak{t}).$$

Write $\pi_{\mathfrak{t}} \colon \mathrm{CFL}^\infty_{UV}(\mathcal{H}, \mathfrak{s}) \to \mathrm{CFL}^\infty(\mathcal{H}, \mathfrak{t})$ for the projection onto $\mathrm{CFL}^\infty(\mathcal{H}, \mathfrak{t})$.

Finally, we note that in $\mathrm{CFL}^\infty(Y, \mathbb{L}, \mathfrak{t})$ the multi-index J in a monomial $U_{\boldsymbol{w}}^I V_{\boldsymbol{z}}^J \cdot \boldsymbol{x} \in \mathrm{CFL}^\infty(Y, \mathbb{L}, \mathfrak{t})$ is determined by the multi-index I, as well as the choice of $\mathfrak{t}$. Thus the full link Floer complex in [10] is described instead as the module generated by monomials $U_{\boldsymbol{w}}^I \cdot \boldsymbol{x}$, but with a filtration by $\mathrm{Spin}^c(Y, L)$. Given a $\mathfrak{t} \in \mathrm{Spin}^c(Y, L)$, it is straightforward to write down an isomorphism of filtered chain complexes between these two objects.

2.4 Colorings and $\mathfrak{P}$–filtrations

As was the case in [14], to define functorial maps it is important to work in a category of chain complexes over a fixed ring. As the link Floer complexes are modules over a ring which depends on the link, we need to formally "color" the complexes to make them modules over a fixed ring. Different choices of base rings will be useful for different applications, but for a single computation, a single ring must be fixed.

If $\mathfrak{P}$ is a finite set, we let $\mathbb{Z}_2[U_{\mathfrak{P}}, U_{\mathfrak{P}}^{-1}]$ denote the ring generated by the formal variables U_p and their inverses U_p^{-1} for $p \in \mathfrak{P}$.

Definition 2.5 If $\mathfrak{P}$ is a finite set, a *$\mathfrak{P}$–filtered chain complex* is a chain complex with a filtration of $\mathbb{Z}^{\mathfrak{P}}$, ie if C is a chain complex, then a $\mathfrak{P}$–filtration is a collection of subcomplexes $\mathcal{F}_I \subseteq C$ ranging over $I \in \mathbb{Z}^{\mathfrak{P}}$ such that if $I \le I'$, then $\mathcal{F}_{I'} \subseteq \mathcal{F}_I$. A $\mathfrak{P}$–filtered homomorphism is a homomorphism $\phi \colon C \to C'$ where C and C' are $\mathfrak{P}$–filtered with filtrations $\mathcal{F}_I$ and $\mathcal{F}'_I$ such that

$$\phi(\mathcal{F}_I) \subseteq \mathcal{F}'_I.$$

Definition 2.6 A *coloring of a multibased link* $\mathbb{L} = (L, \boldsymbol{w}, \boldsymbol{z})$ in Y is a pair $(\sigma, \mathfrak{P})$ where $\mathfrak{P}$ is a finite set and $\sigma \colon \boldsymbol{w} \cup \boldsymbol{z} \to \mathfrak{P}$ is a map which sends all of the $\boldsymbol{z}$ basepoints on a given link component to the same color (this condition ensures that the differential squares to zero).

If $(\sigma, \mathfrak{P})$ is a coloring of a link $\mathbb{L} = (L, \boldsymbol{w}, \boldsymbol{z})$, let $\mathcal{C}_{\sigma,\mathfrak{P}}$ denote the module

$$\mathbb{Z}_2[U_{\boldsymbol{w}}, U_{\boldsymbol{w}}^{-1}, V_{\boldsymbol{z}}, V_{\boldsymbol{z}}^{-1}, U_{\mathfrak{P}}, U_{\mathfrak{P}}^{-1}]/I_{\sigma,\mathfrak{P}},$$

where $I_{\sigma,\mathfrak{P}}$ is the submodule generated by elements of the form $U_w - U_{\sigma(w)}$ and $V_z - U_{\sigma(z)}$. The colored complex is then defined as

$$\mathit{CFL}^\infty_{UV}(\mathcal{H}, \sigma, \mathfrak{P}, \mathfrak{s}) = \mathit{CFL}^\infty_{UV,0}(\mathcal{H}, \sigma) \otimes_{\mathbb{Z}_2[U_{\boldsymbol{w}}, U_{\boldsymbol{w}}^{-1}, V_{\boldsymbol{z}}, V_{\boldsymbol{z}}^{-1}]} \mathcal{C}_{\sigma,\mathfrak{P}}.$$

Given a coloring $(\sigma, \mathfrak{P})$ of $\boldsymbol{w} \cup \boldsymbol{z}$ of a link $\mathbb{L} = (L, \boldsymbol{w}, \boldsymbol{z})$ in Y, the colored complexes $\mathit{CFL}^\infty_{UV}(Y, \mathbb{L}, \sigma, \mathfrak{P}, \mathfrak{s})$ naturally obtain a $\mathfrak{P}$–filtration by powers of the variables U_p. An element of $\mathit{CFL}^\infty_{UV}(Y, \mathbb{L}, \sigma, \mathfrak{P}, \mathfrak{s})$ is uniquely written as a sum of elements of the form $\boldsymbol{x} \cdot U_{\mathfrak{P}}^I$, and given an $I \in \mathbb{Z}^{\mathfrak{P}}$ we define $\mathcal{F}_I$ to be the $\mathbb{Z}_2[U_{\mathfrak{P}}]$–submodule generated by $\boldsymbol{x} \cdot U_{\mathfrak{P}}^J$ with $J \geq I$.

Remark 2.7 Asking that a $\mathbb{Z}_2[U_{\mathfrak{P}}]$–equivariant map

$$F \colon \mathit{CFL}^\infty_{UV}(\mathcal{H}, \sigma, \mathfrak{P}, \mathfrak{s}) \to \mathit{CFL}^\infty_{UV}(\mathcal{H}', \sigma', \mathfrak{P}, \mathfrak{s}')$$

be $\mathfrak{P}$–filtered is just asking that F can be written as

$$F(\boldsymbol{x}) = \sum_{I \geq 0} U_{\mathfrak{P}}^I \cdot H_I(\boldsymbol{x}),$$

where the maps H_I do not involve the $U_{\mathfrak{P}}$ variables. Most maps which appear in Heegaard Floer homology are $\mathfrak{P}$–filtered. The differential, the triangle maps, the quadrilateral maps, and the maps Φ_w, Φ_z and $S^{\pm}_{w,z}$ are all $\mathfrak{P}$–filtered.

Given an arbitrary coloring $(\sigma, \mathfrak{P})$ of basepoints $\boldsymbol{w} \cup \boldsymbol{z}$, we may not always be able to define submodules corresponding to relative Spin^c structures $\mathfrak{t}$. However, if no two basepoints from distinct link components are given the same color, then one can use a modification of (1) to define a $\mathfrak{P}$–filtered $\mathbb{Z}_2$–submodule $\mathit{CFL}^\infty(Y, \mathbb{L}, \sigma, \mathfrak{P}, \mathfrak{t})$. For our purposes, we just observe that in the case that $(\sigma, \mathfrak{P})$ is the trivial coloring (ie $\mathfrak{P} = \boldsymbol{w} \cup |L|$ and σ is the map sending $w \in \boldsymbol{w}$ to w and $z \in \boldsymbol{z}$ to the link component containing it), then $\mathit{CFL}^\infty_{UV}(\mathcal{H}, \sigma, \mathfrak{P}, \mathfrak{s})$ is equal to just $\mathit{CFL}^\infty_{UV}(\mathcal{H}, \mathfrak{s})$ and the maps $\pi_{\mathfrak{t}}$ and $\iota_{\mathfrak{t}}$ are still defined. The following lemma is essentially trivial, though it is useful for relating endomorphisms of $\mathit{CFL}^\infty_{UV}(Y, \mathbb{L}, \mathfrak{s})$ to endomorphisms of the subcomplexes $\mathit{CFL}^\infty(Y, \mathbb{L}, \mathfrak{t})$:

Lemma 2.8 *Suppose that $(L, \boldsymbol{w}, \boldsymbol{z})$ is a link in an integer homology sphere Y and that $(\sigma, \mathfrak{P})$ is the trivial coloring. Suppose f and g are $\mathfrak{P}$–filtered $\mathbb{Z}_2[U_{\mathfrak{P}}]$–module endomorphisms of $\mathit{CFL}^\infty_{UV}(Y, \mathbb{L}, \sigma, \mathfrak{P}, \mathfrak{s})$ such that f and g are chain homotopic via a chain homotopy which is $\mathfrak{P}$–filtered on $\mathit{CFL}^\infty_{UV}(Y, \mathbb{L}, \sigma, \mathfrak{P}, \mathfrak{s})$. Then $\pi_{\mathfrak{t}} \circ f \circ \iota_{\mathfrak{t}}$ and $\pi_{\mathfrak{t}} \circ g \circ \iota_{\mathfrak{t}}$ are $\mathbb{Z}^{|\boldsymbol{w}|} \oplus \mathbb{Z}^{|L|}$–filtered $\mathbb{Z}_2[\bar{U}_{\boldsymbol{w}}]$–chain homotopic.*

Proof First note that the filtration on $\mathit{CFL}^\infty(\mathcal{H},\mathfrak{t})$ is just the pullback under $\iota_\mathfrak{t}$ of the $\mathfrak{P}$–filtration on $\mathit{CFL}^\infty_{UV}(\mathcal{H},\sigma,\mathfrak{P},\mathfrak{s})$. If f and g are $\mathfrak{P}$–filtered chain homotopic, we have that

$$f-g=\partial H+H\partial$$

for a $\mathfrak{P}$–filtered map H. Pre- and postcomposing with the $\mathfrak{P}$–filtered maps $\iota_\mathfrak{t}$ and $\pi_\mathfrak{t}$ yields a $\mathbb{Z}^{|\boldsymbol{w}|}\oplus\mathbb{Z}^{|L|}$–filtered chain homotopy between $\pi_\mathfrak{t}\circ f\circ\iota_\mathfrak{t}$ and $\pi_\mathfrak{t}\circ g\circ\iota_\mathfrak{t}$ because $\pi_\mathfrak{t}$ and $\iota_\mathfrak{t}$ are $\mathfrak{P}$–filtered chain maps. The chain homotopy is $\mathbb{Z}_2[\bar{U}_{\boldsymbol{w}}]$–equivariant since $\iota_\mathfrak{t}$ and $\pi_\mathfrak{t}$ are $\mathbb{Z}_2[\bar{U}_{\boldsymbol{w}}]$–equivariant, as we mentioned above (recall that $\bar{U}_w=U_wV_z$, where z is any base point on the link component containing z). □

2.5 Why we use the larger $\mathit{CFL}^\infty_{UV}(Y,L,\mathfrak{s})$ instead of other versions

We briefly explain why we use the object $\mathit{CFL}^\infty_{UV}(Y,\mathbb{L},\mathfrak{s})$ to prove formulas for basepoint moving maps, instead of other versions of link Floer homology. In the next sections, we will define maps Φ_w and Ψ_z, which are endomorphisms of $\mathit{CFL}^\infty_{UV}(Y,\mathbb{L},\mathfrak{s})$. However, due to the extra factors of U_w^{-1} or V_z^{-1} in the definitions, these do not preserve $\mathit{CFL}^\infty(Y,\mathbb{L},\mathfrak{t})$ for a relative Spin^c structure. Instead they change the relative Spin^c structure by $\pm\,\mathrm{PD}[\mu]$, where μ is the meridian of the component containing w and z (note, however, that the composition $\Phi_w\Psi_z$ does actually preserve relative Spin^c structure). Although this is not insurmountable, what's worse is that the maps $S^+_{w,z}$ and $S^-_{w,z}$ are not even endomorphisms of the same complex, and since $S^+_{w,z}S^-_{w,z}\simeq\Phi_w$, we know that they can't preserve relative Spin^c structures. Similarly, one could try to use the version of link Floer homology described in [10] as a $\mathrm{Spin}^c(Y,L)$–filtration on $\mathit{CF}^\infty(Y)$, but we have the same problem since the map Φ_w is not $\mathrm{Spin}^c(Y,L)$–filtered.

The solution is clearly to work with the larger complexes $\mathit{CFL}^\infty_{UV}(Y,\mathbb{L},\mathfrak{s})$.

There are also other algebraic advantages to working with $\mathit{CFL}^\infty_{UV}(Y,\mathbb{L},\mathfrak{s})$. For instance, we can think of Φ_w and Ψ_z as formal derivatives of the differential. Using our expression for ∂^2, we can quickly derive many relations between various Φ_w and Ψ_z maps.

3 The maps Φ_w and Ψ_z

We now define maps Φ_w and Ψ_z, which are endomorphisms of $\mathit{CFL}^\infty_{UV}(Y,\mathbb{L},\sigma,\mathfrak{P},\mathfrak{s})$. These are denoted by $\Phi_{i,j}$ and $\Psi_{i,j}$ in [13]. We define $\Phi_w:\mathit{CFL}^\infty_{UV}(\mathcal{H},\sigma,\mathfrak{P},\mathfrak{s})\to\mathit{CFL}^\infty_{UV}(\mathcal{H},\sigma,\mathfrak{P},\mathfrak{s})$ by the formula

$$\Phi_w(\boldsymbol{x})=U_w^{-1}\sum_{\boldsymbol{y}\in\mathbb{T}_\alpha\cap\mathbb{T}_\beta}\sum_{\substack{\phi\in\pi_2(\boldsymbol{x},\boldsymbol{y})\\ \mu(\phi)=1}}n_w(\phi)\#\widehat{\mathcal{M}}(\phi)U_{\boldsymbol{w}}^{n_{\boldsymbol{w}}(\phi)}V_{\boldsymbol{z}}^{n_{\boldsymbol{z}}(\phi)}\cdot\boldsymbol{y},$$

which we can alternatively think of as $(d\partial/dU_w)$. Similarly we define

$$\Psi_z(\boldsymbol{x}) = V_z^{-1} \sum_{\boldsymbol{y}\in\mathbb{T}_\alpha\cap\mathbb{T}_\beta} \sum_{\substack{\phi\in\pi_2(\boldsymbol{x},\boldsymbol{y})\\ \mu(\phi)=1}} n_z(\phi)\#\widehat{\mathcal{M}}(\phi) U_{\boldsymbol{w}}^{n_{\boldsymbol{w}}(\phi)} V_{\boldsymbol{z}}^{n_{\boldsymbol{z}}(\phi)} \cdot \boldsymbol{y},$$

which we can alternatively write as $(d\partial/dV_z)$, where the derivative is taken on $\mathrm{CFL}^\infty_{UV,0}$ (ie before tensoring with the module $\mathcal{L}$ and thus setting all of the V_z on a link component equal to each other).

We have the following (compare [13, Lemma 4.1]):

Lemma 3.1 *On $\mathrm{CFL}^\infty_{UV}(\mathcal{H},\mathfrak{s})$, we have $\Phi_w\partial + \partial\Phi_w = 0$. Also $\Psi_z\partial + \partial\Psi_z = U_w + U_{w'}$, where w and w' are the $\boldsymbol{w}$ basepoints adjacent to z.*

Proof One takes the derivative of $\partial\circ\partial$ with respect to either V_z or U_w, before one tensors $\mathrm{CFL}^\infty_{UV,0}$ with $\mathcal{L}$. The map ∂^2 is computed in Lemma 2.1. After tensoring with $\mathcal{L}$, one immediately arrives at the equalities described above. □

In addition, we have the following (compare [13, Theorem 4.2]):

Lemma 3.2 *The maps Φ_w and Ψ_z commute with change of diagram maps $\Phi_{\mathcal{H}_1\to\mathcal{H}_2}$ up to $\mathfrak{P}$–filtered, $\mathbb{Z}_2[U_{\mathfrak{P}}]$–chain homotopy.*

Proof Consider the complex $\mathrm{CFL}^\infty_{UV,0}$ (ie the complex before we set all of the V_z variables on each link component equal to each other). The differential doesn't square to zero, though we can still consider the maps $\Phi_{\mathcal{H}_1\to\mathcal{H}_2}$. These can be written as a composition of maps associated to changing the almost complex structure, triangle maps (corresponding to $\boldsymbol{\alpha}$– or $\boldsymbol{\beta}$–isotopies or handleslides), $(1,2)$–stabilization maps, and maps corresponding to isotoping the Heegaard surface inside of Y via an isotopy which fixes $\mathbb{L}$. We claim that the maps $\Phi_{\mathcal{H}_1\to\mathcal{H}_2}$ satisfy

$$\Phi_{\mathcal{H}_1\to\mathcal{H}_2}\partial + \partial\Phi_{\mathcal{H}_1\to\mathcal{H}_2} = 0,$$

even before tensoring with $\mathcal{L}$. The maps $\Phi_{\mathcal{H}_1\to\mathcal{H}_2}$ are defined as a composition of maps which count holomorphic triangles (handleslides or isotopy maps), holomorphic disks with dynamic almost complex structure (change of almost complex structure maps) or maps which are defined via simple, explicit formulas (stabilization and diffeomorphism). The maps which associated to $(1,2)$–stabilizations and diffeomorphisms obviously satisfy $\partial\phi + \phi\partial = 0$ before tensoring with $\mathcal{L}$. The maps induced by counting disks with dynamic almost complex structure also satisfy $\partial\phi + \phi\partial = 0$ before tensoring with ∂, since that follows from a Gromov compactness argument. Maps induced by handleslides or isotopies of the $\boldsymbol{\alpha}$–curves take the form

$$\boldsymbol{x} \mapsto F_{\boldsymbol{\alpha}'\boldsymbol{\alpha}\boldsymbol{\beta}}(\Theta \otimes \boldsymbol{x}),$$

where Θ is the top-degree generator of a complex $\mathrm{CFL}^-_{UV}(\Sigma, \boldsymbol{\alpha}', \boldsymbol{\alpha}, \boldsymbol{w}, \boldsymbol{z})$ and $F_{\boldsymbol{\alpha}'\boldsymbol{\alpha}\boldsymbol{\beta}}$ is the map which counts holomorphic triangles. For this to be a chain map before tensoring with $\mathcal{L}$, it is sufficient that $\partial\Theta = 0$ before tensoring with $\mathcal{L}$, since the triangle map

$$F_{\boldsymbol{\alpha}'\boldsymbol{\alpha}\boldsymbol{\beta}}\colon \mathrm{CFL}^-_{UV,0}(\Sigma, \boldsymbol{\alpha}', \boldsymbol{\alpha}, \boldsymbol{w}, \boldsymbol{z}) \otimes \mathrm{CFL}^\infty_{UV,0}(\Sigma, \boldsymbol{\alpha}, \boldsymbol{\beta}, \boldsymbol{w}, \boldsymbol{z}) \to \mathrm{CFL}^\infty_{UV,0}(\Sigma, \boldsymbol{\alpha}', \boldsymbol{\beta}, \boldsymbol{w}, \boldsymbol{z})$$

is a chain map by a Gromov compactness argument. We note now that the diagram $(\Sigma, \boldsymbol{\alpha}', \boldsymbol{\alpha}, \boldsymbol{w}, \boldsymbol{z})$ represents an unlink embedded in $(S^1 \times S^2)^{\# n}$ for some n, and this unlink has exactly two basepoints per link component. By the differential computation in Lemma 2.1, the complex

$$\mathrm{CFL}^-_{UV,0}(\Sigma, \boldsymbol{\alpha}', \boldsymbol{\alpha}, \boldsymbol{w}, \boldsymbol{z})$$

is a chain complex before tensoring with anything, and in particular the homology group $\mathrm{HFL}^-_{UV,0}(\Sigma, \boldsymbol{\alpha}', \boldsymbol{\alpha}, \boldsymbol{w}, \boldsymbol{z})$, is well defined even before tensoring with anything. An easy computation shows that if $\mathrm{HFL}^-_{UV,0,\max}$ denotes the subset of maximal homological grading (here the homological grading is obtained by ignoring the $\boldsymbol{z}$–basepoints, and assigning U variables degree -2, and V variables degree 0), then we have an isomorphism

$$\mathrm{HFL}^-_{UV,0,\max}(\Sigma, \boldsymbol{\alpha}', \boldsymbol{\alpha}, \boldsymbol{w}, \boldsymbol{z}) \cong \mathbb{Z}_2[V_{\boldsymbol{z}}],$$

and in particular $\mathrm{HFL}^-_{UV,0}(\Sigma, \boldsymbol{\alpha}', \boldsymbol{\alpha}, \boldsymbol{w}, \boldsymbol{z})$ admits a "generator" Θ which is distinguished by the property of generating the maximally graded subset as a $\mathbb{Z}_2[V_{\boldsymbol{z}}]$–module. In particular, $\partial\Theta = 0$ even before tensoring with $\mathcal{L}$, as we needed.

Hence

$$\Phi_{\mathcal{H}_1 \to \mathcal{H}_2}\partial + \partial\Phi_{\mathcal{H}_1 \to \mathcal{H}_2} = 0,$$

even before tensoring with $\mathcal{L}$. Differentiating with respect to U_w yields that

$$\Phi'_{\mathcal{H}_1 \to \mathcal{H}_2}\partial + \Phi_{\mathcal{H}_1 \to \mathcal{H}_2}\Phi_w + \Phi_w\Phi_{\mathcal{H}_1 \to \mathcal{H}_2} + \partial\Phi'_{\mathcal{H}_1 \to \mathcal{H}_2} = 0,$$

immediately implying that $\Phi_{\mathcal{H}_1 \to \mathcal{H}_2}\Phi_w + \Phi_w\Phi_{\mathcal{H}_1 \to \mathcal{H}_2} \simeq 0$. The only point to check is that the chain homotopy $H = \Phi'_{\mathcal{H}_1 \to \mathcal{H}_2}$ is $\mathfrak{P}$–filtered and $\mathbb{Z}_2[U_{\mathfrak{P}}]$–equivariant. The equivariance condition is trivial. The filtration condition is also easy to check, since whenever F has a decomposition with only nonnegative powers of U_w and V_z, the map (dF/dU_w) also has a decomposition with nonnegative powers of U_w and V_z. $\square$

Remark 3.3 Using the Leibniz rule, we have that

$$\Phi_w = \frac{d}{dU_w} \circ \partial + \partial \circ \frac{d}{dU_w},$$

as long as U_w doesn't share the same color as any other basepoint. Similarly $\Psi_z \simeq 0$ if z doesn't share the same color with any other basepoint, though in both cases the chain homotopy $H = d/dU_w$ or $H = d/dV_z$ is neither $\mathfrak{P}$–filtered nor $\mathbb{Z}_2[U_{\mathfrak{P}}]$–equivariant.

4 Cylindrical boundary degenerations

We consider holomorphic curves whose boundary is mapped to only the $\boldsymbol{\alpha}$–curves, or only the $\boldsymbol{\beta}$ curves. These will be called *cylindrical $\boldsymbol{\alpha}$–boundary degenerations* or *cylindrical $\boldsymbol{\beta}$–boundary degenerations*.

We now define cylindrical $\boldsymbol{\alpha}$–boundary degenerations. Suppose that S is a Riemann surface with d punctures $\{p_1, \dots, p_d\}$ on its boundary. We consider holomorphic maps

$$u\colon S \to \Sigma \times (-\infty, 1] \times \mathbb{R}$$

such that the following hold:

(1) u is smooth;

(2) $u(\partial S) \subseteq (\boldsymbol{\alpha} \times \{1\} \times \mathbb{R})$;

(3) $\pi_{\mathbb{D}} \circ u$ is nonconstant on each component of S;

(4) $u^{-1}(\alpha_i \times \{1\} \times \mathbb{R})$ consists of exactly one component of $\partial S \setminus \{p_1, \dots, p_d\}$, for each i;

(5) the energy of u is finite;

(6) u is an embedding;

(7) if $z_i \in S$ is a sequence of points approaching a puncture p_j, then $(\pi_{\mathbb{D}} \circ u)(z_i)$ approaches -1 in the compactification of $(-\infty, 1] \times \mathbb{R}$ as the unit complex disk (with the point at ∞ identified with -1).

We organize such curves into moduli spaces $\mathcal{N}(\phi)$ for $\phi \in \pi_2^{\alpha}(\boldsymbol{x})$, modding out by automorphisms of the source, as usual. There is an action of $\mathrm{PSL}_2(\mathbb{R})$ on $\mathcal{N}(\phi)$, which is just the action on the $(-\infty, 1] \times \mathbb{R}$ coordinate of a disk u, and we denote the quotient space $\widehat{\mathcal{N}}(\phi)$. One defines cylindrical $\boldsymbol{\beta}$–boundary degenerations analogously. We now discuss transversality. In the original setup (singly pointed diagrams and disks mapped into $\mathrm{Sym}^g(\Sigma)$), a generic almost complex structure J on $\mathrm{Sym}^g(\Sigma)$ in a neighborhood of $\mathrm{Sym}^g(\mathrm{j})$ achieves transversality for Maslov index 2 holomorphic $\boldsymbol{\alpha}$–degenerate disks [9, Proposition 3.14]. In the cylindrical setup, if a sequence of holomorphic strips for the almost complex structures considered in [5] has a cylindrical boundary degeneration in its limit, the boundary degeneration will be $j_\Sigma \times j_\mathbb{D}$–holomorphic. Thus we need transversality for cylindrical boundary degenerations for split almost complex structures. For the standard proof that $\partial^2 = 0$ and for the purposes of this paper, we only need transversality for Maslov index 2 boundary degenerations. Each of these domains has multiplicity 1 in one component of $\Sigma \setminus \boldsymbol{\alpha}$, and zero everywhere else. If $u\colon S \to \Sigma \times (-\infty, 1] \times \mathbb{R}$ is a component of a holomorphic curve representing an element of $\mathcal{N}(\phi)$ for a $\phi \in \pi_2^\alpha(\boldsymbol{x})$ such that $\pi_\Sigma \circ u$ is nonconstant, then by easy complex analysis $u|_C$ is injective, where $C \subseteq \partial S$ is the part of S mapping to $\partial \mathcal{D}(\phi)$. Adapting the strategy of perturbing boundary conditions instead of almost complex structures, as in [5, Proposition 3.9], [9, Proposition 3.9] or [7], for generic choice of $\boldsymbol{\alpha}$–curves, we can thus achieve transversality for Maslov index 2 cylindrical boundary degenerations.

An important result for our purposes is a count of Maslov index 2 boundary degenerations produced by Ozsváth and Szabó:

Theorem 4.1 [10, Theorem 5.5] *Consider a surface Σ of genus g equipped with a set of attaching circles $\boldsymbol{\alpha} = \{\alpha_1, \dots, \alpha_{g+\ell-1}\}$ which span a g–dimensional lattice in $H_1(\Sigma;\mathbb{Z})$. If $\mathcal{D}(\phi) \geq 0$ and $\mu(\phi) = 2$, then $\mathcal{D}(\phi) = A_i$ for some i, and indeed*

$$\#\widehat{\mathcal{N}}(\phi) = \begin{cases} 0 \pmod 2 & \text{if } \ell = 1, \\ 1 \pmod 2 & \text{if } \ell > 1. \end{cases}$$

Here A_i denotes a component of $\Sigma \setminus \boldsymbol{\alpha}$.

5 Preliminaries on the quasistabilization operation

Suppose that $\mathbb{L} = (L, \boldsymbol{w}, \boldsymbol{z})$ is an oriented link in Y and that w and z are two points, both in a single component of $L \setminus (\boldsymbol{w} \cup \boldsymbol{z})$, such that $(L, \boldsymbol{w} \cup \{w\}, \boldsymbol{z} \cup \{z\})$ has basepoints which alternate between $\boldsymbol{w}$ and $\boldsymbol{z}$ as one traverses the link. We assume that the point w comes after z according to the orientation of L. In Section 7 we prove invariance for quasistabilization maps

$$S^+_{w,z}\colon \mathrm{CFL}^\infty_{UV}(Y, L, \boldsymbol{w}, \boldsymbol{z}, \sigma, \mathfrak{P}, \mathfrak{s}) \to \mathrm{CFL}^\infty_{UV}(Y, L, \boldsymbol{w} \cup \{w\}, \boldsymbol{z} \cup \{z\}, \sigma', \mathfrak{P}, \mathfrak{s})$$

and

$$S^-_{w,z}\colon \mathrm{CFL}^\infty_{UV}(Y, L, \boldsymbol{w} \cup \{w\}, \boldsymbol{z} \cup \{z\}, \sigma', \mathfrak{P}, \mathfrak{s}) \to \mathrm{CFL}^\infty_{UV}(Y, L, \boldsymbol{w}, \boldsymbol{z}, \sigma, \mathfrak{P}, \mathfrak{s}),$$

which are defined up to $\mathfrak{P}$–filtered $\mathbb{Z}_2[U_\mathfrak{P}]$–chain homotopy. Here σ' is a coloring which extends σ.

Though it will take several sections to construct the maps and prove they are well defined, we now summarize that the maps will be defined by the formulas

$$S^+_{w,z}(\boldsymbol{x}) = \boldsymbol{x} \times \theta^+$$

and

$$S^-_{w,z}(\boldsymbol{x} \times \theta^+) = 0, \quad S^-_{w,z}(\boldsymbol{x} \times \theta^-) = \boldsymbol{x},$$

for suitable choices of Heegaard diagrams and almost complex structures.

To define the quasistabilization map, we use the special connected sum operation from [6]. There, Manolescu and Ozsváth describe a way of adding new w and z basepoints to Heegaard multidiagrams. They prove that for multidiagrams with at least three sets of attaching curves (eg Heegaard triples or quadruples), there is an identification of certain moduli spaces of holomorphic curves on the unstabilized diagram and certain moduli spaces of holomorphic curves on the stabilized diagram. They conjecture an analogous result for the holomorphic curves on a Heegaard diagram with two sets of attaching curves (ie for the differentials of quasistabilized diagrams), but only prove the result for grid diagrams using somewhat ad hoc techniques, since in general they run into transversality issues. We will soon prove Proposition 5.3, computing the differential on quasistabilized diagrams for appropriate almost complex structures, showing how to avoid any transversality issues and using no more gluing technology than is used in showing that $\partial^2 = 0$ on multipointed diagrams.

5.1 Topological preliminaries on quasistabilization

Suppose that $\mathcal{H} = (\Sigma, \boldsymbol{\alpha}, \boldsymbol{\beta}, \boldsymbol{w}, \boldsymbol{z})$ is a diagram for $(Y, L, \boldsymbol{w}, \boldsymbol{z})$. Given new basepoints w, z in the same component of $L \setminus (\boldsymbol{w} \cup \boldsymbol{z})$, such that w occurs after z, we now describe a new diagram $\bar{\mathcal{H}}_{p,\alpha_s}$, which depends on a choice of point $p \in \Sigma$ and curve $\alpha_s \subseteq \Sigma \setminus \boldsymbol{\alpha}$ which passes through the point p. For fixed α_s and p, the diagram $\bar{\mathcal{H}}_{p,\alpha_s}$ will be defined up to an isotopy of Y which fixes $\boldsymbol{w} \cup \boldsymbol{z} \cup \{w, z\}$ and maps L to L.

Given a diagram $\mathcal{H} = (\Sigma, \boldsymbol{\alpha}, \boldsymbol{\beta}, \boldsymbol{w}, \boldsymbol{z})$ as above, let A denote the component of $\Sigma \setminus \boldsymbol{\alpha}$ which contains the basepoints adjacent to w and z on L. Let $p \in A \setminus (\boldsymbol{\alpha} \cup \boldsymbol{\beta} \cup \boldsymbol{w} \cup \boldsymbol{z})$ be a point. If U_α denotes the handlebody component of $Y \setminus \Sigma$ such that the $\boldsymbol{\alpha}$–curves bound compressing disks in U_α, then there is a path λ in U_α from p to a point on L between w and z. Such a curve λ is specified up to an isotopy fixing $\boldsymbol{w} \cup \boldsymbol{z} \cup \{w, z\}$ which maps L to L by requiring that λ be isotopic in $\bar{U}_\alpha$ to a segment of L concatenated with an embedded arc on $\Sigma \setminus \boldsymbol{\alpha}$.

Let $N(\lambda)$ denote a regular neighborhood of λ inside of U_α such that $\partial N(\lambda)$, the boundary of $N(\lambda)$ inside of U_α, satisfies

$$\partial N(\lambda) \cap L = \{w, z\}.$$

Topologically $\partial N(\lambda)$ is just a disk, which we denote by D_1. Also let D_2 denote $N(\lambda)\cap\Sigma$, which we note is also a disk. We can assume that $D_2\cap(\boldsymbol{\alpha}\cup\boldsymbol{\beta}\cup\boldsymbol{w}\cup\boldsymbol{z})=\varnothing$. Define

$$\overline{\Sigma}_p=(\Sigma\setminus D_2)\cup D_1.$$

The surface $\overline{\Sigma}_p$ is specified up to an isotopy which fixes $(\boldsymbol{\alpha}\cup\boldsymbol{\beta}\cup\boldsymbol{w}\cup\boldsymbol{z})$. Figure 1 shows the situation schematically.

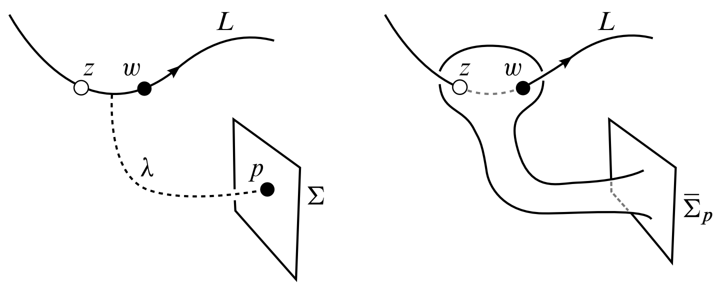

Figure 1: The path λ and the surfaces Σ and $\overline{\Sigma}_p$

We wish to extend the arc $\alpha_s\setminus D_2$ over all of D_1 to get a curve $\overline{\alpha}_s$ on $\overline{\Sigma}_p$. As is demonstrated in Figure 2, there is not an isotopically unique way to do this relative to the new basepoints w and z.

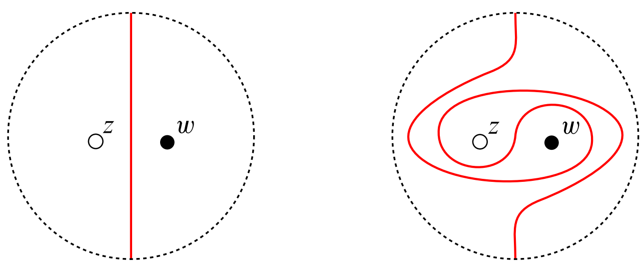

Figure 2: Different choices of $\overline{\alpha}_s$ curve on D_1 interpolating $\alpha_s\setminus D_2$. There is a unique isotopy class of such curves such that the resulting $\overline{\alpha}_s$ curve on $\overline{\Sigma}_p$ bounds a compressing disk which doesn't intersect L.

The set of such curves is easily seen to consist of those generated by the images of the curve on the left in Figure 2 under finger moves of w around z. Fortunately, the arc $\alpha_s\setminus D_2$ can be extended over D_1 uniquely (up to isotopy) by requiring the resulting curve $\overline{\alpha}_s\subseteq\overline{\Sigma}_p$ to bound a compressing disk in $U_{\overline{\alpha}}$ which doesn't intersect L, where here $U_{\overline{\alpha}}$ denotes the component of $Y\setminus\overline{\Sigma}_p$ in which the $\boldsymbol{\alpha}$–curves bound compressing disks.

Suppose $\mathcal{H}=(\Sigma,\boldsymbol{\alpha},\boldsymbol{\beta},\boldsymbol{w},\boldsymbol{z})$ is a diagram, and $p\in\Sigma\setminus\boldsymbol{\alpha}$ is a chosen point, and let $N(p_0)$ denote a neighborhood of the connected sum point p_0 on S^2, which intersects α_0 in an arc and doesn't intersect β_0. Given a diffeomorphism $\psi\colon \Sigma \to \overline{\Sigma}_p$ which is the identity outside of D_2 and an embedding $\iota\colon S^2 \setminus N(p_0) \to D_1$ which sends $\alpha_0 \setminus N(p_0)$ to $\overline{\alpha}_s$, we can form a diagram

$$\overline{\mathcal{H}}_{p,\alpha_s} = (\overline{\Sigma}_p, \overline{\boldsymbol{\alpha}}, \overline{\boldsymbol{\beta}}, \boldsymbol{w} \cup \{w\}, \boldsymbol{z} \cup \{z\}),$$

where $\overline{\boldsymbol{\alpha}} = \boldsymbol{\alpha} \cup \{\overline{\alpha}_s\}$ and $\overline{\boldsymbol{\beta}} = \boldsymbol{\beta} \cup \{\iota(\beta_0)\}$. Such a choice of ψ and ι will be part of a larger collection of data $\mathcal{J}$ which we will consider in the next section and will call "gluing data". If we need to emphasize the distinction, we will write $\overline{\boldsymbol{\alpha}}$ for $\boldsymbol{\alpha} \cup \{\overline{\alpha}_s\}$, the curves on $\overline{\Sigma}_p$, and we will write $\boldsymbol{\alpha}^+$ for $\boldsymbol{\alpha} \cup \{\alpha_s\}$, the curves on Σ. By abuse of notation, we will often write α_s to denote both $\alpha_s \subseteq \Sigma$ and $\overline{\alpha}_s \subseteq \overline{\Sigma}_p$. Similarly, when no confusion will arise, we will write β_0 for both the curve β_0 on S^2 and the curve $\iota(\beta_0)$ on $\overline{\Sigma}_p$.

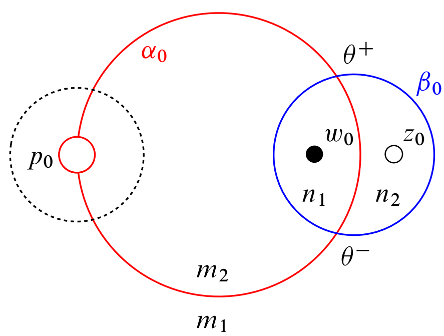

Figure 3: The diagram $\mathcal{H}_0$ used for quasistabilization, with multiplicities labeled. The dashed circle denotes where we will perform the neck stretching in the special connected sum.

5.2 Gluing data and almost complex structures

In [14] the author describes a systematic way of constructing and proving invariance of maps corresponding to adding or removing a basepoint from a closed 3–manifold. A key ingredient was a choice of auxiliary data which we call "gluing data" for patching two almost complex structures together in a systematic way. Here we introduce the analogous idea for quasistabilization.

Suppose that $\mathcal{H} = (\Sigma, \boldsymbol{\alpha}, \boldsymbol{\beta}, \boldsymbol{w}, \boldsymbol{z})$ is a diagram for $\mathbb{L} = (L, \boldsymbol{w}, \boldsymbol{z})$ and w, z are two new consecutive basepoints on L with z following w. Suppose $p \in A \setminus (\boldsymbol{w} \cup \boldsymbol{z} \cup \boldsymbol{\alpha} \cup \boldsymbol{\beta})$ is a distinguished point, where here A denotes the component of $\Sigma \setminus \boldsymbol{\alpha}$ containing the basepoints on L adjacent to w and z. Let $\overline{\Sigma}_p$ denote the Heegaard surface described in the previous subsection.

Definition 5.1 We define *gluing data* to be a collection

$$\mathcal{J} = (\psi, J_s, J_{s,0}, B, B_0, r, r_0, p_0, \iota, \phi),$$

where

(1) $\psi\colon \Sigma \to \overline{\Sigma}_p$ is a diffeomorphism which is fixed outside of D_2 and maps α_s to $\overline{\alpha}_s$;

(2) $B \subseteq \Sigma$ is a closed ball containing p which doesn't intersect $(\boldsymbol{w} \cup \boldsymbol{z} \cup \boldsymbol{\alpha} \cup \boldsymbol{\beta})$ and such that $\alpha_s \cap B$ is a closed arc;

(3) the point $p_0 \in \alpha_0 \setminus \beta_0$ is the connected sum point;

(4) $B_0 \subseteq S^2$ is a closed ball containing p_0 which doesn't intersect β_0 and such that $B_0 \cap \alpha_0$ is a closed arc;

(5) J_s is an almost complex structure on $\Sigma \times [0,1] \times \mathbb{R}$ which is split on B;

(6) $J_{s,0}$ is an almost complex structure on $S^2 \times [0,1] \times \mathbb{R}$ which is split on B_0;

(7) r and r_0 are real numbers such that $0 < r, r_0 < 1$;

(8) using the unique (up to rotation) conformal identifications of (B, p) and (B_0, p_0) as $(\mathbb{D}, 0)$, where $\mathbb{D}$ denotes the unit complex disk, ι is an embedding of $S^2 \setminus r_0 \cdot B_0$ into $r \cdot B \subseteq \Sigma$ such that

$$\iota(\alpha_0) \subseteq \alpha_s, \quad (\psi \circ \iota)(z_0) = z, \quad (\psi \circ \iota)(w_0) = w,$$

and

$$(r \cdot B) \setminus \iota(S^2 \setminus r_0 \cdot B_0)$$

is a closed annulus;

(9) letting $\widetilde{A}$, A and A_0 denote the closures of the annuli $B \setminus \iota(S^2 \setminus B_0)$, $B \setminus r \cdot B$ and $B_0 \setminus r_0 \cdot B_0$, respectively,

$$\phi\colon \widetilde{A} \to S^1 \times [-a, 1+b]$$

is a diffeomorphism which sends the annulus A to $[-a, 0]$ and $\iota(A_0)$ to $[1, 1+b]$ and is conformal on A and A_0.

The space of embeddings ι is connected since if a denotes the arc on the left side of Figure 2, the space of diffeomorphisms $f\colon B \to B$ mapping $\partial B \cup a$ to itself and fixing $\{z, w\}$ is connected. That the space of diffeomorphisms $\psi\colon \Sigma \to \overline{\Sigma}_p$ in the definition is also connected follows for similar reasons.

Gluing data $\mathcal{J}$ and a choice of neck length T determines an almost complex structure $\mathcal{J}(T)$ on $\overline{\Sigma}_p \times [0,1] \times \mathbb{R}$.

5.3 Computing the quasistabilized differential

We now wish to compute the differential after performing quasistabilization. We have the following Maslov index computation:

Lemma 5.2 *If ϕ_0 is a homology class of disks on $\mathcal{H}_0$, then using the multiplicities in Figure 3, we have*

$$\mu(\phi_0) = (n_1 + n_2 + m_1 + m_2)(\phi_0).$$

Proof The formula is easily verified for the constant disk and respects splicing in any of the Maslov index 1 strips. □

Let $\mathcal{J}$ denote gluing data as in the previous section, and let $\mathcal{J}(T)$ denote the almost complex structure on $\bar{\mathcal{H}}_{p,\alpha_s}$ determined by $\mathcal{J}$ for a choice of neck length T. We have the following:

Proposition 5.3 *Suppose that $\mathcal{H}$ is a strongly $\mathfrak{s}$–admissible diagram and that $\mathcal{J}$ is gluing data with almost complex structure J_s on $\Sigma \times [0,1] \times \mathbb{R}$. Then $\bar{\mathcal{H}}_{p,\alpha_s}$ is also strongly $\mathfrak{s}$–admissible and for sufficiently large T there is an identification of uncolored differentials (ie before we tensor with $\mathcal{L}$)*

$$\partial_{\bar{\mathcal{H}}_{p,\alpha_s},\mathcal{J}(T)} = \begin{pmatrix} \partial_{\mathcal{H},J_s} & U_w + U_{w'} \\ V_z + V_{z'} & \partial_{\mathcal{H},J_s} \end{pmatrix},$$

where the basepoints w and z are placed between w' and z' on $\mathbb{L}$.

Proof Suppose that u_i is a sequence of Maslov index 1 holomorphic curves on $\bar{\mathcal{H}}_{p,\alpha_s}$ in a fixed homology class for the almost complex structure $\mathcal{J}(T_i)$ for a sequence of T_i with $T_i \to \infty$. From the sequence u_i we can extract a weak limit of curves on the diagrams $(\Sigma, \boldsymbol{\alpha}^+, \boldsymbol{\beta}, \boldsymbol{w}, \boldsymbol{z})$ and $\mathcal{H}_0$. Let U_Σ, and U_0 denote these collections of curves. The curves in U_Σ consist of flowlines on $(\Sigma, \boldsymbol{\alpha}^+, \boldsymbol{\beta}, \boldsymbol{w}, \boldsymbol{z})$ as well as $\boldsymbol{\alpha}$– and $\boldsymbol{\beta}$–boundary degenerations on $(\Sigma, \boldsymbol{\alpha}^+)$ and $(\Sigma, \boldsymbol{\beta})$, and closed surfaces mapped into Σ. The holomorphic curves are now allowed to have a puncture along the α–boundary which is mapped asymptotically to p.

We first note that any flowline in the limit (ie a map $u\colon S \to \Sigma \times [0,1] \times \mathbb{R}$ which maps ∂S to $(\boldsymbol{\beta} \times \{0\} \cup \boldsymbol{\alpha}^+ \times \{1\} \times \mathbb{R}$ such that each component of S has both $\boldsymbol{\alpha}^+$ and $\boldsymbol{\beta}$ components) on the diagram $\mathcal{H}^+ = (\Sigma, \boldsymbol{\alpha}^+, \boldsymbol{\beta}, \boldsymbol{w}, \boldsymbol{z})$ must actually be a legitimate flow line on $(\Sigma, \boldsymbol{\alpha}, \boldsymbol{\beta}, \boldsymbol{w}, \boldsymbol{z})$. This is because if u is any holomorphic curve which is part of a weak limit of the curves u_{T_i}, then u cannot have a puncture asymptotic to an intersection point $\alpha_s \cap \beta_j$ for $\beta_j \in \boldsymbol{\beta}$. Hence if u is part of the weak limit of u_i, and if S denotes the source of u, then if ∂S has any points mapped to α_s, then S must have boundary component with a single puncture which is mapped to α_s. Projecting to $[0,1]\times\mathbb{R}$, we note that either $u|_{\partial S}$ attains a local extremum, or u is asymptotic to both $+\infty$ and $-\infty$ as one approaches the puncture. If $u|_{\partial S}$ attains a local extremum, then one can use the doubling trick to create an analytic function mapping $\mathbb{D}$ into $\mathbb{D}$ (where here $\mathbb{D}=\{z:|z|<1\}$) which maps $\mathbb{D}\cap\{\mathrm{im}(z)\geq 0\}$ to $\mathbb{D}\cap\{\mathrm{im}(z)\geq 0\}$ but which satisfies $f'(z)=0$ for some $z\in\mathbb{R}$, which is impossible by writing down a local model. The case that u is asymptotic to both $+\infty$ and $-\infty$ at the puncture is impossible since u must extend to a continuous function over the punctures. Hence any such u must be constant in the $[0,1]\times\mathbb{R}$ component, which implies that u cannot have any portion of ∂S mapped onto a $\boldsymbol{\beta}$–curve. Hence the curves in the weak limit can be taken to be holomorphic disks on $(\Sigma,\boldsymbol{\alpha},\boldsymbol{\beta},\boldsymbol{w},\boldsymbol{z})$, $\boldsymbol{\alpha}^+$– or $\boldsymbol{\beta}$–degenerations, or closed surfaces.

Though not essential for our argument, to avoid "annoying" curves (ie maps into $\Sigma\times[0,1]\times\mathbb{R}$ which are constant in the $[0,1]\times\mathbb{R}$–component) among the $\boldsymbol{\beta}$– or $\boldsymbol{\alpha}^+$–degenerations, we observe that by rescaling the $[0,1]\times\mathbb{R}$ component, we could instead get curves that map into $\Sigma\times(-\infty,1]\times\mathbb{R}$ or $\Sigma\times S^2$ such that the $(-\infty,1]\times\mathbb{R}$ or S^2 components are nonconstant. Maps into $\Sigma\times(-\infty,1]\times\mathbb{R}$ are cylindrical $\boldsymbol{\alpha}^+$–boundary degenerations.

We now wish to compute exactly which of the above degenerations can occur in a weak limit of the sequence u_i of Maslov index 1 $\mathcal{J}(T_i)$–holomorphic curves. Assume without loss of generality that all of the u_i are in the same homology class ϕ.

Suppose that U_Σ consists of a collection U'_Σ of curves on $(\Sigma,\boldsymbol{\alpha},\boldsymbol{\beta})$ (flowlines, boundary degenerations, closed surfaces) and a collection of curves $\mathcal{A}$ in $(\Sigma,\boldsymbol{\alpha}^+,\boldsymbol{\beta})$ which have a boundary component which maps to α_s. As we've already remarked, the collection $\mathcal{A}$ consists exactly of cylindrical $\boldsymbol{\alpha}^+$–boundary degenerations. Letting ϕ'_Σ denote the underlying homology class of U'_Σ, we define a combinatorial Maslov index for U_Σ by

$$\mu(U_\Sigma)=\mu(\phi'_\Sigma)+m_1(\mathcal{A})+m_2(\mathcal{A})+2\sum_{\substack{\mathcal{D}\in C(\Sigma\setminus\boldsymbol{\alpha}),\\ \alpha_s\cap\mathcal{D}=\varnothing}} n_{\mathcal{D}}(\mathcal{A}),$$

where $C(\Sigma\setminus\boldsymbol{\alpha})$ denotes the connected components of $\Sigma\setminus\boldsymbol{\alpha}$. By Lemma 5.2 the Maslov index of U_0 satisfies

$$\mu(U_0)=m_1(\phi)+m_2(\phi)+n_1(\phi)+n_2(\phi).$$

The formula for $\mu(U_\Sigma)$ does not necessarily count the expected dimension of anything since we've only defined it combinatorially, though we can compute the Maslov index

$\mu(\phi)$ using these formulas, as follows:

$$\begin{aligned}(2)\qquad \mu(\phi) &= \mu(U_\Sigma)+\mu(U_0)-m_1(\phi)-m_2(\phi)\\ &= \mu(\phi'_\Sigma)+n_1(\phi)+n_2(\phi)+m_1(\mathcal{A})+m_2(\mathcal{A})+2\sum_{\substack{\mathcal{D}\in C(\Sigma\setminus\boldsymbol{\alpha})\\ \alpha_s\cap\mathcal{D}=\varnothing}} n_{\mathcal{D}}(\mathcal{A}).\end{aligned}$$

Each term in this sum is nonnegative, and by assumption the total sum is equal to 1. If $\mu(\phi)=1$, we immediately have that $n_{\mathcal{D}}(\mathcal{A})=0$ for $\mathcal{D}\in C(\Sigma\setminus\boldsymbol{\alpha})$, with $\alpha_s\cap\mathcal{D}=\varnothing$. Now $\mu(\phi'_\Sigma)$ does actually count the expected dimension of the moduli space of ϕ'_Σ, and in particular if ϕ'_Σ has a representative as a broken curve, we must have $\mu(\phi'_\Sigma)\ge 0$ with equality if and only if ϕ'_Σ is the constant disk.

As a consequence we see that if $\mu(\phi)=1$, we have that exactly one of $\mu(\phi'_\Sigma)$, $n_1(\phi)$, $n_2(\phi)$, $m_1(\mathcal{A})$ or $m_2(\mathcal{A})$ is equal to 1, and the rest are zero. The cases where $n_1(\phi)=1$ or $n_2(\phi)=1$ are easy to analyze, and those possibilities contribute summands of

$$\begin{pmatrix}0 & U_w\\ 0 & 0\end{pmatrix}\quad\text{and}\quad\begin{pmatrix}0 & 0\\ V_z & 0\end{pmatrix},$$

respectively, to $\partial_{\bar{\mathcal{H}}_{p,\alpha_s}}$.

We now consider broken curves in the limit with $\mu(\phi'_\Sigma)=1$ and the remaining terms zero. In this case we have that $m_1(\mathcal{A})=m_2(\mathcal{A})=0$ (so $\mathcal{A}=0$) and $n_1(\phi)=n_2(\phi)=0$. In this case, we observe that ϕ'_Σ is represented by U_Σ and $\mu(\phi'_\Sigma)=1$, so the limit cannot contain any boundary degenerations or closed surfaces. Furthermore, by Maslov index considerations we have that U_Σ consists of a single Maslov index 1 flowline, which we denote by u_Σ.

We now consider the curves in U_0. There must be a component of U_0 which satisfies a matching condition with u_Σ. Note also that since U_Σ consists only of a single disk on $(\Sigma,\boldsymbol{\alpha},\boldsymbol{\beta})$, there cannot be any curves in U_0 which have a point on the boundary mapped to p_0 or have a puncture along their boundary which is asymptotic to p_0.

Let u_0 denote the component of U_0 which satisfies the matching condition

$$\rho^p(u_\Sigma)=\rho^{p_0}(u_0).$$

In particular, this forces $m_1(u_0)=m_2(u_0)$. We also have $n_1(u_0)=n_2(u_0)=0$. Here, if $u\colon S\to\Sigma\times[0,1]\times\mathbb{R}$ is a holomorphic disk, $\rho^q(u)$ is the divisor

$$(\pi_{\mathbb{D}}\circ u)(\pi_\Sigma\circ u)^{-1}(q)\in\operatorname{Sym}^{n_q(u)}(\mathbb{D}).$$

Any additional components u'_0 of U_0 must also satisfy $n_1(u'_0)=n_2(u'_0)=0$ and also can't have an interior point or boundary point mapped to p_0, and hence must be constant. Hence U_0 consists exactly of a holomorphic strip u_0 with $m_2(u_0)=m_1(u_0)$ which satisfies a matching condition with u_Σ, ie (u_Σ, u_0) are prematched strips.

We thus have shown that if $\mu(\phi'_\Sigma)=1$, then the weak limit of the curves u_i is a prematched strip, so following standard gluing arguments (see eg [5, Appendix A]), the count of $\widehat{\mathcal{M}}_{\mathcal{J}(T)}(\phi)$ is equal to the count of prematched strips with total homology class ϕ, for sufficiently large T. If ϕ_0 is a homology class of disks in $\pi_2(\theta^+,\theta^+)$ or $\pi_2(\theta^-,\theta^-)$, let $\mathcal{M}(\phi_0,\boldsymbol{d})$ denote the set of holomorphic strips u representing ϕ_0 with $\rho^{p_0}(u)=\boldsymbol{d}$. Note that there is a unique homology class of disks $\phi_0\in\pi_2(\theta^+,\theta^+)$ with $m_1(\phi_0)=m_2(\phi_0)=|\boldsymbol{d}|$ and $n_1(\phi_0)=n_2(\phi_0)=0$.

We claim that

$$\mathcal{M}(\phi_0,\boldsymbol{d})\equiv 1 \pmod 2$$

if $m_1(\phi_0)=m_2(\phi_0)=|\boldsymbol{d}|$ and $n_1(\phi_0)=n_2(\phi_0)=0$. We consider a path $\boldsymbol{d}_t$ between two divisors $\boldsymbol{d}_0$ and $\boldsymbol{d}_1$ and consider the 1–dimensional space

$$\mathcal{M}=\bigsqcup_{t\in[0,1]}\mathcal{M}(\phi_0,\boldsymbol{d}_t).$$

We count the ends of $\mathcal{M}$. There are ends corresponding to $\mathcal{M}(\phi_0,\boldsymbol{d}_0)$ and $\mathcal{M}(\phi_0,\boldsymbol{d}_1)$. On the other hand, there are ends corresponding to strip breaking or other types of degenerations. No curve in the degeneration can have p_0 in its boundary, which constrains any degeneration to be into disks of the form $\pi_2(\theta^+,\theta^+)$ or $\pi_2(\theta^-,\theta^-)$. But if any nontrivial strip breaking occurs, the Maslov index of the matching component drops, contradicting the formula for the Maslov index. Hence the only ends of $\mathcal{M}$ correspond to $\mathcal{M}(\phi_0,\boldsymbol{d}_0)$ and $\mathcal{M}(\phi_0,\boldsymbol{d}_1)$, implying that

$$\#\mathcal{M}(\phi_0,\boldsymbol{d}_0)\equiv\#\mathcal{M}(\phi_0,\boldsymbol{d}_1) \pmod 2.$$

We now consider a path of divisors $\boldsymbol{d}_T$ consisting of k points in $[0,1]\times\mathbb{R}$ spaced at least T apart which approach the line $\{0\}\times\mathbb{R}$ as $T\to\infty$. Letting $T\to\infty$, since p_0 is not on β_0, we know that the Gromov limit of the curves in $\mathcal{M}(\phi_0,\boldsymbol{d}_T)$ consists of k cylindrical β_0–degenerations, and a single constant holomorphic strip. Applying Theorem 4.1, we get that the total count of the boundary of

$$\overline{\bigsqcup_T\mathcal{M}(\phi_0,\boldsymbol{d}_T)}$$

is $\#\mathcal{M}(\phi_0,\boldsymbol{d}_1)+1$, implying the claim.

Disks which consist of preglued flowlines (u_Σ,u_0) glued together thus provide a total contribution of

$$\begin{pmatrix}\partial_{\mathcal{H},J_s} & 0\\ 0 & \partial_{\mathcal{H},J_s}\end{pmatrix}$$

to the differential.

We now consider the last contributions to the differential. These correspond to having $\mathcal{D}(\phi_1') = 0$ and $n_1 = n_2 = 0$, and $m_1(\mathcal{A}) + m_2(\mathcal{A}) = 1$. In this case $\mathcal{A}$ is an $\boldsymbol{\alpha}^+$–boundary degeneration on $(\Sigma, \boldsymbol{\alpha}^+, \boldsymbol{\beta})$. Since

$$\sum_{\substack{\mathcal{D} \in C(\Sigma \setminus \boldsymbol{\alpha}) \\ \alpha_s \cap \mathcal{D} = \varnothing}} n_{\mathcal{D}}(\mathcal{A}) = 0,$$

we have that $\mathcal{D}(\mathcal{A})$ is constrained to one of two domains. For each of the two possible domains of $\mathcal{D}(\mathcal{A})$, there is exactly one corresponding choice of domain for ϕ_0, the homology class of U_0, which is just the domain with exactly one of m_1 and m_2 equal to 1, and the other equal to zero, and n_1 and n_2 also zero.

On $\overline{\mathcal{H}}_{p,\alpha_s}$ these correspond to exactly two homology classes of disks. We now describe two strategies to count such disks. The first would be to perform a gluing argument to glue holomorphic representatives of the bigon on $\mathcal{H}_0$ to Maslov index 2 $\boldsymbol{\alpha}$–boundary degeneration on $(\Sigma, \boldsymbol{\alpha}^+)$ at punctures along their boundaries. As we remarked, one could rescale the curves so that they were genuine cylindrical $\boldsymbol{\alpha}^+$, and by perturbing the $\boldsymbol{\alpha}^+$ curves we could achieve transversality since the domains of such curves are α–injective. By a gluing argument, one could prove that the count on $\overline{\mathcal{H}}_{p,\alpha_s}$ was equal to the product of the counts for the two pieces, for a sufficiently stretched neck. Although the author isn't aware of any obstruction to do this, we will describe another approach which uses more established gluing results and a nice trick.

Let $\boldsymbol{x}$ be an intersection point on the unstabilized diagram. By our work up to now, there are two homology classes we have left to count: a disk $\phi_{z'} \in \pi_2(\boldsymbol{x} \times \theta^+, \boldsymbol{x} \times \theta^-)$ which goes over z' once, and a disk $\phi_{w'} \in \pi_2(\boldsymbol{x} \times \theta^-, \boldsymbol{x} \times \theta^+)$, which goes over w' once. To count the number of representatives of $\phi_{w'}$ and $\phi_{z'}$, we consider the ends of the moduli spaces associated to certain Maslov index 2 homology classes in $\pi_2(\boldsymbol{x} \times \theta^+, \boldsymbol{x} \times \theta^+)$. On $\overline{\mathcal{H}}_{p,\alpha_s}$, we consider the two components of $\overline{\Sigma}_p \setminus \overline{\boldsymbol{\alpha}}$ which have boundary along α_s. For an intersection point $\boldsymbol{x}$ on the unstabilized diagram, each of these two domains yields a homotopy class $\pi_2(\boldsymbol{x} \times \theta^+, \boldsymbol{x} \times \theta^+)$. Let us call these homotopy classes $A_{w'}$ and $A_{z'}$, depending on whether they go over w' or z'. Let us consider the ends of the 1–dimensional space of holomorphic disks $\widehat{\mathcal{M}}(A_{w'})$. The ends correspond to boundary degenerations and strip breaking. By our work so far, for sufficiently stretched almost complex structure, there is a single domain which can appear as the domain of a Maslov index 1 homology class with $n_1 \neq 0$ and which admits a holomorphic representative, namely the bigon going over w once. Let us call this bigon b_w. Hence if a 1-parameter family of holomorphic disks in $\widehat{\mathcal{M}}(A_{z'})$ breaks into a pair of holomorphic disks, one of them must be have domain equal to b_w. This forces the other to have domain $A_{z'} - b_w$, ie the homology class must be $\phi_{z'}$. As no other homotopy classes can appear in strip breaking, due to our degenerated almost complex structure, we conclude that

$$\#\widehat{\mathcal{N}}(A_{z'}) + \#\widehat{\mathcal{M}}(\phi_{z'})\#\widehat{\mathcal{M}}(b_w) = 0,$$

as the latter count is the number of ends of $\widehat{\mathcal{M}}(A_{z'})$. Since $\#\widehat{\mathcal{N}}(A_{z'}) = 1$ by Theorem 4.1, and the bigon certainly has a unique holomorphic representative, we conclude that $\widehat{\mathcal{M}}(\phi_{z'}) = 1 \in \mathbb{Z}_2$. By an analogous argument, we conclude that $\widehat{\mathcal{M}}(\phi_{w'}) = 1$, as well.

With the above count we see that such curves make contributions of

$$\begin{pmatrix} 0 & U_{w'} \\ 0 & 0 \end{pmatrix} \quad \text{and} \quad \begin{pmatrix} 0 & 0 \\ V_{z'} & 0 \end{pmatrix}.$$

Summing together all of the contributions, we see that the differential takes the form

$$\partial_{\overline{\mathcal{H}}_{p,\alpha_s},\mathcal{J}(T)} = \begin{pmatrix} \partial_{\mathcal{H},J_s} & U_w + U_{w'} \\ V_z + V_{z'} & \partial_{\mathcal{H},J_s} \end{pmatrix}. \qquad \square$$

Note that we tensor $\mathrm{CFL}^{\infty}_{UV,0}(\mathcal{H},\mathfrak{s})$ with $\mathcal{L}$ so that the differential squares to zero. When we do this, we set $V_z = V_{z'}$, and the bottom left entry of the differential vanishes.

Example 5.4 We now briefly give an example which helps to illustrate the technique we used to count some of the disks appearing in the off-diagonal entries of the differential. We consider a nested quasistabilization, shown in Figure 4, where we stretch along the dashed curve on the inside quasistabilization. We haven't drawn any basepoints in the figure. We've illustrated a homology class $A \in \pi_2(\boldsymbol{x} \times \theta, \boldsymbol{x} \times \theta)$ whose domain is just a component of $\Sigma \setminus (\overline{\alpha})$ and the ends of $\widehat{\mathcal{M}}(A)$. We've illustrated how the homology class can split into either pairs of Maslov index 1 disks, or a boundary degeneration. When we stretch the neck sufficiently, the weak limits argument from the previous proposition prohibits the middle pair of homology disks from both having a representative. Hence the boundary of $\widehat{\mathcal{M}}(\phi)$ consists of exactly $\widehat{\mathcal{N}}(A)$ (which has a unique representative) and $\widehat{\mathcal{M}}(b) \times \widehat{\mathcal{M}}(\phi)$, where b is a bigon and $\phi \in \pi_2(\boldsymbol{x} \times \theta, \boldsymbol{x} \times \theta')$ is one of the disks we were trying to count at the end of the previous proposition.

5.4 Dependence of quasistabilization on gluing data

In this subsection we prove some initial results about quasistabilization and change of almost complex structure maps. The reader should compare this to [14, Section 6], where the analogous arguments are presented for free stabilization.

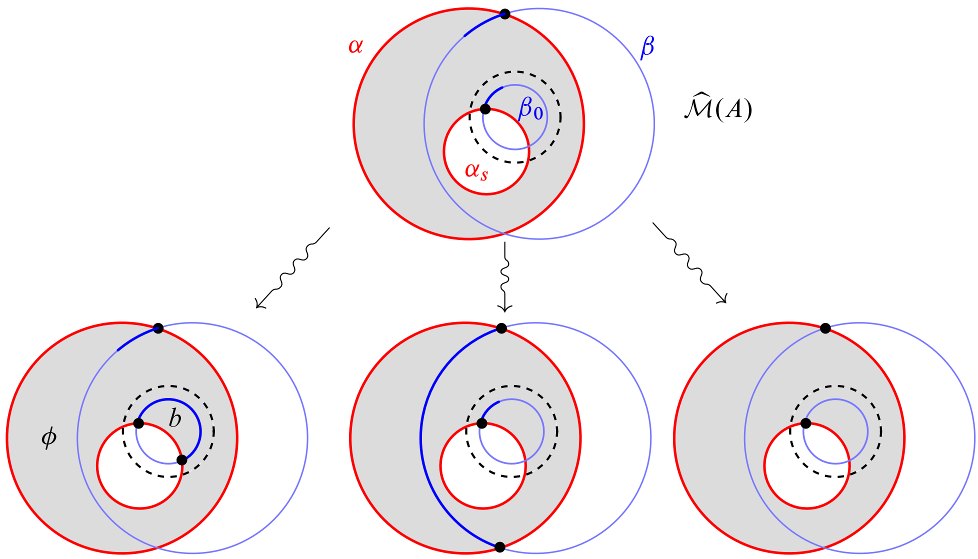

Figure 4: An example of the possible strip breaking which can occur for the homology class A. By degenerating the almost complex structure, our weak limits argument in the previous proposition rules out the middle degeneration. This allows us to count the representatives for the Maslov index 1 homology class ϕ, appearing on the left, which is otherwise hard to count.

Lemma 5.5 *Suppose that $\mathcal{J}$ is gluing data. Then there is an N such that if $T, T' > N$ and if $\mathcal{J}(T)$ and $\mathcal{J}(T')$ achieve transversality, then*

$$\Phi_{\mathcal{J}(T)\to\mathcal{J}(T')} \simeq \begin{pmatrix} 1 & 0 \\ 0 & 1 \end{pmatrix}.$$

The proof is analogous to the proof of [14, Lemma 6.8], using the techniques of Proposition 5.3. Note that in [14], the upper right entry appeared as a $*$. Due to the Maslov index computation in (2), both off-diagonal entries are forced to be zero in our case. Philosophically this is because quasistabilization is a stronger degeneration than free stabilization. As in [14], we make the following definition:

Definition 5.6 We say that N is *sufficiently large* for gluing data $\mathcal{J}$ if $\Phi_{\mathcal{J}(T)\to\mathcal{J}(T')}$ is of the form in the previous lemma for all $T, T' \geq N$. We say T is *large enough to compute $S^{\pm}_{w,z}$* for the gluing data $\mathcal{J}$ if $T > N$ for some N which is sufficiently large.

Adapting the proofs of [14, Lemmas 6.10–6.16], we have the following:

Lemma 5.7 *If $\mathcal{J}$ and $\bar{\mathcal{J}}$ are two choices of gluing data with almost complex structures J_s and $\bar{J}_s$ on $\Sigma\times[0,1]\times\mathbb{R}$, respectively, then there is an N such that if $T>N$ and if $\mathcal{J}(T)$ and $\bar{\mathcal{J}}(T)$ achieve transversality, then*

$$\Phi_{\mathcal{J}(T)\to\bar{\mathcal{J}}(T)}\simeq\begin{pmatrix}\Phi_{J_s\to\bar{J}_s} & 0\\ 0 & \Phi_{J_s\to\bar{J}_s}\end{pmatrix}.$$

The previous lemma will be used to show that the quasistabilization maps are independent of the choice of gluing data.

6 Quasistabilization and triangle maps

In this section we prove several results about quasistabilizing Heegaard triples, which we will use to prove invariance of the quasistabilization maps. The results for quasistabilization of Heegaard triples along a single α_s curve are established in [6], so we focus on quasistabilizing a Heegaard triple along two curves, α_s and β_s. To compute the quasistabilization maps $S^{\pm}_{w,z}$, we pick a curve α_s in the surface Σ, but there are many choices of such an α_s curve, so in order to address invariance of the quasistabilization maps, we need to show that the maps $S^{\pm}_{w,z}$ commute with the change of diagram map corresponding to moving α_s to α_s', which can be computed using a Heegaard triple which has been quasistabilized along two curves. Our main result is Theorem 6.5, which is an analogue of our computation of the differential after quasistabilizing in Proposition 5.3, but for certain Heegaard triples which we have quasistabilized along two curves which are allowed to travel throughout the diagram.

6.1 Quasistabilizing Heegaard triples along a single curve

We now consider Heegaard triples which are quasistabilized along a single α_s curve which is allowed to run through the diagram. This was first considered in [6]. We state a result from that paper, which considers the quasistabilized configuration shown in Figure 5. The result will be useful in showing that the quasistabilization maps are invariant under $\boldsymbol{\beta}$–handleslides and $\boldsymbol{\beta}$–isotopies.

Lemma 6.1 [6, Proposition 5.2] *Suppose that $\mathcal{T}=(\Sigma,\boldsymbol{\alpha},\boldsymbol{\beta},\boldsymbol{\gamma},\boldsymbol{w},\boldsymbol{z})$ is a strongly $\mathfrak{s}$–admissible triple and suppose that α_s is a new $\boldsymbol{\alpha}$–curve, passing through the point $p\in\Sigma$. Let $\overline{\mathcal{T}}_{\alpha_s,p}$ denote the Heegaard triple resulting from quasistabilizing along α_s at p, as in Figure 5. If $\mathcal{J}$ is gluing data, then for sufficiently large T, with the almost complex structure $\mathcal{J}(T)$ we have the following identifications:*

$$F_{\overline{\mathcal{T}}_{\alpha_s,p},\bar{\mathfrak{s}}}(\boldsymbol{x}\times\cdot,\boldsymbol{y}\times y^+)=\begin{pmatrix}F_{\mathcal{T},\mathfrak{s}}(\boldsymbol{x},\boldsymbol{y}) & 0\\ 0 & F_{\mathcal{T},\mathfrak{s}}(\boldsymbol{x},\boldsymbol{y})\end{pmatrix}$$

where $\cdot \in \{x^+, x^-\} = \alpha_s \cap \beta_0$ *and the matrix on the right denotes the expansion into the upper and lower generator components of* $\alpha_s \cap \beta_0$ *and* $\alpha_s \cap \gamma_0$*.*

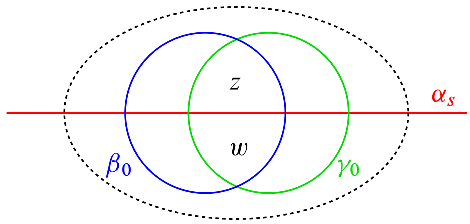

Figure 5: The version of quasistabilization discussed in Lemma 6.1

6.2 Strong positivity condition for diagrams of $(S^1 \times S^2)^{\#k}$

In this subsection we describe a class of simple diagrams for $(S^1 \times S^2)^{\#k}$ which we will use in a technical condition in Theorem 6.5 for quasistabilizing Heegaard triples along two curves, α_s and β_s, passing through a Heegaard triple.

Suppose that $(\Sigma, \boldsymbol{\alpha}, \boldsymbol{\beta}, \boldsymbol{w})$ is a diagram for $(S^1 \times S^2)^{\#k}$ such that

$$|\alpha_i \cap \beta_j| = \begin{cases} 1 \text{ or } 2 & \text{if } i = j, \\ 0 & \text{if } i \neq j \end{cases}$$

and that if $\alpha_i \cap \beta_i = \{p_i^-, p_i^+\}$, then p_i^- and p_i^+ differ by Maslov grading 1. We do not assume that the α_i curves are small isotopies of the β_j curves. Let $\theta^+ = p_1^+ \times \cdots \times p_{n-1}^+$ denote the top graded (partial) intersection point. Assume that $|\alpha_n \cap \beta_n| = 2$ and write p_n^- and p_n^+ for the two points of $\alpha_n \cap \beta_n$.

Definition 6.2 Under the same assumptions as the previous paragraph, we say that $(\Sigma, \boldsymbol{\alpha}, \boldsymbol{\beta}, \boldsymbol{w})$ is *strongly positive* with respect to p_n^+ if for every nonnegative disk $\phi \in \pi_2(\theta^+ \times p_n^+, \boldsymbol{y} \times p_n^+)$ we have that

$$(\mu - (m_1 + m_2))(\phi) = (\mu - (n_1 + n_2))(\phi) \geq 0,$$

with equality to zero if and only if ϕ is the constant disk. Here m_1, m_2, n_1, n_2 denote the multiplicities adjacent to the point p_n^+, appearing in the following counterclockwise order: n_1, m_1, n_2, then m_2.

Note that $m_1 + m_2 = n_1 + n_2$ for any disk $\phi \in \pi_2(\boldsymbol{x} \times p_n^+, \boldsymbol{y} \times p_n^+)$, by the vertex relations.

We now describe a class of diagrams which are strongly positive at an intersection point, which will be sufficient for our purposes:

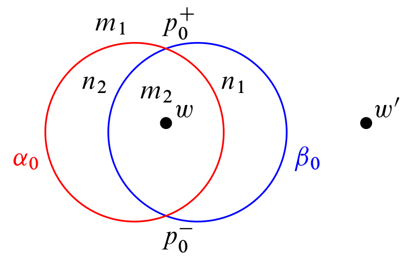

Figure 6: The diagram $\mathcal{H}_0 = (S^2, \alpha_0, \beta_0, w, w')$ in Lemma 6.3 which is strongly positive at p_0^+, and the multiplicities m_1, n_1, m_2 and n_2

Lemma 6.3 *The diagram $\mathcal{H}_0 = (S^2, \alpha_0, \beta_0, w, w')$ in Figure 6 is strongly positive with respect to p_0^+, the intersection point of α_0 and β_0 with higher relative grading. If $\mathcal{H} = (\Sigma, \boldsymbol{\alpha}, \boldsymbol{\beta}, \boldsymbol{w})$ is a diagram with a distinguished intersection point $p_n^+ \in \alpha_n \cap \beta_n$ where $|\alpha_n \cap \beta_n| = 2$, and $\mathcal{H}' = (\Sigma', \boldsymbol{\alpha}', \boldsymbol{\beta}', \boldsymbol{w}')$ is the result of any of the following moves, then $\mathcal{H}'$ is strongly positive with respect to p_n^+ if and only if $\mathcal{H}$ is strongly positive with respect to p_n^+:*

1. *$(1,2)$–stabilization[1];*
2. *taking the disjoint union of $\mathcal{H}$ with the standard diagram $(\mathbb{T}^2, \alpha_0, \beta_0, w)$ for (S^3, w);*
3. *performing surgery on an embedded 0–sphere $\{q_1, q_2\} \subseteq \Sigma \setminus (\boldsymbol{\alpha} \cup \boldsymbol{\beta})$ by removing small disks from Σ, and connecting the resulting boundary components with an annulus with new α_0 and β_0 curves with $|\alpha_0 \cap \beta_0| = 2$, and which are isotopic to each other, and homotopically nontrivial in the annulus.*

Proof We first note that $\mathcal{H}_0$ is strongly positive with respect to p_0^+, because the Maslov index of any disk is given by

$$\mu(\phi) = (m_1 + m_2 + n_1 + n_2)(\phi),$$

by Lemma 5.2, where m_1, m_2, n_1, n_2 are multiplicities appearing in the counterclockwise order m_1, n_1, m_2, n_2 around p_0^+, as in Figure 6. Hence for any disk ϕ, we have

$$(\mu - (n_1 + n_2))(\phi) = (m_1 + m_2)(\phi),$$

which is certainly nonnegative. For a disk $\phi \in \pi_2(p_0^+, p_0^+)$ we also have

$$(m_1 + m_2)(\phi) = (n_1 + n_2)(\phi),$$

so the above quantity is positive if and only if ϕ has positive multiplicities.

[1] If $\mathcal{H} = (\Sigma, \boldsymbol{\alpha}, \boldsymbol{\beta}, \boldsymbol{w})$ is a Heegaard diagram for Y, a $(1,2)$–stabilization of $\mathcal{H}$ is obtained by taking an embedded torus $\mathbb{T}^2$ inside of a 3–ball in $Y \setminus \Sigma$, together with curves α_0 and β_0 with $|\alpha_0 \cap \beta_0| = 1$, which bound compressing disks with boundary on Σ, and letting $\mathcal{H}'$ be the diagram $(\Sigma \# \mathbb{T}^2, \boldsymbol{\alpha} \cup \{\alpha_0\}, \boldsymbol{\beta} \cup \{\beta_0\}, \boldsymbol{w})$, where $\Sigma \# \mathbb{T}^2$ is the internal connected sum.

We now address moves (1)–(3).

Move (1) If $\mathcal{H}$ is a diagram, and $\mathcal{H}'$ is the result of $(1,2)$–stabilization, there is an isomorphism

$$\sigma_*\colon \pi_2^{\mathcal{H}}(\boldsymbol{x}\times p_n^+, \boldsymbol{y}\times p_n^+)\to \pi_2^{\mathcal{H}'}(\boldsymbol{x}\times c\times p_n^+, \boldsymbol{y}\times c\times p_n^+),$$

where c is the intersection of the new $\boldsymbol{\alpha}$– and $\boldsymbol{\beta}$–curves. Furthermore,

$$(\mu-(n_1+n_2))(\phi)=(\mu-(n_1+n_2))(\sigma_*\phi),$$

from which the claim follows easily.

Move (2) Suppose $\mathcal{H}'$ is formed from $\mathcal{H}$ by taking the disjoint union of $\mathcal{H}$ with a diagram $(\mathbb{T}^2,\alpha_0,\beta_0,w)$. Homology classes on $\mathcal{H}'$ are of the form $\phi\sqcup k\cdot[\mathbb{T}^2]$, where ϕ is a homology disk on $\mathcal{H}$. One has

$$\mu(\phi\sqcup k\cdot[\mathbb{T}^2])=\mu(\phi)+2k,$$

from which the claim follows easily.

Move (3) This move corresponds to surgering on an embedded 0–sphere $\{q_1,q_2\}\subseteq \Sigma\setminus(\boldsymbol{\alpha}\cup\boldsymbol{\beta}\cup\boldsymbol{w})$. Write α_0 and β_0 for the new curves on the annulus, and $\{\theta_0^+,\theta_0^-\}=\alpha_0\cap\beta_0$. Suppose that $y\in\alpha_0\cap\beta_0$ is a choice of intersection point. We can define (noncanonically) an injection

$$\iota_y\colon \pi_2^{\mathcal{H}}(\theta^+\times p_n^+, \boldsymbol{y}\times p_n^+)\to \pi_2^{\mathcal{H}'}(\theta^+\times\theta_0^+\times p_n^+, \boldsymbol{y}\times y\times p_n^+).$$

For $y=\theta_0^+$, we define $\iota_{\theta_0^+}(\phi)$ to be the disk on the surgered diagram which has no change across the curve β_0, but which agrees with the disk ϕ away from the α_0 and β_0 curves. For $y=\theta_0^-$, a map $\iota_{\theta_0^-}$ can be defined by defining it to be the map $\iota_{\theta_0^+}$, defined above, composed with the map on disks obtained by splicing in a choice of one of the bigons from θ_0^+ to θ_0^-. An easy computation shows that

$$(\mu-(m_1+m_2))(\iota_{\theta_0^+}(\phi))=(\mu-(m_1+m_2))(\phi),$$

while

$$(\mu-(m_1+m_2))(\iota_{\theta_0^-}(\phi))=(\mu-(m_1+m_2))(\phi)+1.$$

Any disk in $\pi_2(\theta^+\times\theta_0^+\times p_n^+, \boldsymbol{y}\times y\times p_n^+)$ is equal to one which is in the image of ι_y, with $n\cdot\mathcal{P}$ spliced in, where $\mathcal{P}$ is the periodic domain which is $+1$ in one of the small strips between α_0 and β_0, and -1 in the other. We note that

$$\mu(\mathcal{P})=m_1(\mathcal{P})=m_2(\mathcal{P})=0.$$

From these observations it follows easily that $\mathcal{H}$ is strongly positive with respect to p_n^+ if and only if $\mathcal{H}'$ is. $\square$

Remark 6.4 Suppose $\mathcal{H}=(\Sigma,\boldsymbol{\alpha}',\boldsymbol{\alpha},\boldsymbol{w})$ is obtained by taking attaching curves $\boldsymbol{\alpha}$ and letting $\boldsymbol{\alpha}'$ be small Hamiltonian isotopies of the curves in $\boldsymbol{\alpha}$. Let α_s be a new curve in $\Sigma\setminus\boldsymbol{\alpha}$ which doesn't intersect any $\boldsymbol{\alpha}'$–curves. If α_s' is the result of handlesliding α_s across a curve in $\boldsymbol{\alpha}$, then $(\Sigma,\boldsymbol{\alpha}'\cup\{\alpha_s'\},\boldsymbol{\alpha}\cup\{\alpha_s\},\boldsymbol{w}\cup\{w\})$ is strongly positive at p^+, the intersection point of $\alpha_s'\cap\alpha_s$ with higher grading. Here w is a new basepoint in one of the regions adjacent to p^+.

Similarly, if $\mathcal{H}=(\Sigma,\boldsymbol{\alpha}',\boldsymbol{\alpha},\boldsymbol{w})$ is the result of handlesliding a curve in $\boldsymbol{\alpha}$ across another curve in $\boldsymbol{\alpha}$, and α_s and α_s' are two new curves which are Hamiltonian isotopies of each other, then $(\Sigma,\boldsymbol{\alpha}'\cup\{\alpha_s'\},\boldsymbol{\alpha}\cup\{\alpha_s\},\boldsymbol{w}\cup\{w\})$ is strongly positive with respect to the intersection point of $\alpha_s'\cap\alpha_s$ of higher relative grading.

Note that a diagram $(\Sigma_g,\boldsymbol{\alpha}',\boldsymbol{\alpha},w)$ where the curves in $\boldsymbol{\alpha}'$ are small isotopies of the curves in $\boldsymbol{\alpha}$ with $g(\Sigma_g)=|\boldsymbol{\alpha}'|=|\boldsymbol{\alpha}|=g$ is not a strongly positive diagram at any point, since $[\Sigma_g]$ represents a positive homology class in $\pi_2(\theta^+,\theta^+)$ with

$$\mu([\Sigma_g])-m_1-m_2=2-1-1=0.$$

Strongly positive diagrams always have multiple basepoints. The prototypical example is the one resulting from handlesliding a quasistabilization curve α_s across an $\boldsymbol{\alpha}$–curve, as in Figure 7.

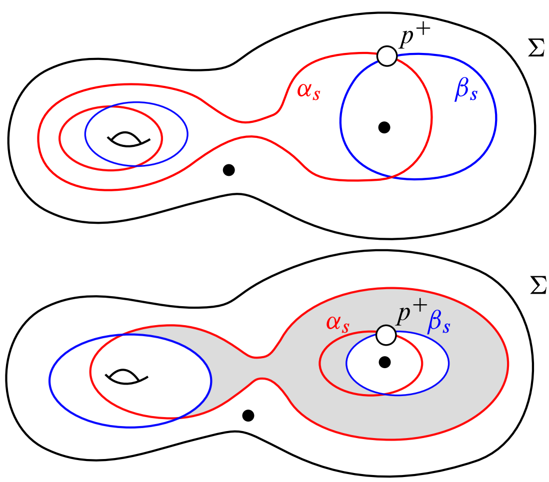

Figure 7: The diagram on the top is strongly positive with respect to the point p^+. The curves α_s and β_s are curves on which one could perform the quasistabilization operation of triangles in Theorem 6.5. The diagram on the bottom is not, and the nonzero, nonnegative domain of a disk ϕ with $\mu(\phi)-(n_1+n_2)(\phi)=0$ is shown.

A more interesting example of a diagram which doesn't satisfy the strong positivity condition would be the pair $(\Sigma, \boldsymbol{\alpha}' \cup \{\alpha_s'\}, \boldsymbol{\alpha} \cup \{\alpha_s\}, \boldsymbol{w})$ that arises in a triple $(\Sigma, \boldsymbol{\alpha}' \cup \{\alpha_s'\}, \boldsymbol{\alpha} \cup \{\alpha_s\}, \boldsymbol{\beta} \cup \{\beta_0\}, \boldsymbol{w})$ for handlesliding an $\boldsymbol{\alpha}$ curve across α_s. Fortunately, such a move is not required in the proof of invariance of the quasistabilization maps.

6.3 Quasistabilizing Heegaard triples along two curves

We now consider the effect on the triangle maps of quasistabilizing along two curves. Our analysis follows a similar spirit to the proof of [6, Proposition 5.2]. Suppose that $(\Sigma, \boldsymbol{\alpha}, \boldsymbol{\beta}, \boldsymbol{\gamma}, \boldsymbol{w}, \boldsymbol{z})$ is a Heegaard triple with a distinguished point

$$p^+ \in \Sigma \setminus (\boldsymbol{\alpha} \cup \boldsymbol{\beta} \cup \boldsymbol{\gamma} \cup \boldsymbol{w} \cup \boldsymbol{z}).$$

Suppose also that α_s and β_s are choices of curves in $\Sigma \setminus (\boldsymbol{\alpha} \cup \boldsymbol{w} \cup \boldsymbol{z})$ and $(\Sigma \setminus (\boldsymbol{\beta} \cup \boldsymbol{w} \cup \boldsymbol{z})$, respectively, which intersect only at p^+ and another point $p^- \in \Sigma$. We can form the diagram $\overline{\mathcal{T}}_{\alpha_s, \beta_s, p^+}$, obtained by quasistabilizing along both α_s and β_s, simultaneously, at the point p^+. This corresponds to removing a small disk containing p^+, and inserting the diagram shown in Figure 8, with a disk centered around p_0^- removed.

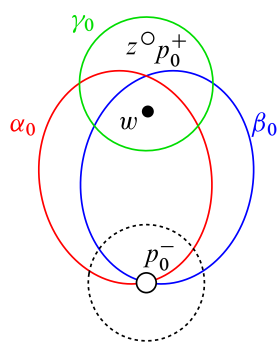

Figure 8: The diagram we insert into a Heegaard triple diagram $\mathcal{T}$ along the curves α_s and β_s to form the diagram $\overline{\mathcal{T}}_{\alpha_s, \beta_s, p^+}$. We cut out the solid circle marked with p_0^- and stretch the almost complex structure along the dashed circle.

Theorem 6.5 *Suppose that $\mathcal{T} = (\Sigma, \boldsymbol{\alpha}, \boldsymbol{\beta}, \boldsymbol{\gamma}, \boldsymbol{w}, \boldsymbol{z})$ is a Heegaard triple with curves α_s and β_s, intersecting at two points p^+ and p^-, and let $\overline{\mathcal{T}}_{\alpha_s, \beta_s, p^+}$ be the Heegaard triple resulting from quasistabilization, as described above. If $(\Sigma, \boldsymbol{\alpha} \cup \{\alpha_s\}, \boldsymbol{\beta} \cup \{\beta_s\}, \boldsymbol{w} \cup \{w\})$ is a strongly positive diagram for $(S^1 \times S^2)^{\# k}$ with respect to p^+ (Definition 6.2), and $\mathcal{J}$ is gluing data for stretching along the dashed circle, then for sufficiently large T, with respect to the almost complex structure $\mathcal{J}(T)$, there are identifications*

$$F_{\mathcal{T}^+_{\alpha_s,\beta_s,p^+},\bar{\mathfrak{s}},\mathcal{J}(T)}(\Theta^+_{\alpha\beta}\times p_0^+,\boldsymbol{x}\times\cdot)=\begin{pmatrix}F_{\mathcal{T},\mathfrak{s},J}(\Theta^+_{\alpha\beta},\boldsymbol{x}) & 0\\ 0 & F_{\mathcal{T},\mathfrak{s},J}(\Theta^+_{\alpha\beta},\boldsymbol{x})\end{pmatrix},$$

where $\cdot$ denotes $x^\pm\in\beta_0\cap\gamma_0$ and the matrix on the right denotes the matrix decomposition of the map based on the decompositions given $x^\pm$ and $y^\pm$.

As usual, the argument proceeds by a Maslov index calculation, which we use to put constraints on the homology classes of holomorphic curves which can appear in a weak limit as we let the parameter T approach $+\infty$. Once we determine which homology classes of triangles can appear, we can use standard gluing results to explicitly count holomorphic curves.

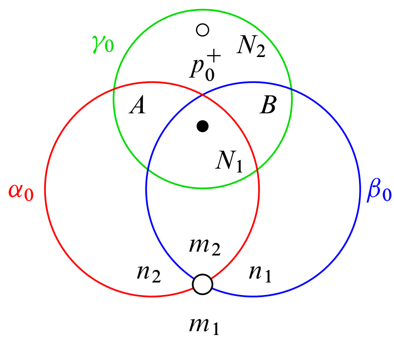

Figure 9: Multiplicities for a triangle on the diagram $(S^2,\alpha_0,\beta_0,\gamma_0,w,z)$

Lemma 6.6 *Suppose $\psi\in\pi_2(x,y,z)$ is a homology disk on $(S^2,\alpha_0,\beta_0,\gamma_0,w,z)$, shown in Figure 9. Then*

$$\mu(\psi)=n_1+n_2+N_1+N_2.$$

Proof The formula is easily checked for any of the Maslov index 0 small triangles, and respects splicing in any Maslov index 1 strip. Since any two triangles on this diagram differ by splicing in some number of the Maslov index 1 strips, the formula follows in full generality. □

We can now prove Theorem 6.5.

Proof of Theorem 6.5 Suppose that u_i is a sequence of holomorphic triangles of Maslov index 0 representing a class $\psi\in\pi_2(\Theta^+_{\alpha\beta}\times p_0^+,\boldsymbol{x}\times x,\boldsymbol{y}\times y)$, for almost complex structure $\mathcal{J}(T_i)$, where T_i is a sequence of neck lengths approaching $+\infty$. Adapting the proof of Proposition 5.3, the limiting curves which appear can be arranged into three classes of broken holomorphic curves:

(1) a broken holomorphic triangle u_Σ which represents a homology class ψ_Σ on $(\Sigma, \boldsymbol{\alpha}, \boldsymbol{\beta}, \boldsymbol{\gamma})$ which has no boundary components on α_s or β_s;

(2) a broken holomorphic disk $u_{\alpha\beta}$ on $(\Sigma, \boldsymbol{\alpha} \cup \{\alpha_s\}, \boldsymbol{\beta} \cup \{\beta_s\})$ which represents a class $\phi_{\alpha\beta} \in \pi_2(\Theta^+_{\alpha\beta} \times p^+, \boldsymbol{y} \times p^+)$, for some $\boldsymbol{y} \in \mathbb{T}_\alpha \cap \mathbb{T}_\gamma$;

(3) a broken holomorphic triangle u_0 on $(S^2, \alpha_0, \beta_0, \gamma_0)$ which represents a homology triangle $\psi_0 \in \pi_2(p_0^+, x, y)$.

We now wish to write down the Maslov index of ψ in terms of the Maslov indices and multiplicities of ψ_Σ, ψ_0 and $\phi_{\alpha\beta}$. Let $m_1(\cdot)$, $m_2(\cdot)$, $n_1(\cdot)$ and $n_2(\cdot)$ denote the multiplicities of a homology curve in the regions surrounding p^+ or p_0^-, as in Figure 9. In [12], Sarkar derives a formula for the Maslov index of a homology triangle $\rho \in \pi_2(\boldsymbol{x}, \boldsymbol{y}, \boldsymbol{z})$ which can be computed entirely from the domain $\mathcal{D}(\rho)$. Writing $\mathcal{D} = \mathcal{D}(\rho)$, the formula reads

$$\mu(\rho) = e(\mathcal{D}) + n_{\boldsymbol{x}}(\mathcal{D}) + n_{\boldsymbol{y}}(\mathcal{D}) + a(\mathcal{D}).c(\mathcal{D}) - \tfrac{1}{2}d,$$

where $d = |\boldsymbol{\alpha}| = |\boldsymbol{\beta}| = |\boldsymbol{\gamma}|$. Here $a(\mathcal{D})$ is defined to be the intersection $\partial\mathcal{D} \cap \boldsymbol{\alpha}$ (viewed as a 1–chain), and $c(\mathcal{D})$ is defined similarly, using the $\boldsymbol{\gamma}$–curves. The quantity $a(\mathcal{D}).c(\mathcal{D})$ is defined as the average of the four algebraic intersection numbers of $a'(\mathcal{D})$ and $c(\mathcal{D})$, where $a'(\mathcal{D})$ is a translate of $a(\mathcal{D})$ in any of the four "diagonal directions". If $s \in \alpha_i \cap \beta_j$, then $n_s(\mathcal{D})$ is the average of the multiplicities in the regions surrounding s, and if $\boldsymbol{s}$ is a set of such intersection points, then $n_{\boldsymbol{s}}(\mathcal{D})$ is the sum of the $n_s(\mathcal{D})$ ranging over $s \in \boldsymbol{s}$.

For a homology triangle $\psi \in \pi_2(\Theta^+_{\alpha\beta} \times p_0^+, \boldsymbol{x} \times x, \boldsymbol{y} \times y)$ which can be decomposed into homology classes ψ_Σ, $\phi_{\alpha\beta}$ and ψ_0 as above (as any homology class admitting holomorphic representatives for arbitrarily large neck length can) we observe that $\mu(\psi)$ can be computed by adding up $\mu(\psi_\Sigma)$, $\mu(\phi_{\alpha\beta})$ and $\mu(\psi_0)$, then subtracting the quantities which are over-counted. This corresponds to subtracting

$$\tfrac{1}{2}(m_1 + m_2 + n_1 + n_2)(\psi),$$

which is the excess of Euler measure resulting from removing balls centered at p^+ and at p_0^- $\big($note that the Euler measure of a quarter disk is $\tfrac{1}{4}\big)$, and subtracting

$$2n_{p^+}(\phi_{\alpha\beta}) = \tfrac{1}{2}(n_1 + n_2 + m_1 + m_2)(\phi_{\alpha\beta}),$$

which is the quantity in the expression

$$\begin{aligned}\mu(\phi_{\alpha\beta}) &= e(\mathcal{D}(\phi_{\alpha\beta})) + n_{\Theta^+_{\alpha\beta} \times p^+}(\phi_{\alpha\beta}) + n_{\boldsymbol{y} \times p^+}(\phi_{\alpha\beta}) \\ &= e(\mathcal{D}(\phi_{\alpha\beta})) + n_{\Theta^+_{\alpha\beta}}(\phi_{\alpha\beta}) + n_{\boldsymbol{y}}(\phi_{\alpha\beta}) + \tfrac{1}{2}(n_1 + n_2 + m_1 + m_2)(\phi_{\alpha\beta})\end{aligned}$$

which does not contribute to $\mu(\psi)$. Adding these contributions, we get

$$\begin{aligned}(3)\quad \mu(\psi) = {}& \mu(\psi_\Sigma) + \mu(\psi_0) + \mu(\phi_{\alpha\beta}) \\ & - \tfrac{1}{2}(n_1+n_2+m_1+m_2)(\psi) - \tfrac{1}{2}(n_1+n_2+m_1+m_2)(\phi_{\alpha\beta}).\end{aligned}$$

Writing $\psi_0 \in \pi_2(p_0^+, x, y)$, using the vertex multiplicity relations around p_0^-, it is an easy computation that

$$(m_1+m_2)(\psi) = (n_1+n_2)(\psi).$$

Note also that $m_i(\psi_0) = m_i(\psi)$ and similarly for the multiplicities n_i, since we are grouping all holomorphic curves on $(S^2, \alpha_0, \beta_0, \gamma_0)$ appearing in the weak limit into the homology class ψ_0. Using the Maslov index formula from Lemma 6.6 for ψ_0, we get from (3) that

$$\begin{aligned}\mu(\psi) = {}& \mu(\psi_\Sigma) + \mu(\phi_{\alpha\beta}) + (m_1+m_2+N_1+N_2)(\psi_0) \\ & - \tfrac{1}{2}(m_1+m_2+n_1+n_2)(\psi_0) - \tfrac{1}{2}(n_1+n_2+m_1+m_2)(\phi_{\alpha\beta}),\end{aligned}$$

which reduces to

$$(4)\quad \mu(\psi) = \mu(\psi_\Sigma) + (N_1+N_2)(\psi_0) + \mu(\phi_{\alpha\beta}) - \tfrac{1}{2}(n_1+n_2+m_1+m_2)(\phi_{\alpha\beta}),$$

since ψ_0 does not have p^+ as a vertex, so the vertex relations at p^+ yield

$$\tfrac{1}{2}(n_1+n_2+m_1+m_2)(\psi_0) = (n_1+n_2)(\psi_0) = (m_1+m_2)(\psi_0).$$

We now use the assumption that $(\Sigma, \boldsymbol{\alpha} \cup \{\alpha_s\}, \boldsymbol{\beta} \cup \{\beta_s\}, \boldsymbol{w})$ is strongly positive with respect to p^+, and hence

$$\mu(\phi_{\alpha\beta}) - \tfrac{1}{2}(n_1+n_2+m_1+m_2)(\phi_{\alpha\beta}) \geq 0,$$

with equality if and only if $\phi_{\alpha\beta}$ is a constant disk. We note that $\mu(\psi_\Sigma) \geq 0$, since ψ_Σ admits a broken holomorphic representative. Hence the formula for $\mu(\psi)$ in (4) can be written as a sum of nonnegative expressions, and hence each must be zero if $\mu(\psi) = 0$. Thus

$$0 = \mu(\psi) = \mu(\psi_\Sigma) = \mu(\phi_{\alpha\beta}) = N_1 = N_2.$$

Note first that this implies that $\phi_{\alpha\beta}$ is a constant disk, since generically there are no nonconstant, Maslov index 0 disks which admit broken holomorphic representatives. From here the argument proceeds in a familiar manner. Note that ψ_Σ is a Maslov index 0 broken holomorphic triangle, and hence must be a genuine holomorphic triangle, as nonconstant holomorphic disks, boundary degenerations, and closed surfaces all have strictly positive Maslov index. Hence, since ψ_Σ is represented by a holomorphic triangle with no boundary components mapped to α_s or β_s, we must have $m_1(\psi) = m_2(\psi) = n_1(\psi) = n_2(\psi)$.

We now claim that this implies that the off-diagonal entries of the matrix representing the triangle map in the statement are zero. Writing $\psi_0 \in \pi_2(p_0^+, x, y)$, and using the multiplicities in Figure 9, the vertex relations at p_0^+ read

$$A + B = 1,$$

and hence exactly one of A and B is 1, and the other is 0, since $A, B \geq 0$. Since $n_1 = n_2 = m_1 = m_2$, we know that by subtracting some number of copies of the γ_0–boundary degeneration of Maslov index 2 with $N_1 = N_2 = 0$, we get a homology triangle in $\pi_2(p_0^+, x, y)$ with N_1, N_2, m_1, m_2, n_1 and n_2 all zero. There are only two homology triangles satisfying that condition. One is in $\pi_2(p_0^+, x^+, y^+)$ and the other is in $\pi_2(p_0^+, x^-, y^-)$, implying that ψ_0 itself must be in one of those sets. Hence the off-diagonal entries of the matrix are zero.

Since u_Σ is a genuine Maslov index 0 holomorphic triangle, there must be a curve in u_0' in the broken holomorphic triangle u_0 which matches, ie which satisfies

$$\rho^{p^+}(u_\Sigma) = \rho^{p_0}(u_0').$$

Recall that if $u\colon S \to \Sigma \times \Delta$ is a holomorphic map and $q \in \Sigma$ is a point, we define

$$\rho^q(u) = (\pi_\Delta \circ u)(\pi_\Sigma \circ u)^{-1}(q) \in \mathrm{Sym}^{n_q(u)}(\Delta).$$

Since this in particular forces $n_{p^+}(u_\Sigma) = n_{p_0^-}(u_0')$, it is easy to see that there can be no other curves in the broken curve u_0 since there are no multiplicities on $(S^2, \alpha_0, \beta_0, \gamma_0)$ which could be increased without increasing n_1, m_1, n_2, m_2, N_1 and N_2 while still preserving the vertex relations. By standard gluing arguments (see eg [5, Appendix A]) the count of prematched triangles[2] is equal to the count of holomorphic triangles in $\#\mathcal{M}_{\mathcal{J}(T)}(\psi_\Sigma \# \psi_0)$ for sufficiently large T.

For x and y of the same relative grading (both the top intersection points or both the lower intersection points), for each k there is a unique homology class ψ_k on $(S^2, \alpha_0, \beta_0, \gamma_0)$ in $\pi_2(p_0^+, x, y)$ with $n_1 = n_2 = m_1 = m_2 = k$. Thus, adapting the proof of Proposition 5.3, it is sufficient to count holomorphic triangles on $(S^2, \alpha_0, \beta_0, \gamma_0)$ of homology class ψ_k which match a fixed divisor $\boldsymbol{d} \in \mathrm{Sym}^k(\Delta)$. The count of such holomorphic triangles matching $\boldsymbol{d}$ is generically 1 (mod 2), as can be seen from a Gromov compactness argument nearly identical to the one done at the

[2] Recall that a prematched triangle is a pair (u_Σ, u_0) where u_Σ and u_0 are holomorphic triangles representing ψ_Σ and ψ_0 on $(\Sigma, \boldsymbol{\alpha}, \boldsymbol{\beta}, \boldsymbol{\gamma})$ and $(S^2, \alpha_0, \beta_0, \gamma_0)$ respectively and $\rho^{p^+}(u_\Sigma) = \rho^{p_0}(u_0')$.

end of Proposition 5.3. Hence the diagonal entries of the triangle map matrix are as claimed, completing the proof. □

Remark 6.7 Without the "strongly positive" condition, the counts of the previous theorem are false. The bottom of Figure 7 shows a diagram which is not strongly positive, along with a Maslov index 1 disk which could appear on $(\Sigma, \boldsymbol{\alpha}', \boldsymbol{\alpha})$ when we degenerate. Fortunately such pairs $(\Sigma, \boldsymbol{\alpha}', \boldsymbol{\alpha})$ don't appear when proving invariance of the quasistabilization maps, as we don't need to handleslide other $\boldsymbol{\alpha}$ curves across α_s.

7 Invariance of the quasistabilization maps

In this section, we combine the results of the previous section to prove invariance of the quasistabilization maps:

Theorem A *Assume that $(\sigma, \mathfrak{P})$ is a coloring of the basepoints $\boldsymbol{w} \cup \boldsymbol{z}$ which is extended by the coloring $(\sigma', \mathfrak{P})$ of the basepoints $\boldsymbol{w} \cup \boldsymbol{z} \cup \{w, z\}$. The quasistabilization operation induces well-defined maps*

$$S^+_{w,z}\colon \mathrm{CFL}^\infty_{UV}(Y, L, \boldsymbol{w}, \boldsymbol{z}, \sigma, \mathfrak{P}, \mathfrak{s}) \to \mathrm{CFL}^\infty_{UV}(Y, L, \boldsymbol{w} \cup \{w\}, \boldsymbol{z} \cup \{z\}, \sigma', \mathfrak{P}, \mathfrak{s})$$

and

$$S^-_{w,z}\colon \mathrm{CFL}^\infty_{UV}(Y, L, \boldsymbol{w} \cup \{w\}, \boldsymbol{z} \cup \{z\}, \sigma', \mathfrak{P}, \mathfrak{s}) \to \mathrm{CFL}^\infty_{UV}(Y, L, \boldsymbol{w}, \boldsymbol{z}, \sigma, \mathfrak{P}, \mathfrak{s}),$$

which are well-defined invariants up to $\mathfrak{P}$–filtered $\mathbb{Z}_2[U_{\mathfrak{P}}]$–chain homotopy.

The proof is to construct the maps for choices of Heegaard diagram and auxiliary data, and show that the maps we describe are independent of that auxiliary data and the choice of diagram.

If $\mathcal{H} = (\Sigma, \boldsymbol{\alpha}, \boldsymbol{\beta}, \boldsymbol{w}, \boldsymbol{z})$ is a diagram for $\mathbb{L} = (L, \boldsymbol{w}, \boldsymbol{z})$, recall from Section 5.1 that if A denotes the component of $\Sigma \setminus \boldsymbol{\alpha}$ containing the basepoints of $(L, \boldsymbol{w}, \boldsymbol{z})$ adjacent to w and z, then we pick a point $p \in A \setminus (\boldsymbol{\alpha} \cup \boldsymbol{\beta} \cup \boldsymbol{w} \cup \boldsymbol{z})$ and a simple closed curve $\alpha_s \subseteq A \setminus \boldsymbol{\alpha}$ to form a diagram $\bar{\mathcal{H}}_{p,\alpha_s}$. Let $\mathcal{J}$ denote gluing data (see Section 5.2) for performing the special connected sum operation at $p \in \Sigma$ and $p_0 \in S^2$ and gluing almost complex structures on $\mathcal{H}$ and $\mathcal{H}_0$ together.

We now define maps

$$S^+_{w,z,\mathcal{H},p,\alpha_s,\mathcal{J},T}\colon \mathrm{CFL}^\infty_{UV,J_s}(\mathcal{H}, \mathfrak{s}) \to \mathrm{CFL}^\infty_{UV,\mathcal{J}(T)}(\bar{\mathcal{H}}_{p,\alpha_s}, \mathfrak{s})$$

and

$$S^-_{w,z,\mathcal{H},p,\alpha_s,\mathcal{J},T}\colon \mathrm{CFL}^\infty_{UV,\mathcal{J}(T)}(\bar{\mathcal{H}}_{p,\alpha_s}, \mathfrak{s}) \to \mathrm{CFL}^\infty_{UV,J_s}(\mathcal{H}, \mathfrak{s})$$

by the formulas

$$S^+_{w,z,\mathcal{H},p,\alpha_s,\mathcal{J}}(\boldsymbol{x}) = \boldsymbol{x} \times \theta^+$$

and

$$S^-_{w,z,\mathcal{H},p,\alpha_s,\mathcal{J}}(\boldsymbol{x} \times \theta^+) = 0, \quad S^+_{w,z,\mathcal{H},p,\alpha_s,\mathcal{J}}(\boldsymbol{x} \times \theta^-) = \boldsymbol{x},$$

where J_s denotes the almost complex structure on Σ associated to the gluing data $\mathcal{J}$ and T is sufficiently large. Here θ^+ denotes the top-degree intersection point with respect to the Maslov grading (the grading obtained by using the $\boldsymbol{w}$–basepoints and ignoring the $\boldsymbol{z}$–basepoints).

The maps $S^{\pm}_{w,z,\mathcal{H},p,\alpha_s,\mathcal{J},T}$ can be extended to the entire $\mathfrak{P}$–filtered chain homotopy-type invariant by pre- and postcomposing with change of diagram maps and change of almost complex structure maps. By functoriality of the change of diagrams maps, we get well-defined maps $S^{\pm}_{w,z,\mathcal{H},p,\alpha_s,\mathcal{J},T}$ between the coherent chain homotopy type invariants $\mathrm{CFL}^\infty_{UV}(Y, L, \boldsymbol{w}, \boldsymbol{z}, \sigma, \mathfrak{P}, \mathfrak{s})$ and $\mathrm{CFL}^\infty_{UV}(Y, L, \boldsymbol{w} \cup \{w\}, \boldsymbol{z} \cup \{z\}, \sigma', \mathfrak{P}, \mathfrak{s})$, though of course we need to show independence from the choices of $\mathcal{H}$, p, α_s, $\mathcal{J}$ and T.

Any diagram $\overline{\mathcal{H}}$ for $(Y, L, \boldsymbol{w} \cup \{w\}, \boldsymbol{z} \cup \{z\})$ can be connected to one of the form $\overline{\mathcal{H}}_{p,\alpha_s}$ for a diagram $\mathcal{H}$ and a choice of p and α_s by a sequence of handleslides and isotopies of the attaching curves, $(1,2)$–stabilizations, and isotopies of Y relative the basepoints and preserving the link, since we can always find a diagram for the unstabilized link and quasistabilize it, and any two diagrams for the same multibased link can be connected by a sequence of Heegaard moves by [4, Proposition 2.37], for example. This is somewhat unsatisfying since it would be nice to have an actual algorithm for reducing an arbitrary Heegaard diagram for the quasistabilized link to a quasistabilized diagram, but for our purposes it is sufficient to know that such a path exists.

We now begin our proof of invariance of the maps $S^{\pm}_{w,z}$. We first address independence from $\mathcal{J}$ and the parameter T. Recalling Lemma 5.5, there is an N such that if $T, T' > N$ we have

$$\Phi_{\mathcal{J}(T)\to\mathcal{J}(T')} \simeq \begin{pmatrix} \mathrm{id} & 0 \\ 0 & \mathrm{id} \end{pmatrix}.$$

Hence, as with the free stabilization maps from [14], we define the maps $S^{\pm}_{w,z,\mathcal{H},p,\alpha_s,\mathcal{J}}$ to be between the complexes $\mathrm{CFL}^\infty_{J_s,UV}(\mathcal{H}, \mathfrak{s})$ and $\mathrm{CFL}^\infty_{\mathcal{J}(T),UV}(\overline{\mathcal{H}}_{p,\alpha_s}, \mathfrak{s})$ for any T greater than any such N.

Lemma 7.1 *The maps $S^{\pm}_{w,z,\mathcal{H},p,\alpha_s,\mathcal{J}}$ are independent of $\mathcal{J}$ and the parameter T.*

Proof Lemma 5.5 implies that $S^{\pm}_{w,z,\mathcal{H},p,\alpha_s,\mathcal{J},T}$ is independent of T for any T which is sufficiently large. Let $S^{\pm}_{w,z,\mathcal{H},p,\alpha_s,\mathcal{J}}$ denote the common map. Lemma 5.7 implies that the maps $S^{\pm}_{w,z,\mathcal{H},p,\alpha_s,\mathcal{J}}$ are independent of $\mathcal{J}$. We denote the common map from now on by $S^{\pm}_{w,z,\mathcal{H},p,\alpha_s}$. □

Lemma 7.2 *For a fixed diagram $\mathcal{H}$ with fixed $p \in \Sigma$, the maps $S^{\pm}_{w,z,\mathcal{H},p,\alpha_s}$ are independent of α_s.*

Proof This follows from the triangle map computation in Theorem 6.5, which allows one to change the α_s curve through a sequence of isotopies of the α_s curve, and handleslides of the α_s curve over other $\boldsymbol{\alpha}$–curves, each of which can be realized by quasistabilizing a Heegaard triple $(\Sigma, \boldsymbol{\alpha}', \boldsymbol{\alpha}, \boldsymbol{\beta}, \boldsymbol{w}, \boldsymbol{z})$ along two curves α_s' and α_s with $\alpha_s' \cap \alpha_s = \{p^+, p^-\}$, such that $(\Sigma, \boldsymbol{\alpha}' \cup \{\alpha_s'\}, \boldsymbol{\alpha} \cup \{\alpha_s\}, \boldsymbol{w})$ is strongly positive at p^+ (see Remark 6.4). For each of these moves, by Theorem 6.5 the change of diagrams map can be written as

$$\Phi_{\boldsymbol{\beta}\cup\{\beta_s\}}^{\boldsymbol{\alpha}\cup\{\alpha_s\}\to\boldsymbol{\alpha}'\cup\{\alpha_s'\}} = \begin{pmatrix} \Phi_{\boldsymbol{\beta}}^{\boldsymbol{\alpha}\to\boldsymbol{\alpha}'} & 0 \\ 0 & \Phi_{\boldsymbol{\beta}}^{\boldsymbol{\alpha}\to\boldsymbol{\alpha}'} \end{pmatrix},$$

where the curves in $\boldsymbol{\alpha}'$ are small Hamiltonian isotopies of the curves in $\boldsymbol{\alpha}$. Similarly, by Theorem 6.5 we also have

$$\Phi_{\boldsymbol{\beta}\cup\{\beta_s\}}^{\boldsymbol{\alpha}\cup\{\alpha_s\}\to\boldsymbol{\alpha}'\cup\{\alpha_s\}} = \begin{pmatrix} \Phi_{\boldsymbol{\beta}}^{\boldsymbol{\alpha}\to\boldsymbol{\alpha}'} & 0 \\ 0 & \Phi_{\boldsymbol{\beta}}^{\boldsymbol{\alpha}\to\boldsymbol{\alpha}'} \end{pmatrix},$$

completing the proof. □

We now let $S^{\pm}_{w,z,\mathcal{H},p}$ denote the map $S^{\pm}_{w,z,\mathcal{H},p,\alpha_s}$ for any choice of α_s. We now prove independence from the choice of point $p \in \Sigma$.

Lemma 7.3 *Given a fixed diagram $\mathcal{H}$, the maps $S^{\pm}_{w,z,\mathcal{H},p}$ are independent of the choice of point $p \in \Sigma$.*

Proof Let A denote the component of $\Sigma \setminus \boldsymbol{\alpha}$ containing the basepoints on $\mathbb{L}$ which are adjacent to w and z. Let p and p' be two choices of points in $A \setminus (\boldsymbol{\beta} \cup \boldsymbol{w} \cup \boldsymbol{z})$. Let ϕ_t be an isotopy $\phi_t\colon \Sigma \to \Sigma$ which fixes $\Sigma \setminus A$ and maps p to p'. Recall that the surfaces $\overline{\Sigma}_p$ were well defined up to an isotopy fixing $\boldsymbol{\alpha} \cup \boldsymbol{\beta} \cup \boldsymbol{w} \cup \boldsymbol{z}$ and mapping L to L. Extend $\phi = \phi_1$ to an isotopy of Y which fixes $(\Sigma \setminus A) \cup \boldsymbol{w} \cup \boldsymbol{z} \cup \{w, z\}$ and maps L to L. By definition

$$(\phi)_*(\overline{\Sigma}_p) = \overline{\Sigma}_{p'},$$

as embedded surfaces. The diffeomorphism ϕ fixes all the curves in $\boldsymbol{\alpha}$, but moves some of the $\boldsymbol{\beta}$–curves which pass through the region A.

Observe the factorizations

$$\Phi_{(\Sigma,\boldsymbol{\alpha},\boldsymbol{\beta},J_s)\to(\Sigma,\boldsymbol{\alpha},\boldsymbol{\beta},\phi_* J_s)} \simeq \Phi^{\boldsymbol{\alpha}}_{\phi_*\boldsymbol{\beta}\to\boldsymbol{\beta}} \circ \phi_* \tag{5}$$

and similarly

$$\Phi_{(\overline{\Sigma}_p,\boldsymbol{\alpha}\cup\{\alpha_s\},\boldsymbol{\beta}\cup\{\beta_0\},\mathcal{J}(T))\to(\overline{\Sigma}_{p'},\boldsymbol{\alpha}\cup\{\phi_*\alpha_s\},\boldsymbol{\beta}\cup\{\phi_*\beta_0\},\phi_*\mathcal{J}(T))} \simeq \Phi^{\boldsymbol{\alpha}\cup\{\phi_*\alpha_s\}}_{(\phi_*\boldsymbol{\beta})\cup\{\phi_*\beta_0\}\to\boldsymbol{\beta}\cup\{\phi_*\beta_0\}}\circ\phi_*.$$

Using Theorem 6.5, for sufficiently stretched almost complex structure we can write

$$\Phi^{\boldsymbol{\alpha}\cup\{\phi_*\alpha_s\}}_{(\phi_*\boldsymbol{\beta})\cup\{\phi_*\beta_0\}\to\boldsymbol{\beta}\cup\{\phi_*\beta_0\}} \simeq \begin{pmatrix} \Phi^{\boldsymbol{\alpha}}_{\phi_*\boldsymbol{\beta}\to\boldsymbol{\beta}} & 0 \\ 0 & \Phi^{\boldsymbol{\alpha}}_{\phi_*\boldsymbol{\beta}\to\boldsymbol{\beta}} \end{pmatrix},$$

and hence

$$\Phi^{\boldsymbol{\alpha}\cup\{\phi_*\alpha_s\}}_{(\phi_*\boldsymbol{\beta})\cup\{\phi_*\beta_0\}\to\boldsymbol{\beta}\cup\{\phi_*\beta_0\}}\circ\phi_* \simeq \begin{pmatrix} \Phi^{\boldsymbol{\alpha}}_{\phi_*\boldsymbol{\beta}\to\boldsymbol{\beta}}\circ\phi_* & 0 \\ 0 & \Phi^{\boldsymbol{\alpha}}_{\phi_*\boldsymbol{\beta}\to\boldsymbol{\beta}}\circ\phi_* \end{pmatrix}.$$

Combining this with (5), we see that for sufficiently large T, we have

$$\Phi_{(\overline{\Sigma}_p,\boldsymbol{\alpha}\cup\{\alpha_s\},\boldsymbol{\beta}\cup\{\beta_0\},\mathcal{J}(T))\to(\overline{\Sigma}_{p'},\boldsymbol{\alpha}\cup\{\phi_*\alpha_s\},\boldsymbol{\beta}\cup\{\phi_*\beta_0\},\phi_*\mathcal{J}(T))} \simeq \begin{pmatrix} \Phi_{(\Sigma,\boldsymbol{\alpha},\boldsymbol{\beta},J_s)\to(\Sigma,\boldsymbol{\alpha},\boldsymbol{\beta},\phi_*J_s)} & 0 \\ 0 & \Phi_{(\Sigma,\boldsymbol{\alpha},\boldsymbol{\beta},J_s)\to(\Sigma,\boldsymbol{\alpha},\boldsymbol{\beta},\phi_*J_s)} \end{pmatrix}.$$

Since this map is upper triangular with diagonal entries equal to the change of diagrams maps, the change of diagrams maps commute with the maps $S^{\pm}_{w,z,\mathcal{H},p}$ and $S^{\pm}_{w,z,\mathcal{H},p'}$ in the appropriate sense. Since any two choices of points p and p' at which we can perform quasistabilization are in the region A, we know that the maps on the filtered chain homotopy invariant $\mathrm{CFL}^{\infty}_{UV}$ induced by $S^{\pm}_{w,z,\mathcal{H},p,\alpha_s\mathcal{J}}$ and $S^{\pm}_{w,z,\mathcal{H},p',\phi_*\alpha_s,\phi_*\mathcal{J}}$ are equal. Since we proved invariance from the gluing data $\mathcal{J}$ in Lemma 5.7, and we proved invariance from the curve α_s in Lemma 7.2, the proof is thus complete. □

We let $S^{\pm}_{w,z,\mathcal{H}}$ denote the map $S^{\pm}_{w,z,\mathcal{H},p}$ for any choice of p in the component of $\Sigma\setminus\boldsymbol{\alpha}$ containing the basepoints of L adjacent to w and z.

Lemma 7.4 *If $\mathcal{H}$ and $\mathcal{H}'$ are two diagrams for $\mathbb{L}=(L,\boldsymbol{w},\boldsymbol{z})$, then the maps $S^{\pm}_{w,z,\mathcal{H}}$ and $S^{\pm}_{w,z,\mathcal{H}'}$ are filtered chain homotopic.*

Proof Suppose that $\mathcal{H}=(\Sigma,\boldsymbol{\alpha},\boldsymbol{\beta},\boldsymbol{w},\boldsymbol{z})$ and $\mathcal{H}'=(\Sigma',\boldsymbol{\alpha}',\boldsymbol{\beta}',\boldsymbol{w},\boldsymbol{z})$ are two diagrams for $(L,\boldsymbol{w},\boldsymbol{z})$. The diagrams $\mathcal{H}$ and $\mathcal{H}'$ are related by a sequence of the following moves:

(1) $\boldsymbol{\alpha}$– and $\boldsymbol{\beta}$–handleslides and isotopies;

(2) (1,2)–stabilizations away from L;

(3) isotopies of Σ inside of Y which fix $\boldsymbol{w}\cup\boldsymbol{z}$, and map L to L.

The maps corresponding to $\boldsymbol{\alpha}$– and $\boldsymbol{\beta}$–handleslides on the unstabilized diagram $\mathcal{H}$ can be computed using triangle maps. For moves of the $\boldsymbol{\beta}$–curves, we simply apply Lemma 6.1 to see that the maps $S^{\pm}_{w,z,\mathcal{H}}$ are invariant under $\boldsymbol{\beta}$–isotopies and handleslides. Theorem 6.5 implies independence under $\boldsymbol{\alpha}$–moves of $\mathcal{H}$ for which there are curves α_s and α_s' in Σ, with top graded intersection point $p \in \alpha_s' \cap \alpha_s$, such that $(\Sigma, \boldsymbol{\alpha}' \cup \{\alpha_s'\}, \boldsymbol{\alpha} \cup \{\alpha_s\}, \boldsymbol{w})$ is strongly positive with respect to p. An arbitrary $\boldsymbol{\alpha}$–move can be realized as a sequence of such moves, along with moves of the point p inside of the region of $\Sigma \setminus \boldsymbol{\alpha}$. Since we've already shown invariance under each of these smaller moves, the maps $S^{\pm}_{w,z,\mathcal{H}}$ are unchanged by handleslides and isotopies of the $\boldsymbol{\alpha}$– and $\boldsymbol{\beta}$–curves.

The maps $S^{\pm}_{w,z,\mathcal{H}}$ obviously commute with the $(1,2)$–stabilization maps.

We now consider isotopies $\phi_t\colon Y \to Y$ which fix $\boldsymbol{w} \cup \boldsymbol{z}$ and map L to L. We note that tautologically we have that

$$\phi_* \circ S^{\pm}_{w,z,\mathcal{H},p,\mathcal{J}} = S^{\pm}_{w,z,\phi_*\mathcal{H},\phi_* p,\phi_*\mathcal{J}} \circ \phi_*.$$

Since we already know that $S^{\pm}_{w,z,\mathcal{H},p,\mathcal{J}}$ is independent from p and $\mathcal{J}$, we thus conclude that $S^{\pm}_{w,z,\mathcal{H}}$ and $S^{\pm}_{w,z,\phi_*\mathcal{H}}$ agree. □

We can now write $S^{\pm}_{w,z}$ for the quasistabilization maps, completing the proof of Theorem A.

Remark 7.5 Given that the triangle map computations in Lemma 6.1 and Theorem 6.5 showed that change of diagrams maps were not only upper triangular, but diagonal, one may ask why it is natural to define $S^{+}_{w,z}$ by $\boldsymbol{x} \mapsto \boldsymbol{x} \times \theta^+$ and not $\boldsymbol{x} \mapsto \boldsymbol{x} \times \theta^-$. We remark that $\boldsymbol{x} \mapsto \boldsymbol{x} \times \theta^-$ is only a chain map when w is given the same color as the other $\boldsymbol{w}$–basepoint adjacent to z, and indeed $\boldsymbol{x} \mapsto \boldsymbol{x} \times \theta^-$ is equal to $\Psi_z S^{+}_{w,z}$. The map Ψ_z is only a chain map if the $\boldsymbol{w}$–basepoints adjacent to z have the same color.

Remark 7.6 We have defined quasistabilization maps $S^{\pm}_{w,z}$ in the case that w comes after z and showed that such maps were invariants, ie that they yielded well-defined maps $S^{\pm}_{w,z}$ on the coherent filtered chain homotopy type invariant. These maps were only constructed if w came after z on the link component. In the case that z comes after w, we can define quasistabilization maps $S^{\pm}_{z,w}$ analogously, picking a choice of β_s. We could call such an operation β quasistabilization. There is no ambiguity between α quasistabilizations or β quasistabilizations because $S^{\pm}_{w,z}$ is always an α quasistabilization and $S^{\pm}_{z,w}$ is always a β quasistabilization.

8 Commutation of quasistabilization maps

In this section we show that if $\{w,z\}\cap\{w',z'\}=\varnothing$, then the maps $S^{\pm}_{w,z}$ and $S^{\pm}_{w',z'}$ all commute. In [14] we showed that the free stabilization maps commute, though commutation was easier to show in that setting, since we could just pick a diagram and an almost complex structure where both free stabilization maps could be computed, and by simply looking at the formulas, one could observe that the maps commuted. In the case of quasistabilization, we cannot always pick an almost complex structure which can be used to compute both maps. Nevertheless, we can compute enough components of the change of almost complex structure map to show that quasistabilization maps commute:

Theorem 8.1 *Suppose that $(L,\boldsymbol{w},\boldsymbol{z})$ is a multibased link in Y^3 and that w,z,w' and z' are new basepoints such that (w,z) and (w',z') are each pairs of adjacent basepoints on $(L,\boldsymbol{w}\cup\{w,w'\},\boldsymbol{z}\cup\{z,z'\})$. Then*

$$S^{\circ_1}_{w,z}\circ S^{\circ_2}_{w',z'}\simeq S^{\circ_2}_{w',z'}\circ S^{\circ_1}_{w,z}$$

for any $\circ_1,\circ_2\in\{+,-\}$.

Pick a diagram $(\Sigma,\boldsymbol{\alpha},\boldsymbol{\beta},\boldsymbol{w},\boldsymbol{z})$ for $(L,\boldsymbol{w},\boldsymbol{z})$, and let α_s and α_s' be curves in $\Sigma\setminus\boldsymbol{\alpha}$ along which we can perform quasistabilization for (w,z) and (w',z'), respectively. Let β_0 and β_0' denote the new $\boldsymbol{\beta}$–curves. Let $\mathcal{J}$ denote gluing data for stretching along circles bounding β_0 and β_0'. There are two distinct cases to consider, corresponding to whether the pairs (w,z) and (w',z') are adjacent or not: either α_s and α_s' lie in the same component of $\Sigma\setminus\boldsymbol{\alpha}$ (this case corresponds to having the pair (w,z) be adjacent to the pair (w',z')), or α_s and α_s' lie in different components of $\Sigma\setminus\boldsymbol{\alpha}$ (this case corresponds to the pair (w,z) not being adjacent to (w',z')).

The first case is the easier to consider. In this case, we now show that we can pick an almost complex structure which computes both quasistabilization maps. To this end, we have the following lemma:

Lemma 8.2 *Suppose that $(\Sigma,\boldsymbol{\alpha},\boldsymbol{\beta},\boldsymbol{w},\boldsymbol{z})$ is a diagram as in the previous paragraph with new curves α_s and α_s' for quasistabilizing at (w,z) and (w',z'), respectively. If α_s and α_s' are not in the same component of $\Sigma\setminus\boldsymbol{\alpha}$, then for all sufficiently large T_1, T_1', T_2, T_2', we have*

$$\Phi_{\mathcal{J}(T_1,T_1')\to\mathcal{J}(T_2,T_2')}\simeq\mathrm{id}$$

with respect to the obvious identification between the two complexes.

Proof To show this, we will perform a computation similar to the one in Proposition 5.3, but for Maslov index 0 disks. Let A be the component of $\Sigma \setminus \boldsymbol{\alpha}$ which contains α_s and let A' denote the component of $\Sigma \setminus \boldsymbol{\alpha}$ which contains α_s'. By assumption $A \neq A'$. Let A_1 and A_2 denote the two components of $A \setminus \alpha_s$. Let A_1' and A_2' denote the components of $A' \setminus \alpha_s'$. Suppose that ϕ is a Maslov index 0 homology disk on the doubly quasistabilized diagram

$$(\overline{\Sigma}, \boldsymbol{\alpha} \cup \{\alpha_s, \alpha_s'\}, \boldsymbol{\beta} \cup \{\beta_0, \beta_0'\}, \boldsymbol{w} \cup \{w, w'\}, \boldsymbol{z} \cup \{z, z'\}).$$

Write $\phi = \phi_\Sigma \# \phi_0 \# \phi_0'$, where ϕ_Σ is a homology class on $(\Sigma, \boldsymbol{\alpha} \cup \{\alpha_s, \alpha_s'\}, \boldsymbol{\beta}, \boldsymbol{w}, \boldsymbol{z})$, ϕ_0 is a homology class on $(S^2, \alpha_0, \beta_0, w, z)$ and $(S^2, \alpha_0', \beta_0', w, z)$. Suppose that $T_{1,n}$, $T_{1,n}'$, $T_{2,n}$ and $T_{2,n}'$ are sequences of neck lengths all approaching $+\infty$ and let $\widehat{\mathcal{J}}_n$ denote interpolating almost complex structures between $\mathcal{J}(T_{1,n}, T_{1,n}')$ and $\mathcal{J}(T_{2,n}, T_{2,n}')$. Pick $\widehat{\mathcal{J}}_n$ so that as $n \to \infty$ the almost complex structures $\widehat{\mathcal{J}}_n$ split into $J_s \vee J_{S^2} \vee J_{S^2}$ on $(\Sigma \vee S^2 \vee S^2) \times [0,1] \times \mathbb{R}$. If u_n is a sequence of Maslov index 0 $\widehat{\mathcal{J}}_n$–holomorphic curves representing ϕ, we can extract a weak limit to broken curves U_Σ, U_0 and U_0' on $(\Sigma, \boldsymbol{\alpha} \cup \{\alpha_s, \alpha_s'\}, \boldsymbol{\beta}, \boldsymbol{w}, \boldsymbol{z})$, (S^2, α_0, β_0) and $(S^2, \alpha_0', \beta_0')$ representing ϕ_Σ, ϕ_0 and ϕ_0' respectively. As in Proposition 5.3, the curves in U_Σ consist of a broken holomorphic strip U_Σ' on $(\Sigma, \boldsymbol{\alpha}, \boldsymbol{\beta})$ and a collection $\mathcal{A}$ of cylindrical $(\boldsymbol{\alpha} \cup \{\alpha_s\} \cup \{\alpha_s'\})$–boundary degenerations. Let ϕ_Σ' denote the underlying homology class of U_Σ'. Let m_1, m_2, n_1, n_2, m_1', m_2', n_1' and n_2' be multiplicities as in Figure 10.

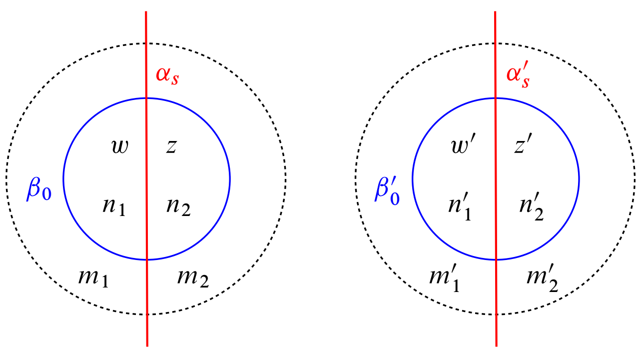

Figure 10: Multiplicities of a disk ϕ near new basepoints w, z, w' and z' on a diagram which has been quasistabilized twice

Adapting the Maslov index computation from Proposition 5.3, we see that

$$\begin{aligned}\mu(\phi) = \mu(\phi_\Sigma') + n_1(\phi) + n_2(\phi) + n_1'(\phi) + n_2'(\phi) \\ + m_1(\mathcal{A}) + m_2(\mathcal{A}) + m_1'(\mathcal{A}) + m_2'(\mathcal{A}) + 2 \sum_{\substack{\mathcal{D} \in C(\Sigma \setminus \boldsymbol{\alpha}) \\ \mathcal{D} \neq A}} n_{\mathcal{D}}(\mathcal{A}),\end{aligned}$$

where $C(\Sigma \setminus \boldsymbol{\alpha})$ denotes the connected components of $\Sigma \setminus \boldsymbol{\alpha}$.

Since U'_Σ is a broken holomorphic curve for an $\mathbb{R}$–invariant almost complex structure, we conclude that U'_Σ consists only of constant flowlines. Since all of the other summands are zero, it's easy to see that this forces all multiplicities to be zero. Hence only constant disks are counted by the change of almost complex structures map, concluding the proof of the lemma. □

In the case that α_s and α'_s are in the same component, the change of almost complex structure maps will often be nontrivial. Nevertheless, we have the following:

Lemma 8.3 *Suppose (w',z') and (w,z) are adjacent on $(L,\boldsymbol{w}\cup\{w,w'\},\boldsymbol{z}\cup\{z,z'\})$ and that (w',z') comes after (w,z). Let $\theta^\pm$ and $(\theta')^\pm$ denote the intersection points corresponding to quasistabilization. If T_1, T_1', T_2, T_2' are all sufficiently large, then, writing $F=\Phi_{\mathcal{J}(T_1,T_1')\to\mathcal{J}(T_2,T_2')}$, we have*

$$\begin{aligned}
F(\boldsymbol{x}\times\theta^+\times(\theta')^+)&=\boldsymbol{x}\times\theta^+\times(\theta')^+,\\
F(\boldsymbol{x}\times\theta^+\times(\theta')^-)&=\boldsymbol{x}\times\theta^+\times(\theta')^-+C\cdot\boldsymbol{x}\times\theta^-\times(\theta')^+,\\
F(\boldsymbol{x}\times\theta^-\times(\theta')^+)&=\boldsymbol{x}\times\theta^-\times(\theta')^+,\\
F(\boldsymbol{x}\times\theta^-\times(\theta')^-)&=\boldsymbol{x}\times\theta^-\times(\theta')^-
\end{aligned}$$

for some C (which is not independent of T_i and T_i').

Proof We proceed similarly to the previous lemma. Now a single component, which we denote by A, of $\Sigma\setminus\boldsymbol{\alpha}$ contains both α_s and α'_s. Write A_1, A_2 and A_3 for the three different components of $A\setminus(\alpha_s\cup\alpha'_s)$. Two of the A_i share boundary with exactly one of the other A_j, and one of the A_i shares boundary with both of the other A_i. Without loss of generality assume that A_1 shares boundary with A_2, and that A_2 also shares boundary with A_3.

As before, as we simultaneously stretch the necks, a sequence of Maslov index 0 disks u_i has a weak limit as before. Now, however, the Maslov index computation is different. Let $a_i(\mathcal{A})$ denote the multiplicity of the $(\boldsymbol{\alpha}\cup\{\alpha_s\}\cup\{\alpha'_s\})$–degeneration $\mathcal{A}$ in the region A_i. One computes that the Maslov index now satisfies

$$\mu(\phi)=\mu(\phi'_\Sigma)+n_1(\phi)+n_2(\phi)+n'_1(\phi)+n'_2(\phi)+a_1(\mathcal{A})+a_3(\mathcal{A})+2\sum_{\substack{\mathcal{D}\in C(\Sigma\setminus\boldsymbol{\alpha})\\ \mathcal{D}\neq A}}n_{\mathcal{D}}(\mathcal{A}).$$

As usual, this implies that all of the terms above are zero. Hence ϕ'_Σ, which has a broken representative for a cylindrical almost complex structure, must be the constant disk by transversality. The only multiplicities which may be nonzero are $a_2(\mathcal{A})$, $m_i(\phi)$ and $m'_i(\phi)$, none of which appear in the sum above. As is easily observed, this constrains the disk ϕ to be in $\pi_2(\boldsymbol{x}\times\theta^+\times(\theta')^-,\boldsymbol{x}\times\theta^-\times(\theta')^+)$, completing the proof. An example of a disk which might appear in the change of almost complex structure map is shown in Figure 11. $\square$

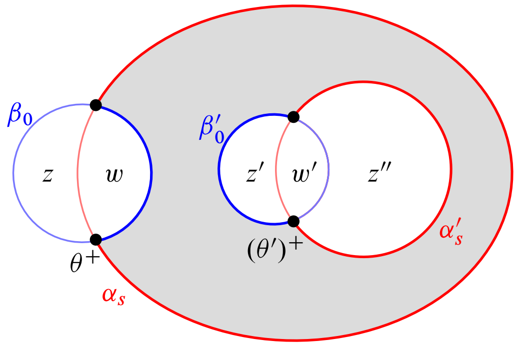

Figure 11: An example of a Maslov index 0 disk which might be counted by $\Phi_{\mathcal{J}(T_1,T_1')\to\mathcal{J}(T_2,T_2')}$ in Lemma 8.3 for arbitrarily large T_i and T_i'

Proof of Theorem 8.1 The proof is easy algebra in all cases using Lemmas 8.2 and 8.3. $\square$

9 Further relations between the maps Ψ_z, Φ_w and $S^{\pm}_{w,z}$

In this section we prove several relations between the maps $S^{\pm}_{w,z}$, Ψ_z and Φ_w. We highlight the convenience of viewing Φ_w and Ψ_z as formal derivatives of the differential, since basically all of the relations in this section are derived by either formally differentiating the expression for $\partial\circ\partial$ from Lemma 2.1, or by differentiating our expression of the quasistabilized differential in Proposition 5.3.

Lemma 9.1 *If w and z are not adjacent, or if w and z are the only basepoints on a link component, then*

$$\Phi_w\Psi_z+\Psi_z\Phi_w\simeq 0.$$

If w and z are adjacent and there are other basepoints on the link component, then

$$\Phi_w\Psi_z+\Psi_z\Phi_w\simeq \mathrm{id}.$$

Proof Take the expression for ∂^2 from Lemma 2.1 and differentiate it with respect to U_w. We obtain

$$\partial\Phi_w+\Phi_w\partial=V_{z'}+V_{z''},$$

where z' and z'' are the variables adjacent to w on its link component. Suppose first that $z' \neq z''$, ie that w and z are not the only basepoints on their link component.

Differentiating the expression above with respect to V_z, we see that

$$\Psi_z \Phi_w + \Phi_w \Psi_z \simeq \begin{cases} \mathrm{id} & \text{if } w \text{ is adjacent to } z, \\ 0 & \text{if } w \text{ is not adjacent to } z, \end{cases}$$

from which the claim follows as long as w and z are not the only basepoints on their link component.

If w and z are the only basepoints on their link component, then $z = z' = z''$ and the argument above is easily modified to give the stated result. □

Lemma 9.2 *We have*

$$\Psi_z \Psi_{z'} + \Psi_{z'} \Psi_z \simeq 0 \quad \textit{and} \quad \Phi_w \Phi_{w'} + \Phi_{w'} \Phi_w \simeq 0$$

for any choice of z, z', w and w'.

Proof This is proven identically to the previous lemma. □

As with the free stabilization maps in [14], we have the following:

Lemma 9.3 *The following relation holds:*

$$S^+_{w,z} S^-_{w,z} = \Phi_w.$$

Proof The differential on the uncolored quasistabilized diagram takes the form

$$\partial_{\overline{\mathcal{H}}} = \begin{pmatrix} \partial_{\mathcal{H}} & U_w + U_{w'} \\ V_z + V_{z'} & \partial_{\mathcal{H}} \end{pmatrix}$$

where $\partial_{\mathcal{H}}$ is the differential on the unstabilized diagram. After taking the U_w derivative we get

$$\Phi_w = \begin{pmatrix} 0 & \mathrm{id} \\ 0 & 0 \end{pmatrix},$$

which is exactly $S^+_{w,z} S^-_{w,z}$. □

We now consider commutators of the quasistabilization maps and the maps Φ_w and Ψ_z.

Lemma 9.4 *Suppose that w and z are two new basepoints for a link. If w is not adjacent to z', then*

$$S^{\pm}_{w,z} \Psi_{z'} + \Psi_{z'} S^{\pm}_{w,z} \simeq 0.$$

With no assumptions on adjacency, we have

$$S^{\pm}_{w,z} \Phi_{w'} + \Phi_{w'} S^{\pm}_{w,z} \simeq 0.$$

Proof Suppose that w and z are inserted between basepoints z'' and w'' on the link $\mathbb{L}$. The quasistabilized differential takes the form

$$\partial_{\bar{\mathcal{H}}} = \begin{pmatrix} \partial_{\mathcal{H}} & U_w + U_{w''} \\ V_z + V_{z''} & \partial_{\mathcal{H}} \end{pmatrix},$$

by Proposition 5.3. By assumption $z' \neq z''$. Differentiating with respect to $V_{z'}$ thus yields

$$\widetilde{\Psi}_{z'} = \begin{pmatrix} \Psi_{z'} & 0 \\ 0 & \Psi_{z'} \end{pmatrix},$$

where $\widetilde{\Psi}_{z'}$ denotes the map on the stabilized diagram and $\Psi_{z'}$ denotes the map on the unstabilized diagram. In matrix notation, the maps $S^{\pm}_{w,z}$ take the form

$$S^+_{w,z} = \begin{pmatrix} \mathrm{id} \\ 0 \end{pmatrix} \quad \text{and} \quad S^-_{w,z} = \begin{pmatrix} 0 & \mathrm{id} \end{pmatrix}. \tag{6}$$

The stated equality involving $\Psi_{z'}$ now follows from matrix multiplication.

The equality involving $\Phi_{w'}$ follows similarly. □

We also have the following:

Lemma 9.5 *Suppose that z' is adjacent to w and that $z' \neq z$. Then we have*

$$S^+_{w,z}\Psi_{z'} \simeq (\Psi_{z'} + \Psi_z)S^+_{w,z} \quad \textit{and} \quad \Psi_{z'}S^-_{w,z} \simeq S^-_{w,z}(\Psi_{z'} + \Psi_z).$$

Proof Once again we consider the quasistabilized differential, which is

$$\partial_{\bar{\mathcal{H}}} = \begin{pmatrix} \partial_{\mathcal{H}} & U_w + U_{w'} \\ V_z + V_{z'} & \partial_{\mathcal{H}} \end{pmatrix}.$$

Differentiating with respect to z' yields

$$\widetilde{\Psi}_{z'} = \begin{pmatrix} \Psi_{z'} & 0 \\ \mathrm{id} & \Psi_{z'} \end{pmatrix} \quad \text{and} \quad \widetilde{\Psi}_z = \begin{pmatrix} 0 & 0 \\ \mathrm{id} & 0 \end{pmatrix}.$$

Here $\widetilde{\Psi}_z$ denotes the map on the complex after quasistabilization, and Ψ_z denotes the map on the complex before quasistabilization. Using the matrix notation from (6), the desired relations follow from matrix multiplication. □

The reader can compare the following lemma to [14, Lemma 7.7], the analogous result for the closed three-manifold invariants.

Lemma 9.6 *Suppose that $\mathbb{L} = (L, \boldsymbol{w}, \boldsymbol{z})$ is a multibased link in Y^3 and w and z are two new, consecutive basepoints on $\mathbb{L}$ such that w follows z. If z' is one of the two $\boldsymbol{z}$–basepoints adjacent to w, then we have*

$$S^-_{w,z}\Psi_{z'}S^+_{w,z} \simeq \mathrm{id}.$$

Proof This follows from our usual strategy. Pick a diagram $\mathcal{H}$ for $(L, \boldsymbol{w}, \boldsymbol{z})$ and let $\bar{\mathcal{H}}$ denote a diagram which has been quasistabilized at w and z. Let z'' and w'' denote the basepoints adjacent to w and z on $\mathbb{L}$. Using Proposition 5.3, we have that

$$\partial_{\bar{\mathcal{H}}} = \begin{pmatrix} \partial_{\mathcal{H}} & U_w + U_{w''} \\ V_z + V_{z''} & \partial_{\mathcal{H}} \end{pmatrix}.$$

By assumption, either $z' = z$ or $z' = z''$ (but not both). In both cases, we have that

$$\Psi_{z'} = \Big(\frac{d}{dV_{z'}}\partial_{\bar{\mathcal{H}}}\Big) = \begin{pmatrix} * & * \\ \mathrm{id} & * \end{pmatrix},$$

where the $*$ terms are unimportant. Using the matrix notation from (6), we get the desired equality immediately from matrix multiplication. □

The reader should compare the following to [13, Lemma 4.4].

Lemma 9.7 *We have $\Psi_z^2 \simeq 0$ and $\Phi_w^2 \simeq 0$ as $\mathfrak{P}$–filtered maps of $\mathbb{Z}_2[U_{\mathfrak{P}}]$–modules.*

Proof The proof follows identically to the proof of [14, Lemma 14.19]. □

10 Basepoint moving maps

In this section, we compute several basepoint moving maps. The procedure for computing maps induced by moving basepoints is in a similar spirit to the author's computation of the π_1–action on the Heegaard Floer homology of a closed three-manifold in [14]. We first compute the effect of moving basepoints along a small arc on a link component via a model computation. We then use this to prove Theorem B, the effect of moving all of the basepoints on a link component in one full loop. The final computation is Theorem D, where we compute the effect on certain colored complexes of moving each $\boldsymbol{w}$–basepoint to the next $\boldsymbol{w}$–basepoint, and moving each $\boldsymbol{z}$–basepoint to the next $\boldsymbol{z}$–basepoint.

10.1 Moving basepoints along an arc

Suppose that Y^3 is a three-manifold with embedded multipointed link $\mathbb{L}_0 = (L, \boldsymbol{w}_0, \boldsymbol{z}_0)$, though we allow the case that one of the components of $\mathbb{L}_0$ has no basepoints. Suppose that z, w, z', w' are all points on a single component of $L \setminus (\boldsymbol{w}_0 \cup \boldsymbol{z}_0)$, appearing in that order according to the orientation of $\mathbb{L}$. Let

$$\boldsymbol{w} = \boldsymbol{w}_0 \cup \{w\}, \quad \boldsymbol{z} = \boldsymbol{z}_0 \cup \{z\}, \quad \boldsymbol{w}' = \boldsymbol{w}_0 \cup \{w'\}, \quad \boldsymbol{z}' = \boldsymbol{z}_0 \cup \{z'\}.$$

Finally, assume that $(L, \boldsymbol{w}, \boldsymbol{z})$ has basepoints in each component of L. There is an isotopically unique diffeomorphism of Y which maps L to itself and fixes $\boldsymbol{w}_0 \cup \boldsymbol{z}_0$ and maps w to w' and z to z', which is isotopic to the identity relative to $\boldsymbol{w}_0 \cup \boldsymbol{z}_0$ through isotopies which map L to itself. Let ς_0 denote this diffeomorphism. It induces a map

$$(\varsigma_0)_*\colon \mathrm{CFL}^\infty_{UV}(Y, L, \boldsymbol{w}, \boldsymbol{z}, \mathfrak{s}) \to \mathrm{CFL}^\infty_{UV}(Y, L, \boldsymbol{w}', \boldsymbol{z}', \mathfrak{s}).$$

The map $(\varsigma_0)_*$ is defined as a tautology. That is, if $\mathcal{H} = (\Sigma, \boldsymbol{\alpha}, \boldsymbol{\beta}, \boldsymbol{w}, \boldsymbol{z})$ is a diagram for $(Y, L, \boldsymbol{w}, \boldsymbol{z})$ with almost complex structure J_s, we just apply the map ς_0 to the diagram $\mathcal{H}$ to get a new diagram

$$\varsigma_0(\mathcal{H}) = (\varsigma_0(\Sigma), \varsigma_0(\boldsymbol{\alpha}), \varsigma_0(\boldsymbol{\beta}), \varsigma_0(\boldsymbol{w}), \varsigma_0(\boldsymbol{z})),$$

with almost complex structure $(\varsigma_0)_* J_s$. The diffeomorphism ς_0 tautologically determines a chain map

$$(\varsigma_0)_*\colon \mathrm{CFL}^\infty_{UV,J_s}(\mathcal{H}, \mathfrak{s}) \to \mathrm{CFL}^\infty_{UV,\varsigma_0(J_s)}(\varsigma_0(\mathcal{H}), \mathfrak{s})$$

defined by

$$(\varsigma_0)_*(\boldsymbol{x}) = \varsigma_0(\boldsymbol{x}).$$

By the naturality results of [4], this yields a well-defined morphism on the coherent chain homotopy type invariants (ie it commutes with change of diagrams maps, in the appropriate sense).

Note that $(\varsigma_0)_*$ "appears" like the identity map since it just maps an intersection point $\boldsymbol{x}$ to its image under ς_0. With this in mind, we prove the following:

Lemma 10.1 *The induced map $(\varsigma_0)_*$ is filtered chain homotopic to*

$$(\varsigma_0)_* \simeq S^-_{w,z} \Psi_{z'} S^+_{w',z'}.$$

Proof We first prove the result in the case that the link component containing w and z has at least one extra pair of basepoints. Let z'' denote the basepoint occurring immediately after w'. In this case, we can pick a diagram like the one shown in Figure 12, where the dashed lines show two circles along which the almost complex structure will be stretched. In this diagram, we assume that α_s and α_s' each bound disks on Σ and that α_s, α_s', β_0 and β_0' do not intersect any other $\boldsymbol{\alpha}$– or $\boldsymbol{\beta}$–curves. With this diagram, we can compute all of the maps $\Psi_{z'}$, $S^-_{w,z}$, and $S^+_{w',z'}$ explicitly. We must be careful, though, since we cannot use the same almost complex structure for all of the maps. Instead we will need to use the change of almost complex structure computation from Lemma 8.3. Let J_s be an almost complex structure which is sufficiently stretched along c to compute $S^{\pm}_{w,z}$, and let J_s' be an almost complex structure which is sufficiently stretched along c' to compute $S^{\pm}_{w',z'}$, and assume that both are stretched sufficiently so that the change of almost complex structure map $\Phi_{J_s'\to J_s}$ takes the form described in Lemma 8.3. We wish to compute $S^-_{w,z}\circ\Psi_{z'}\circ\Phi_{J_s'\to J_s}\circ S^+_{w',z'}$.

Let $\theta^{\pm}$ denote the intersection points of $\alpha_s\cap\beta_0$ and let $(\theta')^{\pm}$ denote the intersection points of α_s' and β_0'.

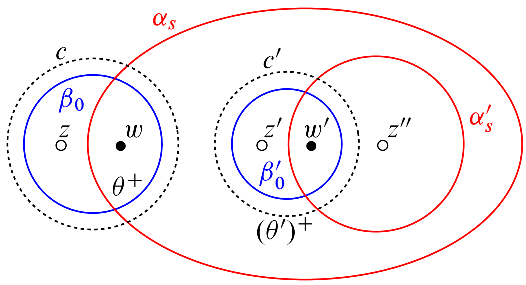

Figure 12: A diagram for Lemma 10.1 when we have another basepoint z'' on the link component containing w, z, w' and z'. The curves α_s and α_s' each bound disks, and $\alpha_s,\alpha_s',\beta_0,\beta_0'$ do not intersect any other $\boldsymbol{\alpha}$– or $\boldsymbol{\beta}$–curves.

Using the analysis in Proposition 5.3, we see that for J_s there are exactly two domains which are the domain of Maslov index 1 disks ϕ which support holomorphic representatives with $n_{z'}(\phi)>0$. These domains are shown in Figure 13. Also every homology disk ϕ which has one of these domains has $\#\widehat{\mathcal{M}}_{J_s}(\phi)=1$.

We wish to show that $S^-_{w,z}\circ\Psi_{z'}\circ\Phi_{J_s'\to J_s}\circ S^+_{w',z'}=(\varsigma_0)_*$, where ς_0 is the diffeomorphism induced by simply pushing w and z to w' and z', respectively. To this end, it is sufficient to show that

$$(S^-_{w,z}\circ\Psi_{z'}\circ\Phi_{J_s'\to J_s}\circ S^+_{w',z'})(\boldsymbol{x}\times\theta^{\pm})=\boldsymbol{x}\times(\theta')^{\pm},$$

since $(\varsigma_0)_*(\boldsymbol{x}\times\theta^{\pm})=\boldsymbol{x}\times(\theta')^{\pm}$.

Homology disks with the left domain in Figure 13 yield a contribution to $\Psi_{z'}$ of

$$\boldsymbol{x}\times\theta^{\pm}\times(\theta')^{+}\longrightarrow\boldsymbol{x}\times\theta^{\pm}\times(\theta')^{-}.$$

Homology disks with the right domain in Figure 13 yield a contribution to $\Psi_{z'}$ of

$$\boldsymbol{x}\times\theta^{+}\times(\theta')^{\pm}\longrightarrow\boldsymbol{x}\times\theta^{-}\times(\theta')^{\pm}.$$

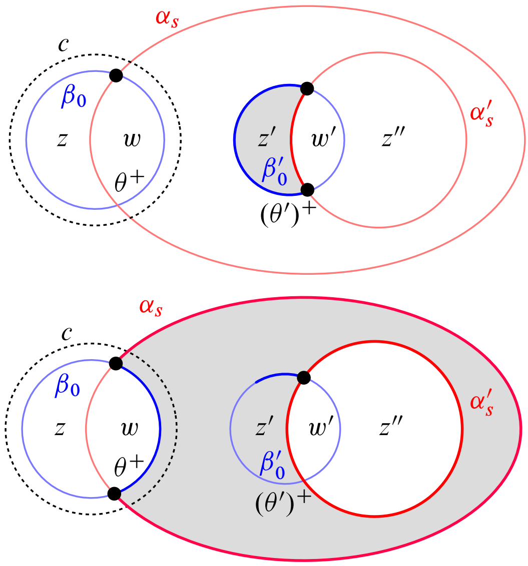

Figure 13: The two domains contributing to $\Psi_{z'}$ in Lemma 10.1 for the almost complex structure J_s stretched first on c', and then stretched on c (possibly much more than on c'). Also drawn in are two examples of holomorphic disks with those domains.

We first compute $(S^-_{w,z} \circ \Psi_{z'} \circ \Phi_{J_s' \to J_s} \circ S^+_{w',z'})(\boldsymbol{x} \times \theta^+)$. Using the computation of $\Psi_{z'}$ above and the computation of $\Phi_{J_s' \to J_s}$ from Lemma 8.3, we have that

$$\begin{aligned}(S^-_{w,z} \circ \Psi_{z'} \circ \Phi_{J_s' \to J_s} \circ S^+_{w',z'})(\boldsymbol{x} \times \theta^+) &= (S^-_{w,z} \circ \Psi_{z'} \circ \Phi_{J_s' \to J_s})(\boldsymbol{x} \times \theta^+ \times (\theta')^+) \\ &= (S^-_{w,z} \circ \Psi_{z'})(\boldsymbol{x} \times \theta^+ \times (\theta')^+) \\ &= S^-_{w,z}(\boldsymbol{x} \times \theta^+ \times (\theta')^- + \boldsymbol{x} \times \theta^- \times (\theta')^+) \\ &= \boldsymbol{x} \times (\theta')^+.\end{aligned}$$

We now compute $(S^-_{w,z} \circ \Psi_{z'} \circ \Phi_{J_s' \to J_s} \circ S^+_{w',z'})(\boldsymbol{x} \times \theta^-)$. Once again using our previous computation of $\Psi_{z'}$ and Lemma 8.3, we have that

$$\begin{aligned}(S^-_{w,z} \circ \Psi_{z'} \circ \Phi_{J_s' \to J_s} \circ S^+_{w',z'})(\boldsymbol{x} \times \theta^-) &= (S^-_{w,z} \circ \Psi_{z'} \circ \Phi_{J_s' \to J_s})(\boldsymbol{x} \times \theta^- \times (\theta')^+) \\ &= (S^-_{w,z} \circ \Psi_{z'})(\boldsymbol{x} \times \theta^- \times (\theta')^+) \\ &= S^-_{w,z}(\boldsymbol{x} \times \theta^- \times (\theta')^-) \\ &= \boldsymbol{x} \times (\theta')^-,\end{aligned}$$

completing the proof of the claim if $\boldsymbol{w}$ and $\boldsymbol{z}$ each have at least two basepoints on L.

We now consider the case that $\mathbb{L}$ doesn't have any basepoints other than w and z. In this case we just introduce two new basepoints w'', z'' which are on the component of $L \setminus \{w, w', z, z'\}$ which goes from w' to z. Note that ς_0 is isotopic relative to $\{w, z\}$ to a diffeomorphism which fixes w'' and z''. Hence $(\varsigma_0)_* S^-_{w'',z''} = S^-_{w'',z''}(\varsigma_0)_*$. We just compute that

$$\begin{aligned}
(\varsigma_0)_* &\simeq (\varsigma_0)_*(S^-_{w'',z''}\Psi_{z''}S^+_{w'',z''}) && \text{(Lemma 9.6)}\\
&\simeq S^-_{w'',z''}(\varsigma_0)_*\Psi_{z''}S^+_{w'',z''} && \text{(observation above)}\\
&\simeq S^-_{w'',z''}(S^-_{w,z}\Psi_{z'}S^+_{w',z'})\Psi_{z''}S^+_{w'',z''} && \text{(previous case)}\\
&\simeq (S^-_{w,z}\Psi_{z'}S^+_{w',z'})(S^-_{w'',z''}\Psi_{z''}S^+_{w'',z''}) && \text{(Theorem 8.1, Lemma 9.4)}\\
&\simeq S^-_{w,z}\Psi_{z'}S^+_{w',z'} && \text{(Lemma 9.6)}
\end{aligned}$$

as we wanted. □

10.2 Sarkar's formula for moving basepoints in a full twist around a link component

In this section, we prove Theorem B, which is Sarkar's conjectured formula for the effect of moving basepoints on a link component in a full twist around the link component for the full link Floer complex. The main technical tool is Lemma 10.1, which computes the effect of moving basepoints on a small arc on a link component. By writing the diffeomorphism of a full twist as a composition of many smaller moves of the previous form, we will obtain Sarkar's formula.

Theorem B *Suppose ς is the diffeomorphism corresponding to a positive Dehn twist around a link component K of $\mathbb{L}$. Suppose that the basepoints on K are $w_1, z_1, \dots, w_n, z_n$. The induced map ς_* on $\mathrm{CFL}^\infty_{UV}(Y, \mathbb{L}, \sigma, \mathfrak{P}, \mathfrak{s})$ has the $\mathfrak{P}$–filtered $\mathbb{Z}_2[U_{\mathfrak{P}}]$ chain homotopy type*

$$\varsigma_* \simeq \mathrm{id} + \Phi_K \Psi_K,$$

where

$$\Phi_K = \sum_{j=1}^n \Phi_{w_j} \quad \textit{and} \quad \Psi_K = \sum_{j=1}^n \Psi_{z_j}.$$

To the reader who is not interested in colorings, we note that one can just take $\mathfrak{P} = \boldsymbol{w} \cup |L|$, where $|L|$ denotes the components of L.

In this section, we also introduce some new formalism to make the computation easier. The maps $\Psi_{z'}$ and $S^{\pm}_{w,z}$ interact strangely (eg Lemma 9.5), which leads to challenging and messy algebra if we are not careful. Suppose that A is an arc on L between two $\boldsymbol{w}$–basepoints which share the same color. We define the map

$$\Psi_A = \sum_{z \in A \cap \boldsymbol{z}} \Psi_z.$$

The maps Ψ_A can be thought of as defining an action of

$$\Lambda^* H_1(L/(\boldsymbol{w}, \sigma); \mathbb{Z})$$

on $\mathit{CFL}^\infty_{UV}(Y, \mathbb{L}, \sigma, \mathfrak{P}, \mathfrak{s})$, where $L/(\boldsymbol{w}, \sigma)$ denotes the space obtained by identifying two $\boldsymbol{w}$–basepoints if they share the same color. This formalism is intriguing, but we will only have use for maps Ψ_A for arcs A between $\boldsymbol{w}$–basepoints of the same color.

Given an arc A between two $\boldsymbol{w}$–basepoints, we define an *endpoint* of A to be a basepoint w such that the sets $\overline{K \setminus A}$ and $\overline{A}$ both contain w (so A has no endpoints if $A = K$).

We now proceed to prove some basic properties of the maps Ψ_A, all of which are recastings of previous lemmas proven about the maps Ψ_z.

Lemma 10.2 *We have*

$$S^{\pm}_{w,z}\Psi_A + \Psi_A S^{\pm}_{w,z} \simeq 0$$

as long as w is not an endpoint of A.

Proof This follows immediately from Lemmas 9.4 and 9.5. □

Lemma 10.3 *If A and A' are two arcs between $\boldsymbol{w}$–basepoints, then*

$$\Psi_A \Psi_{A'} + \Psi_{A'} \Psi_A \simeq 0.$$

Proof This follows from Lemma 9.2. □

Lemma 10.4 *If A is an arc on L, then we have*

$$\Psi_A^2 \simeq 0$$

as filtered equivariant maps.

Proof Simply write $\Psi_A = \sum_{z \in A \cap \boldsymbol{z}} \Psi_z$, multiply out Ψ_A^2, then apply Lemmas 9.2 and 9.7. □

Lemma 10.5 *Suppose $A \subseteq K$ is an arc between $\boldsymbol{w}$–basepoints and let $c(A)$ denote the arc $\overline{K \setminus A}$. Then*

$$\Psi_K \Psi_A = \Psi_{c(A)} \Psi_A.$$

Proof Write $\Psi_K = \Psi_A + \Psi_{c(A)}$ and then use the previous lemma to compute that

$$\Psi_K \Psi_A = (\Psi_A + \Psi_{c(A)})\Psi_A = \Psi_A^2 + \Psi_{c(A)}\Psi_A = \Psi_{c(A)}\Psi_A. \qquad \square$$

Lemma 10.6 *If w is an endpoint of A then we have*

$$\Psi_A \Phi_w + \Phi_w \Psi_A \simeq \mathrm{id}\,.$$

If w is not an endpoint of A, then we have

$$\Psi_A \Phi_w + \Phi_w \Psi_A \simeq 0.$$

Proof The first claim follows from Lemma 9.1. The second claim follows from Lemma 10.2 since we can always write $\Phi_w = S^+_{w,z} S^-_{w,z}$ for z the basepoint immediately preceding w on $\mathbb{L}$. $\square$

We can now prove Theorem B:

Proof of Theorem B Let $w_1, z_1, \dots w_n, z_n$ be the basepoints on K, in the reverse order that they appear on K according to the orientation of K. Let $w_1', z_1', \dots, w_n', z_n'$ be new basepoints on K in the interval between z_n and w_1. Let A_j be the arc on K from w_j to w_j', as in Figure 14.

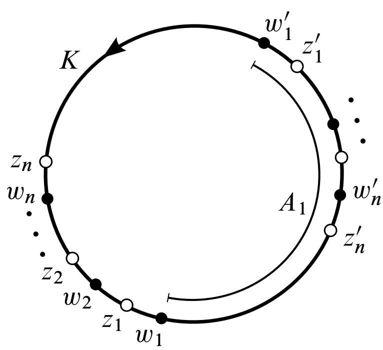

Figure 14: The basepoints $z_1, w_1, \dots, z_n, w_n$ and $z_1', w_1', \dots z_n', w_n'$, and the arcs A_i

Write

$$\boldsymbol{w} = \{w_1, \dots, w_n\}, \quad \boldsymbol{z} = \{z_1, \dots, z_n\}, \quad \boldsymbol{w}' = \{w_1', \dots, w_n'\}, \quad \boldsymbol{z}' = \{z_1', \dots, z_n'\}.$$

As usual, we write ς as a composition of two diffeomorphisms $\varsigma = \varsigma_2 \circ \varsigma_1$, where ς_1 moves the basepoints $\boldsymbol{w}$ and $\boldsymbol{z}$ to $\boldsymbol{w}'$ and $\boldsymbol{z}'$, respectively, and ς_2 moves the basepoints

$\boldsymbol{w}'$ and $\boldsymbol{z}'$ to $\boldsymbol{w}$ and $\boldsymbol{z}$, respectively. Let $c(A_i) = \overline{K \setminus A_i}$. By Lemma 9.6 we have

$$\prod_{j=1}^{n} (S^-_{w'_j,z'_j} \Psi_{A_j} S^+_{w'_j,z'_j}) \simeq \mathrm{id}. \tag{7}$$

Write $S^\pm_{\boldsymbol{w},\boldsymbol{z}}$ for $\prod_{j=1}^n S^\pm_{w_j,z_j}$, and similarly for $S^\pm_{\boldsymbol{w}',\boldsymbol{z}'}$. We compute as follows:

$$\begin{aligned}
\varsigma_* &= (\varsigma_2)_* \circ (\varsigma_1)_* \\
&= \left(\prod_{j=1}^n S^-_{w'_j,z'_j} \Psi_{c(A_j)} S^+_{w_j,z_j}\right)\left(\prod_{j=1}^n S^-_{w_j,z_j} \Psi_{A_j} S^+_{w'_j,z'_j}\right) && \text{(Lemma 10.1)}\\
&= S^-_{\boldsymbol{w}',\boldsymbol{z}'}\left(\prod_{j=1}^n \Psi_{c(A_j)}\right) S^+_{\boldsymbol{w},\boldsymbol{z}} S^-_{\boldsymbol{w},\boldsymbol{z}} \left(\prod_{j=1}^n \Psi_{A_j}\right) S^+_{\boldsymbol{w}',\boldsymbol{z}'} && \text{(Lemmas 10.2, 8.1)}\\
&= S^-_{\boldsymbol{w}',\boldsymbol{z}'}\left(\prod_{j=1}^n \Psi_{c(A_j)}\right)\left(\prod_{j=1}^n \Phi_{w_j}\right)\left(\prod_{j=1}^n \Psi_{A_j}\right) S^+_{\boldsymbol{w}',\boldsymbol{z}'} && \text{(Lemmas 9.3, 8.1)}\\
&= S^-_{\boldsymbol{w}',\boldsymbol{z}'} \sum_{s\in\{0,1\}^n}\left(\prod_{j=1}^n \Phi^{s_j}_{w_j}\right)\left(\prod_{j=1}^n \Psi^{s_j}_{c(A_j)}\right)\left(\prod_{j=1}^n \Psi_{A_j}\right) S^+_{\boldsymbol{w}',\boldsymbol{z}'} && \text{(Lemma 10.6)}\\
&= S^-_{\boldsymbol{w}',\boldsymbol{z}'} \sum_{s\in\{0,1\}^n}\left(\prod_{j=1}^n \Phi^{s_j}_{w_j}\right)\left(\prod_{j=1}^n \Psi^{s_j}_{K}\right)\left(\prod_{j=1}^n \Psi_{A_j}\right) S^+_{\boldsymbol{w}',\boldsymbol{z}'} && \text{(Lemmas 10.3, 10.5)}\\
&= \sum_{s\in\{0,1\}^n}\left(\prod_{j=1}^n \Phi^{s_j}_{w_j}\right)\left(\prod_{j=1}^n \Psi^{s_j}_{K}\right) S^-_{\boldsymbol{w}',\boldsymbol{z}'}\left(\prod_{j=1}^n \Psi_{A_j}\right) S^+_{\boldsymbol{w}',\boldsymbol{z}'} && \text{(Lemmas 10.2, 9.4)}\\
&= \sum_{s\in\{0,1\}^n}\left(\prod_{j=1}^n \Phi^{s_j}_{w_j}\right)\left(\prod_{j=1}^n \Psi^{s_j}_{K}\right) && \text{(Equation (7)).}
\end{aligned}$$

By Lemma 10.4, if $s \in \{0,1\}^n$ then

$$\left(\prod_{j=1}^n \Psi^{s_j}_K\right) \simeq 0$$

if s_j is nonzero for more than one j. Hence the above sum reduces to

$$\varsigma_* \simeq \mathrm{id} + \sum_{j=1}^n \Phi_{w_i} \Psi_K = \mathrm{id} + \Phi_K \Psi_K,$$

completing the proof. $\square$

10.3 The map associated to a partial twist around a link component

In this section, we perform an additional basepoint moving map computation and prove Theorem D. Suppose that $\mathbb{L}$ is a multibased link and K is a component with basepoints z_1, w_1, z_2, $w_2, \dots, z_n$ and w_n, appearing in that order. Let τ be the diffeomorphism induced by twisting $(1/n)^{\text{th}}$ of the way around K, sending z_i to z_{i+1} and w_i to w_{i+1} (with indices taken modulo n). In the case that we pick a coloring $(\sigma, \mathfrak{P})$ where all of the $\boldsymbol{w}$–basepoints have the same color, the map τ induces a map on the complex

$$\mathrm{CFL}^{\infty}_{UV}(Y, \mathbb{L}, \sigma, \mathfrak{P}, \mathfrak{s}).$$

We have the following:

Theorem D *Suppose that $\mathbb{L}$ is an embedded multibased link in Y and K is a component of $\mathbb{L}$ with basepoints $z_1, w_1, \dots, z_n$ and w_n, appearing in that order. Assume that $n > 1$. If τ denotes the $(1/n)^{th}$–twist map, then for a coloring where all $\boldsymbol{w}$–basepoints on K have the same color, we have*

$$\tau_* \simeq (\Psi_{z_1}\Phi_{w_1}\Psi_{z_2}\Phi_{w_2}\cdots\Phi_{w_{n-1}}\Psi_{z_n}\Phi_{w_n}) + (\Phi_{w_1}\Psi_{z_2}\Phi_{w_2}\cdots\Phi_{w_{n-1}}\Psi_{z_n}).$$

Proof Let A_i be the arc from w_i to w_{i+1}, respecting the orientation of K. Let w' and z' be new basepoints in the region between z_n and w_1. Let A' denote the arc from w_n to w' and let A'' denote the arc from w' to w_1. This is illustrated in Figure 15.

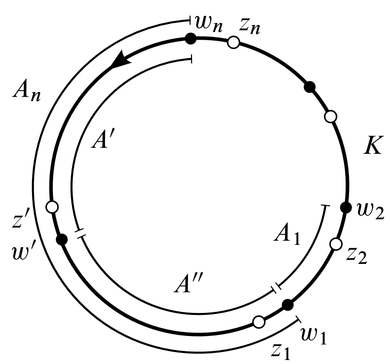

Figure 15: The basepoints $z_1, w_1, \dots, z_n, w_n, z', w'$, and the arcs A_i, A' and A'' from Theorem D

Using Lemma 10.1 repeatedly, we have that

$$\tau_* \simeq (S^-_{w'}\Psi_{A''}S^+_{w_1})(S^-_{w_1}\Psi_{A_1}S^+_{w_2})\cdots(S^-_{w_{n-1}}\Psi_{A_{n-1}}S^+_{w_n})(S^-_{w_n}\Psi_{A'}S^+_{w'}).$$

Using this, we perform the following computation:

$$
\begin{aligned}
\tau_* &\simeq S^-_{w'}\Psi_{A''}\Phi_{w_1}\Psi_{A_1}\Phi_{w_2}\cdots\Phi_{w_{n-1}}\Psi_{A_{n-1}}\Phi_{w_n}\Psi_{A'}S^+_{w'} && \text{(Lemma 9.3)}\\
&\simeq S^-_{w'}\Psi_{A''}\Phi_{w_1}\Psi_{A_1}\Phi_{w_2}\cdots\Phi_{w_{n-1}}\Psi_{A_{n-1}}(\Psi_{A'}\Phi_{w_n}+1)S^+_{w'} && \text{(Lemma 10.6)}\\
&\simeq S^-_{w'}\Psi_{A''}\Phi_{w_1}\Psi_{A_1}\Phi_{w_2}\cdots\Phi_{w_{n-1}}\Psi_{A_{n-1}}\Psi_{A'}\Phi_{w_n}S^+_{w'}\\
&\qquad + S^-_{w'}\Psi_{A''}\Phi_{w_1}\Psi_{A_1}\Phi_{w_2}\cdots\Phi_{w_{n-1}}\Psi_{A_{n-1}}S^+_{w'}\\
&\simeq S^-_{w'}(\Psi_{A''}\Psi_{A'})\Phi_{w_1}\Psi_{A_1}\Phi_{w_2}\cdots\Phi_{w_{n-1}}\Psi_{A_{n-1}}\Phi_{w_n}S^+_{w'}\\
&\qquad + S^-_{w'}\Psi_{A''}\Phi_{w_1}\Psi_{A_1}\Phi_{w_2}\cdots\Phi_{w_{n-1}}\Psi_{A_{n-1}}S^+_{w'} && \text{(Lemmas 10.6, 10.3)}\\
&\simeq S^-_{w'}(\Psi_{A''}\Psi_{A_n})\Phi_{w_1}\Psi_{A_1}\Phi_{w_2}\cdots\Phi_{w_{n-1}}\Psi_{A_{n-1}}\Phi_{w_n}S^+_{w'}\\
&\qquad + S^-_{w'}\Psi_{A''}\Phi_{w_1}\Psi_{A_1}\Phi_{w_2}\cdots\Phi_{w_{n-1}}\Psi_{A_{n-1}}S^+_{w'} && \text{(Lemma 10.4)}\\
&\simeq (S^-_{w'}\Psi_{A''}S^+_{w'})\Psi_{A_n}\Phi_{w_1}\Psi_{A_1}\Phi_{w_2}\cdots\Phi_{w_{n-1}}\Psi_{A_{n-1}}\Phi_{w_n}\\
&\qquad + (S^-_{w'}\Psi_{A''}S^+_{w'})\Phi_{w_1}\Psi_{A_1}\Phi_{w_2}\cdots\Phi_{w_{n-1}}\Psi_{A_{n-1}} && \text{(Lemma 10.2)}\\
&\simeq \Psi_{A_n}\Phi_{w_1}\Psi_{A_1}\Phi_{w_2}\cdots\Phi_{w_{n-1}}\Psi_{A_{n-1}}\Phi_{w_n}\\
&\qquad + \Phi_{w_1}\Psi_{A_1}\Phi_{w_2}\cdots\Phi_{w_{n-1}}\Psi_{A_{n-1}} && \text{(Lemma 9.6),}
\end{aligned}
$$

completing the proof since $\Psi_{A_i}=\Psi_{z_{i+1}}$ on the complex $\mathit{CFL}^\infty_{UV}(Y,\mathbb{L},\sigma,\mathfrak{P},\mathfrak{s})$, by definition. □

References

[1] **K Hendricks**, **C Manolescu**, *Involutive Heegaard Floer homology*, preprint (2015) arXiv

[2] **A Juhász**, *Cobordisms of sutured manifolds and the functoriality of link Floer homology*, Adv. Math. 299 (2016) 940–1038 MR

[3] **A Juhász**, **M Marengon**, *Concordance maps in knot Floer homology*, Geom. Topol. 20 (2016) 3623–3673 MR

[4] **A Juhász**, **D P Thurston**, *Naturality and mapping class groups in Heegaard Floer homology*, preprint (2012) arXiv

[5] **R Lipshitz**, *A cylindrical reformulation of Heegaard Floer homology*, Geom. Topol. 10 (2006) 955–1097 MR

[6] **C Manolescu**, **P Ozsváth**, *Heegaard Floer homology and integer surgeries on links*, preprint (2011) arXiv

[7] **Y-G Oh**, *Fredholm theory of holomorphic discs under the perturbation of boundary conditions*, Math. Z. 222 (1996) 505–520 MR

[8] **P Ozsváth**, **Z Szabó**, *Holomorphic disks and knot invariants*, Adv. Math. 186 (2004) 58–116 MR

[9] **P Ozsváth**, **Z Szabó**, *Holomorphic disks and topological invariants for closed three-manifolds*, Ann. of Math. 159 (2004) 1027–1158 MR

[10] **P Ozsváth**, **Z Szabó**, *Holomorphic disks, link invariants and the multi-variable Alexander polynomial*, Algebr. Geom. Topol. 8 (2008) 615–692 MR

[11] **J A Rasmussen**, *Floer homology and knot complements*, PhD thesis, Harvard (2003) MR Available at `http://search.proquest.com/docview/305332635`

[12] **S Sarkar**, *Maslov index formulas for Whitney n–gons*, J. Symplectic Geom. 9 (2011) 251–270 MR

[13] **S Sarkar**, *Moving basepoints and the induced automorphisms of link Floer homology*, Algebr. Geom. Topol. 15 (2015) 2479–2515 MR

[14] **I Zemke**, *Graph cobordisms and Heegaard Floer homology*, preprint (2015) arXiv

Department of Mathematics, University of California, Los Angeles
520 Portola Plaza, Los Angeles, CA 90025, United States

`ianzemke@math.ucla.edu`

Received: 3 June 2016 Revised: 10 October 2016